

**Mutations in the Extracellular Domain of the  
Neural Cell Adhesion Molecule L1 Impair  
Protein Trafficking *In Vitro* and *In Vivo***

**Dissertation  
zur Erlangung des  
Doktorgrades der Naturwissenschaften  
des Fachbereiches Biologie  
an der Universität Bielefeld**

**vorgelegt von**

**Annette E. Rünker**

**Bielefeld 2002**

## Table of Contents

<b>Abstract</b> .....	<b>1</b>
<b>Zusammenfassung</b> .....	<b>3</b>
<b>I Introduction</b> .....	<b>5</b>
1 Cell adhesion molecules in the nervous system .....	5
2 The immunoglobulin superfamily .....	5
3 The L1 family .....	7
4 The neural cell adhesion molecule L1.....	7
4.1 <i>Characteristics of L1</i> .....	8
4.2 <i>Expression and function of L1 in the nervous system</i> .....	9
4.3 <i>Homophilic and heterophilic adhesion</i> .....	10
4.4 <i>Intracellular events mediated by L1</i> .....	13
4.5 <i>Mutations in the L1 gene cause severe neurological disorders             in humans</i> .....	15
4.6 <i>Genotype-phenotype relationship for L1 mutations</i> .....	17
4.7 <i>The L1-deficient mouse: an animal model for human diseases of             the L1 spectrum</i> .....	19
5 The aim of this study .....	21
<b>II Materials and Methods</b> .....	<b>23</b>
1 Materials .....	23
1.1 <i>Chemicals</i> .....	23
1.2 <i>Solutions and buffers</i> .....	23
1.3 <i>Bacterial and cell culture media</i> .....	26
1.4 <i>Bacterial strains and cell lines</i> .....	27
1.5 <i>Plasmids</i> .....	27
1.6 <i>Antibodies</i> .....	27
2 Methods.....	28

2.1	<i>Molecular biological methods</i> .....	28
2.2	<i>Protein-biochemical methods</i> .....	39
2.3	<i>Cell culture</i> .....	42
2.4	<i>Immunocytochemistry</i> .....	44
2.5	<i>Morphological methods</i> .....	45
<b>III</b>	<b>Results</b> .....	<b>47</b>
1	Part I: Cell culture experiments .....	47
1.1	<i>Mutagenesis of mouse L1cDNA</i> .....	47
1.2	<i>Cell surface expression of L1<math>\Delta</math>hbs and L1C264Y is strongly reduced</i> . 48	
1.3	<i>L1<math>\Delta</math>hbs and L1C264Y are expressed as a protein variant with a reduced molecular weight of 190 kD</i> .....	50
1.4	<i>L1 with a molecular weight of 190 kD is not expressed on the cell surface</i> .....	51
1.5	<i>L1<math>\Delta</math>hbs and L1C264Y are not located at the cell surface, but within the endoplasmic reticulum</i> .....	54
2	Part II: The L1C264Y transgenic mouse .....	55
2.1	<i>Generation of L1C264Y transgenic mice</i> .....	55
2.2	<i>L1C264Y expressed in vivo is endo H-sensitive</i> .....	57
2.3	<i>Expression of L1C264Y protein is restricted to cell bodies of neurons</i> 58	
2.4	<i>General phenotype of L1C264Y mice</i> .....	61
2.5	<i>L1C264Y and L1-deficient mice display a similar morphological phenotype</i> .....	63
<b>IV</b>	<b>Discussion</b> .....	<b>69</b>
1	The short isoform of L1 .....	69
2	The L1 mutations L1C264Y and L1 $\Delta$ hbs result in impaired protein trafficking.....	70
3	Retention of misfolded proteins in the ER.....	71
4	L1 $\Delta$ hbs and L1C264Y are retained in the ER .....	73
5	Studies on L1 extracellular missense mutations .....	74

---

6	Mutations of the intracellular domain .....	76
7	The L1C264Y-transgenic mouse .....	76
8	The fate of intracellularly retained misfolded protein .....	77
9	Concluding remarks and outlook.....	80
<b>V</b>	<b>References .....</b>	<b>83</b>
<b>VI</b>	<b>Appendix .....</b>	<b>109</b>
1	Abbreviations .....	109
2	Oligonucleotides .....	110
2.1	<i>Primer for sequencing of mouse L1 cDNA .....</i>	<i>110</i>
2.2	<i>Primer for sequencing of transgenic construct .....</i>	<i>111</i>
2.3	<i>Primer for genotyping .....</i>	<i>111</i>
2.4	<i>Primer for PCR mutagenesis.....</i>	<i>111</i>
3	Mutations in the of L1cDNA .....	112
4	L1 plasmids.....	114
4.1	<i>Cloning of mutated L1cDNAs into a mammalian expression vector..</i>	<i>114</i>
4.2	<i>Cloning of the L1C264Y transgenic construct .....</i>	<i>115</i>
	<b>Publications.....</b>	<b>117</b>
	<b>Danksagung.....</b>	<b>118</b>

## Abstract

The neural cell adhesion molecule L1, a member of the immunoglobulin superfamily, performs important functions in the developing and adult nervous system. L1 is implicated in neuronal migration and survival, elongation, fasciculation and pathfinding of axons, and synaptic plasticity. Mutations in all parts of the L1 gene might cause serious neurological syndromes in humans, characterized by increased mortality, mental retardation and various malformations of the nervous system. Patients with missense mutations in the extracellular domain of L1 often develop severe phenotypes, while mutations in the cytoplasmic domain usually cause moderate phenotypes. In an attempt to understand the reasons for the frequent occurrence of severe extracellular missense mutations, this study addressed the functional consequences of extracellular and cytoplasmic L1 mutations.

To this aim, we used mutated L1 constructs to study their expression in CHO cells. The L1 missense mutation C264Y (L1C264Y), located in the extracellular domain and causing a severe phenotype in humans, was not expressed at the cell surface. Similar results were obtained for a L1 construct with a deletion of the putative homophilic binding site (L1 $\Delta$ hbs). In contrast, an intracellularly truncated form of L1 showed normal levels of cell surface expression. L1C264Y and L1 $\Delta$ hbs protein had a reduced molecular weight due to the lack of Golgi-type modified N-glycans. These observations suggest that both mutated L1 variants are retained within the endoplasmic reticulum (ER).

To study the expression and the functional consequences of a human pathogenic missense mutation *in vivo*, a transgenic mouse line was generated expressing the extracellular missense mutation C264Y under the control of the L1 promoter in a L1-deficient background. In these mutant mice, the L1C264Y protein was located intracellularly to neuronal cell bodies and displayed an abnormal glycosylation state, in line with the results obtained in cell culture experiments. Analysis of the L1C264Y transgenic mice revealed no phenotypical differences to L1-deficient mice, i.e. both mutants showed reduced survival, a reduced size of the corticospinal tract and pathfinding errors of corticospinal axons, and abnormalities

of unmyelinated fibers in peripheral nerves. Together, these data indicate that the transgenic mice represent functional null mutants.

We suggest an ER retention followed by degradation of the mutated L1 protein as the most likely underlying molecular pathomechanism of the L1C264Y missense mutation, ultimately resulting in the loss of L1 function. The combined *in vitro* and *in vivo* observations corroborate the view that impaired cell surface expression of mutated variants of L1 is a potential explanation for the high number of severe pathogenic mutations identified within the human L1 gene.

## Zusammenfassung

Das neurale Zelladhäsionsmolekül L1 ist ein Mitglied der Immunglobulin Superfamilie und erfüllt wichtige Funktionen im sich entwickelnden und adulten Nervensystem. So ist L1 an verschiedenen Prozessen, wie der Migration und dem Überleben von Neuronen, dem Auswachsen, der Bündelung und der Wegfindung von Axonen und der synaptischen Plastizität, beteiligt. Mutationen in allen Regionen des L1 Gens können beim Menschen zu gravierenden neurologischen Syndromen des sogenannten L1 Spektrums führen. Gemeinsame Merkmale dieser Syndrome sind eine erhöhte Sterblichkeit, geistige Behinderung und verschiedene Mißbildungen des Gehirns. Patienten mit Punktmutationen in der extrazellulären Domäne von L1 entwickeln häufig einen schwereren Phänotyp als solche mit Mutationen im zytoplasmatischen Bereich. Um Einblicke in die Ursachen für das häufige Auftreten von schwerwiegenden Punktmutationen in der extrazellulären Domäne zu gewinnen, wurden in dieser Studie die funktionellen Konsequenzen von Mutationen sowohl der extrazellulären als auch der intrazellulären Domäne von L1 untersucht.

Die Expression von mutierten L1 Konstrukten wurde in CHO- (chinese hamster ovarian) Zellen analysiert. Es konnte gezeigt werden, daß die pathogene L1 Punktmutation C264Y (L1C264Y), die in der extrazellulären Domäne liegt und zu einem schweren Phänotyp beim Menschen führt, nicht auf der Zelloberfläche exprimiert wird. Ähnliche Resultate ergaben sich für ein L1 Konstrukt mit einer Deletion der putativen homophilen Bindungsstelle von L1 (L1 $\Delta$ hbs). Im Gegensatz dazu zeigte eine intrazellulär deletierte L1-Variante normale L1-Mengen auf der Zelloberfläche. Das Molekulargewicht von L1C264Y- und L1 $\Delta$ hbs-Proteinen war reduziert, da die N-gekoppelten Oligosaccharide der Proteine keine Golgi-typische Modifikationen aufwiesen. Diese Beobachtungen lassen vermuten, daß die mutierten Proteine im endoplasmatischen Reticulum (ER) zurückgehalten und nicht weiter zum Golgi-Apparat transportiert werden.

Um die Konsequenzen einer humanpathologischen Mutation auf die Expression und Funktion von L1 *in vivo* zu untersuchen, wurde eine transgene Mauslinie erzeugt, in der die extrazellulär gelegene Punktmutation C264Y unter Kontrolle des L1-Promotors vor einem L1-defizienten Hintergrund exprimiert wird. In diesen

Mausmutanten war das L1C264Y-Protein in neuronalen Zellkörpern lokalisiert und wies einen abnormalen Glykosylierungsgrad auf. Diese Ergebnisse stimmen mit den Befunden der Zellkultur-Untersuchungen überein. Eine phänotypische Analyse der L1C264Y-transgenen Mäuse ergab keine Unterschiede zu L1-defizienten Mäusen, d.h. beide Mutanten zeigten eine verringerte Überlebenswahrscheinlichkeit, eine Reduktion des corticospinalen Traktes, Fehler in der Wegfindung von corticospinalen Axonen, sowie abnormale unmyelinisierte Fasern in peripheren Nerven. Diese Befunde legen nahe, daß die transgenen Mäuse funktionale Null-Mutanten repräsentieren.

Die Ergebnisse der *in vitro* und *in vivo* Untersuchungen deuten darauf hin, daß eine Akkumulation des mutierten L1 Proteins im ER, gefolgt von einer Degradation des Proteins, den zugrundeliegenden molekularen Pathomechanismus der L1C264Y Mutation darstellt. Demnach könnte eine gestörte Zelloberflächenexpression ursächlich für das häufige Auftreten von schweren pathogenen Punktmutationen im humanen L1 Gen sein.

# I Introduction

## 1 Cell adhesion molecules in the nervous system

The development of the nervous system depends on a coordinate sequence of morphoregulatory processes, such as neural induction, proliferation and differentiation of cells, their migration to final destinations, and the patterning of neuronal connectivities (Purves and Lichtman, 1983; Goodman and Shatz, 1993; Edelman, 1986). In the adult nervous system glial cells and, in certain brain regions, also neurons are continuously generated and have to be integrated into the existing tissue. In addition, mature neurons have the capacity to change their synaptic connectivities and the efficacy of synaptic transmission, a process termed synaptic plasticity. A key step in all these processes is the ability of cells and their outgrowing axons and dendrites to interact with other cells and the extracellular matrix (ECM) (Kater and Rehder, 1995; Gordon-Weeks, 2000). Many of these interactions are mediated by a variety of integral membrane proteins, collectively termed cell adhesion molecules (CAMs).

Sequence analysis indicated that many proteins evolved from common precursors by duplication and subsequent diversification of genes. Therefore they were grouped into families and subfamilies according to their structural similarities (Dayhoff et al., 1983). Neural CAMs are divided into three main classes: the  $\text{Ca}^{2+}$ -dependent cadherins (more than 40 members; Angst et al., 2001; Tepass et al., 2000), the heterodimeric integrins (about 17  $\alpha$ - and 8  $\beta$ -subunits; Clark and Brugge, 1995), and the  $\text{Ca}^{2+}$ -independent molecules of the immunoglobulin (Ig) superfamily (for review: Aplin et al., 1998; Juliano, 2002).

## 2 The immunoglobulin superfamily

Members of the Ig superfamily of cell recognition molecules are characterized by the presence of one or more immunoglobulin modules. Prototypical examples of this family are the immunoglobulins themselves (Edelman et al., 1969) and the

MHC-antigens (major histocompatibility complex; Orr et al., 1979) of the immune system. In contrast to these molecules, which are specialized for highly specific antigen recognition, the polypeptide chains constructed by Ig-modules in CAMs (Williams and Barclay, 1988) do not form intermolecular, but intramolecular disulfide bridges within a module. Most cell recognition molecules in the nervous system combine their Ig-like modules with other repeated structures. One of these structures is the fibronectin repeat of the subtype III (FNIII domain). This motif was originally identified as a repeated module of 90 residues in the ECM molecule fibronectin (Kornblihtt et al., 1985) and was later also found in other ECM proteins (Engel, 1991). Functional analysis of fibronectin revealed that FNIII domains are involved in interactions of cells with the EMC (Ruosalahti and Pierschbacher, 1987).

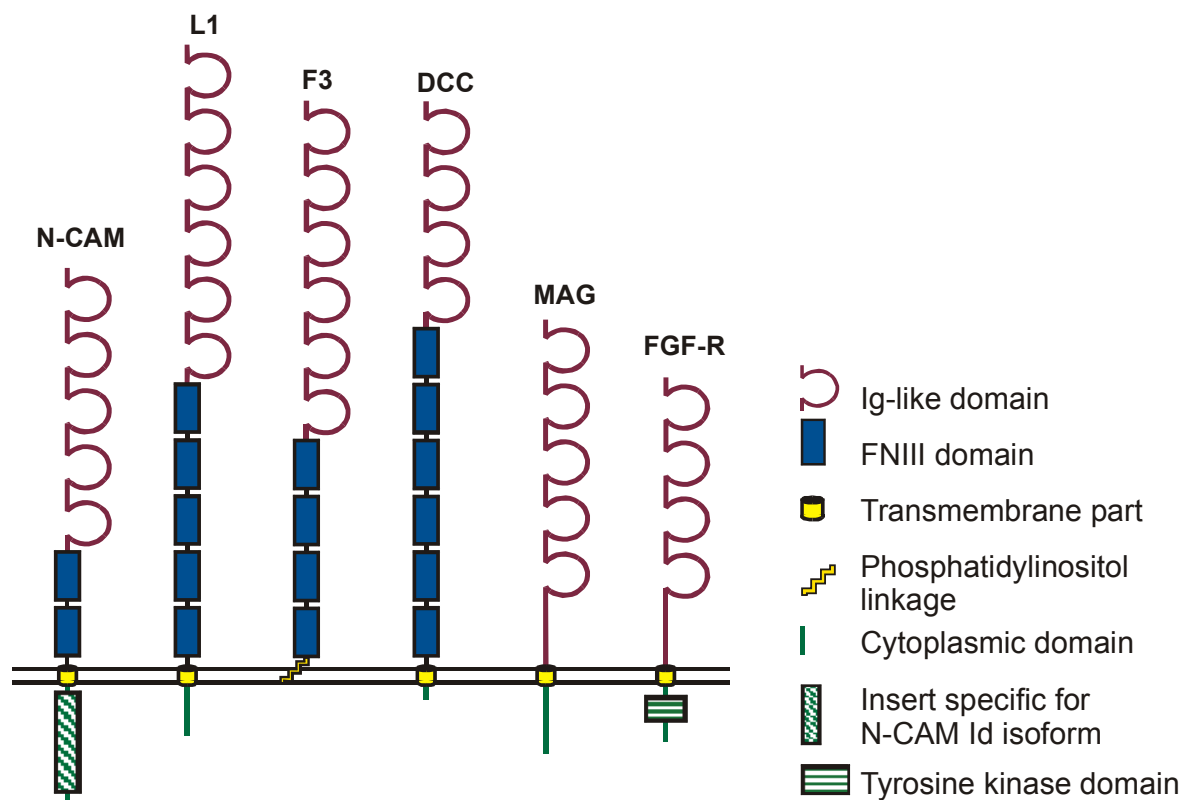


**Figure 1: Representatives of different subgroups of the immunoglobulin superfamily of cell adhesion molecules.** Members of the Ig superfamily consist of an extracellular domain with Ig-like domains and, in part, fibronectin type III (FNIII) repeats, a single transmembrane region or a GPI anchor and, in most cases, an intracellular domain. N-CAM (neural cell adhesion molecule); DCC (deleted in colonrectal carcinoma); MAG (myelin-associated glycoprotein); FGF-R (fibroblast growth factor receptor).

The Ig superfamily is further divided into several subgroups according to the number of Ig-domains, the presence and number of FNIII-domains, the mode of attachment to the cell membrane, and the presence of a catalytic cytoplasmic domain (Fig. 1; Cunningham, 1995). The first isolated and characterized Ig-like CAMs were the neural cell adhesion molecule (N-CAM; Brackenbury et al., 1977; Thiery et al., 1977) and L1 (Salton et al., 1983; Rathjen and Schachner, 1984), representative molecules of two different subgroups. F3 (mouse F3/chicken F11/human contactin), DCC (deleted in colonrectal carcinoma), MAG (myelin associated glycoprotein), and FGF-R (fibroblast growth factor-receptor) represent additional subgroups that occur in the brain (Fig.1)

### 3 The L1 family

The L1 family within the Ig superfamily consists of four vertebrate members: L1, CHL1 (close homologue of L1), Nr-CAM (Ng-CAM related CAM) and neurofascin, and two invertebrate members: neuroglian and tractin (reviewed in Hortsch, 2000; Brümmendorf and Rathjen, 1995). All members of the L1 family share a common modular structure, composed of six amino-terminal Ig-domains, four to five FNIII-repeats, a single hydrophobic membrane-spanning region and a short, phylogenetically highly conserved cytoplasmic tail at the carboxyl terminus (Brümmendorf and Rathjen, 1995). In the developing and adult central nervous system (CNS) and peripheral nervous system (PNS) the molecules are involved in a variety of morphogenetic processes, including cell migration, axon outgrowth, pathfinding and fasciculation, myelination and synaptic plasticity. Members of the L1 family are expressed by neurons and glial cells, and are mainly found on the surface of axons and at sites of cell-cell contact (Hortsch, 1996).

### 4 The neural cell adhesion molecule L1

The neural cell adhesion molecule L1 is one of the most widely studied CAMs and closely related L1 homologous were identified in a variety of species, including L1CAM (or L1, human), NILE (nerve growth factor-inducible large external glycoprotein, rat), L1 (mouse), Ng-CAM (neuron-glia CAM, chick), E587 (goldfish), L1.1 and L1.2 (zebrafish), and neuroglian (drosophila). The sequence similarity

among species homologous of different animal classes ranges between 30 to 60 %, with the intracellular domain showing the highest degree of interspecies homology (Hortsch, 1996 and 2000). The amino acid sequence of L1 from human and mouse, for instance, is 92 % identical, and that between mouse and rat is 97 % identical. The intracellular domain of L1 from these three species shows complete identity.

#### 4.1 Characteristics of L1

L1 was first described in the mouse CNS as a transmembrane glycoprotein of approximately 200 kD. Smaller components of 180, 140, 80, and 50 kD were found, and are generated from the 200 kD form by proteolytic cleavage (Lindner et al., 1983; Rathjen and Schachner, 1984). Mammalian L1 consists of six Ig-domains of the C2-type, five FNIII repeats, a single membrane-spanning region followed by a short cytoplasmic tail (Fig. 2). 21 putative sites for asparagine-(N-) linked glycosylation are distributed over the extracellular domain of L1 (Fig. 2). In addition, a substantial portion of the glycans is O-linked as indicated by tunicamycin inhibition of cotranslational N-glycosylation (Faissner et al., 1985). Glycans contribute about 25 % to the total molecular mass of L1, since deglycosylation revealed an apparent molecular mass of about 150 kD (Lindner et al., 1983; Rathjen and Schachner, 1984).

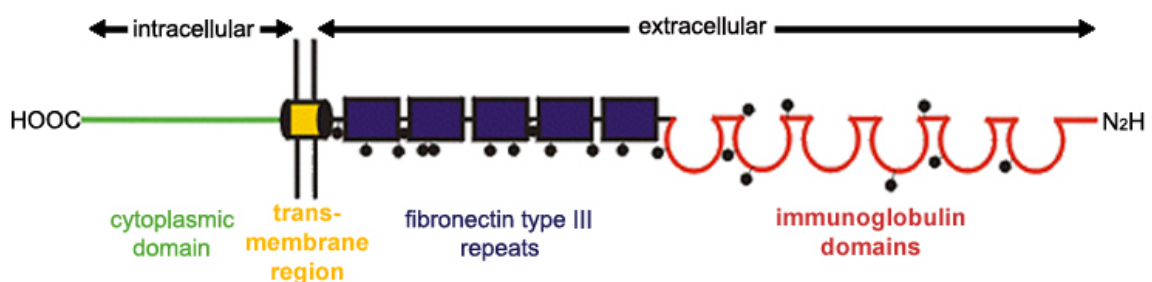


**Figure 2: Structure of L1.** The L1 molecule consists of six immunoglobulin domains and five complete fibronectin type III repeats next to the N-terminal. The transmembrane region is indicated by the yellow box and followed by a short intracellular domain. 21 putative N-glycosylation sites are distributed over the extracellular part and indicated by black lollipops.

The L1 protein is encoded by a single gene, which is located on the X-chromosome and contains 29 exons, 28 exons encode the protein (designated 1b-28) while one exon contains 5' untranslated sequences (exon 1a) (Kohl et al., 1992; Kallunki et al., 1997). The mRNA provides an open reading frame of 3783 nucleotides. The encoded 1260 amino acids comprise a 19 amino acid signal peptide and a mature protein of 1241 amino acids (Moos et al., 1988).

L1 exists as two isoforms that result from alternative splicing. The two isoforms are expressed in a tissue- and cell type-specific pattern. Neurons utilize the entire 28 exon coding sequence of L1 (Takeda et al., 1996). A shorter isoform of L1 (sL1), exclusively expressed in non-neuronal cells, lacks exon 2 and 27. This form was found on cells of hematopoietic origin, in intestinal crypt cells and in the male urogenital tract (Kowitz et al., 1992; Thor et al., 1987; Kujat et al., 1995), in the epidermis and in the kidney (Nolte et al., 1999; Debiec et al., 1998). More recently also oligodendrocytes were found to express sL1 in addition to full-length L1, regulated in a maturation-dependent manner (Itoh et al., 2000).

Differential use of exons 2 and 27 is conserved for L1 orthologous in rodents (Jouet et al., 1995a; Miura et al., 1991), teleost fish and fugu (Coutelle et al., 1998) suggesting that it is of functional importance. Exon 27 encodes for the four amino acids RSLE within the cytoplasmic domain (Fig. 4), which is important as a tyrosine-based sorting motif (YRSL) for clathrin-mediated endocytosis (see below) (Kamiguchi et al., 1998). Inclusion of exon 2 into the mRNA provides the six amino acids YEGHHV in human or YKGGHHV in mouse, respectively, in place of a single leucine residue immediately amino-terminal to the first Ig-domain (Jouet et al., 1995 a).

## **4.2 Expression and function of L1 in the nervous system**

Expression of L1 starts early during neural development, and nerve cells are L1 immunoreactive as they become postmitotic and start to migrate to their final location within the brain. A well-studied example is the L1 positive cells in the inner part of the external granule layer of the cerebellum, which resemble mainly postmitotic, premigratory granule cells. The outer part of the external granular layer which contains proliferating neuroblasts, in contrast, is L1 immunonegative

(Lindner et al., 1983; Persohn and Schachner, 1987). After migration, L1 is predominantly found on outgrowing and fasciculating axons. In adulthood the protein remains expressed on unmyelinated axons, as for example in the molecular layers of the cerebellum or the hippocampus, but disappears from myelinated axons, i.e. white matter (Bartsch et al., 1989; Martini and Schachner, 1986). The cellular expression pattern therefore shows a dependency on the state of differentiation. In the PNS, L1 is also expressed by nonmyelinating Schwann cells (Martin and Schachner, 1986).

The cellular expression pattern of L1 is consistent with its functions. During the development of the nervous system, L1 plays a role in migration of postmitotic neurons (Lindner et al., 1983; Asou et al., 1992), in axon outgrowth, pathfinding and fasciculation (Fischer et al., 1986; Lagenaur and Lemmon, 1987; Chang et al., 1987; Kunz et al., 1996), growth cone morphology (Payne et al., 1992; Burden-Gulley et al., 1995), adhesion between neurons and between neurons and Schwann cells (Rathjen and Schachner, 1984; Faissner et al., 1984; Persohn et al., 1987), and in myelination (Seilheimer et al., 1989; Wood et al., 1990 a, b). In addition, L1 has been implicated in axonal regeneration (Martini and Schachner, 1988), learning and memory formation (Rose, 1995), and the establishment of long-term potentiation in the hippocampus (Luthi et al., 1994 and 1996).

### **4.3 Homophilic and heterophilic adhesion**

The variety of L1 functions within the nervous system is probably related to a multiplicity of binding partners, potential signaling cascades and posttranslational modifications (Fig. 3 and 4). It is generally believed that L1 performs most of its functions via homophilic interactions (Miura et al., 1992; Lemmon et al., 1989; Hankin and Langenaur, 1994). For instance wild-type neurons extend long neurites on purified L1 while neurons from L1 knock-out mice are unable to extend processes on purified L1 (Dahme et al., 1997; Fransen et al., 1998). Several studies attempted to map the regions that are needed for homophilic binding and optimal levels of neurite outgrowth and achieved somewhat different conclusions. While some studies (Appel et al., 1993; Holm et al., 1995) found that several extracellular domains are required for homophilic interactions, Zhao et al. (1995

and 1998) suggested that the second Ig-domain, and more specifically a 14 amino acid peptide within this Ig-domain, is sufficient for homophilic binding.

L1 and its species homologues also interact either in *cis* or in *trans* with a variety of ligands (Fig. 3), including F3/F11/contactin (Brümmendorf et al., 1993), axonin-1/TAG-1 (Kuhn et al., 1991), DM-GRASP (DeBernardo and Chang, 1996), laminin (Grumet et al., 1993), and CD24 (or nectradrin; Kadmon et al., 1995; Sammar et al., 1997). Furthermore, the Arg-Gly-Asp (RGD) site within Ig-domain 6 supports binding with subsets of integrins such as  $\alpha_5\beta_1$ ,  $\alpha_V\beta_1$  or  $\alpha_V\beta_3$  (Ruppert et al., 1995; Ebeling et al., 1996; Montgomery et al., 1996; Felding-Habermann et al., 1997).

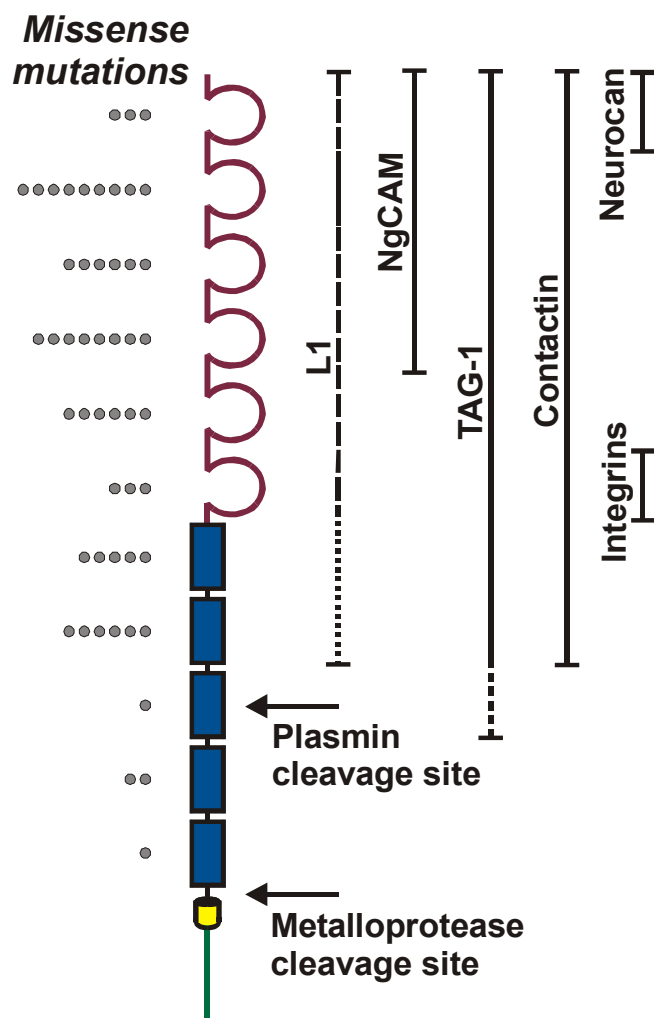


**Figure 3: Interactions of the extracellular domain of L1 and location of all known pathogenic missense mutations.** The distribution of pathogenic missense mutations (indicated by gray dots) within the extracellular domain of L1 in relation to the domains involved in ligand binding and proteolytic cleavage. Broken lines indicate different findings in the mapping of domains, which are important for binding with the indicated partners (modified from Kenwick et al., 2000).

The functional significance of heterophilic L1 interactions is largely unknown. However, some of these heterophilic interactions enhance the effects of L1-L1 interaction. Interactions between L1 and TAG-1/axonin-1 *in cis*, for instance, are

critical in regulating L1-mediated neurite outgrowth (Buchstaller et al., 1996; Rader et al., 1996). In addition, some studies suggested a *cis* interaction of L1 and NCAM, which increase homophilic L1 interactions *in trans*, and thus L1-mediated cell aggregation and neurite outgrowth (Kadmon et al., 1990; Simon et al., 1991; Horstkorte et al., 1993). An action of both molecules through common pathways, but also through different signaling pathways was shown (Williams et al., 1994; Takei et al., 1999).

The findings that neurons from L1-deficient mice fail to respond to the repulsive guidance factor semaphorin3A (Sema3A), and that L1 associates with the semaphorin receptor neuropilin (Castellani et al., 2000) suggest that L1 serves as a co-receptor with neuropilin for Sema3A signal transduction. L1 can also interact with the ECM, namely by binding to the chondroitin sulfate proteoglycans neurocan and phosphacan, major constituents of the ECM (Rauch et al., 1991 and 2001; Milev et al., 1994 and 1995). Mapping of the binding site within the first Ig-domain of L1 led to the suggestion that binding to neurocan may sterically hinder a proper homophilic alignment of L1 (Oleszewski et al., 2000).

In addition to its cell surface localization, L1 is also released as a soluble molecule (Sadoul et al., 1988; Martini and Schachner, 1986; Montgomery et al., 1996; Beer et al., 1999). L1 shedding results from cleavage near the membrane, most likely by a metalloprotease of the ADAM (a distingrin and metalloproteinase) family, ADAM 10, and leads to an amino-terminal 180 kD and a membrane associated 30 kD fragment (Gutwein et al., 2000; Mechtersheimer et al., 2001). This type of L1 cleavage is shown to support integrin-mediated cell adhesion, i.e it can stimulate cell migration on fibronectin and laminin by autocrine binding of soluble L1 to  $\alpha_v\beta_5$  integrins (Beer et al., 1999; Gutwein et al., 2000; Mechtersheimer et al., 2001). Sensitivity to cleavage by the serine protease plasmin is found within the third FNIII-like domain of L1, resulting in a soluble 140 kD and a transmembrane 80 kD fragment (Faissner et al., 1985; Sadoul et al., 1988; Nyboroe et al., 1990; Kayyem et al., 1992; Burgoon et al., 1995; Nayeem et al., 1999). The shedded L1 fragment is suggested to abrogate homophilic L1-L1-mediated aggregation (Nayeem et al., 1999).

#### 4.4 Intracellular events mediated by L1

Evidence for how CAM interactions might promote axonal growth came from studies in which the treatment of neurons with purified CAMs resulted in neurite outgrowth and, in parallel, in changes of intracellular pH and  $\text{Ca}^{2+}$  levels (Doherty and Walsh, 1996). Further, CAM-induced neurite outgrowth was inhibited by treatment with pharmacological reagents, including kinase inhibitors or calcium channel antagonists (Williams et al., 1992). These results suggested that CAMs function by activating second messenger cascades. Indeed, axonal growth in response to homophilic L1-L1 interactions *in trans* seems to be triggered by an activation of the FGF-R (a receptor tyrosine kinase) after *in cis* interactions between the extracellular domains of L1 and FGF-R, leading to an autophosphorylation of the receptor (Williams et al., 1994 a, b; Doherty et al., 1996; Doherty and Walsh, 1996; Brittis et al., 1996; Walsh and Doherty, 1997; Saffell et al., 1997; Lom et al., 1998; Meiri et al., 1998; Kolkova et al., 2000; Rønn et al., 2000). The involved downstream signaling cascade has been worked out in detail (activation of  $\text{PLC}\gamma$  (phospholipase C)  $\rightarrow$  DAG (diacylglycerine)  $\rightarrow$  via DAG lipase: AA (arachidonic acid)) and culminates in transient influx of  $\text{Ca}^{2+}$  through L- and N-type channels at localized submembrane sites (Archer et al., 1999), resulting in a focused signal at a distinct region of the growth cone. How local domains of elevated  $\text{Ca}^{2+}$  levels subsequently promote growth cone advance is not understood, although one possibility might be an action of  $\text{Ca}^{2+}$  dependent modifiers of the actin cytoskeleton (Doherty et al., 1995).

Additional signaling cascades following CAM binding have been suggested. L1 has been shown to be phosphorylated by Cek5 (chicken embryo kinase 5 /EphB2) a receptor-type tyrosine kinase of the ephrin (Eph) kinase family (Zisch et al., 1997; Zisch and Pasquale, 1997), and two serine/threonine protein kinases, casein kinase II and p90<sup>rsk</sup> (Wong et al., 1996 a, b; Kunz et al., 1996). Clustering of L1 at the neural surface is reported to transiently activate the MAP kinase (mitogen-activated protein kinase) and ERK2 (extracellular signal-regulated kinase; Schmid et al., 1999 and 2000). A role of the non-receptor type tyrosine kinase src in L1-dependent neurite outgrowth is indicated by the fact that neurite outgrowth from src-deficient nerve cells is impaired on an L1 substrate (Ignelzi et al., 1994). An example for influences of heterophilic binding on such signaling

casades is the finding that dimerization of L1 with TAG1/axonin-1 is associated with non-receptor tyrosine kinase activation (Kunz et al., 1996).

The most conserved feature among all members of the L1-subgroup is their ability to interact with the spectrin-based membrane skeleton by binding to the adaptor protein ankyrin (Davis and Bennett, 1993 und 1994; Hortsch, 2000). The ankyrin binding motif FIGQY within the cytoplasmic tail of L1 is highly conserved, and phosphorylation of the tyrosine within this sequence abolishes association with ankyrin (Garver et al., 1997; Zhang et al., 1998; Hortsch et al., 1998). Interactions between L1 and ankyrin might be a mechanism by which interactions with the substrate are linked to the cytoskeleton and lead to ankyrin-dependent alterations in the cellular organization or in the targeting of proteins to specific membrane compartments (for review: Bennett and Chen, 2001). Interestingly, one human pathological missense mutation within the ankyrin binding side of L1 (substitution of tyrosine to histidine; Y1229H) results in an abolishment of both ankyrin-binding activity and phospho-tyrosine signaling, indicating a regulation of ankyrin binding via phosphorylation of the tyrosine within the binding site (Kenwrick et al., 2000). Finally, ankyrin-B knock-out mice exhibit a phenotype similar to L1 knock-out mice, and share features of human patients with L1 mutations (Scotland et al., 1998).

L1 has also been shown to colocalize with filamentous actin in the filopodia and lamellipodia of growth cones of cultured chick dorsal root ganglion neurons (Letourneau and Shattuck, 1989) and to bind indirectly to actin (Gumbiner, 1993). The sequence motif crucial for binding to actin stress fibers is close to the serine residue phosphorylated by p90<sup>rsk</sup>, suggesting a link of L1-mediated neurite outgrowth with binding to the actin-based cytoskeleton (Dahlin-Huppe et al., 1997).

Recent studies gave insights into the molecular mechanisms by which L1 might be functionally involved in growth cone migration. Clathrin-mediated endocytosis of L1 occurs preferentially in the central domain of growth cones followed by centrifugal transport of vesicles into the peripheral domains and reinsertion into the membrane at the leading edge (Kamiguchi et al., 1998; Kamiguchi and Lemmon, 2000; Kamiguchi and Yoshihara, 2001). This system may be responsible for producing polarized adhesion and directed migration of the growth

cone. Critical for the clathrin-mediated endocytosis is an interaction of the tyrosine-based motif YRSL (YXX $\Phi$ ; X is any aa;  $\Phi$  is an aa with a hydrophobic bulk chain) within the cytoplasmic domain of L1 with the  $\mu$ 2 chain of the clathrin-adaptor AP-2 (Kamiguchi et al., 1998; Kamiguchi and Lemmon 1998). This interaction may then result in a concentration of L1 in clathrin-coated areas of the plasma membrane. Interestingly, the YRSL motif contains the alternatively spliced RSLE sequence, which is absent from L1 of non-neuronal cells (Kamiguchi and Yoshihara, 2001).

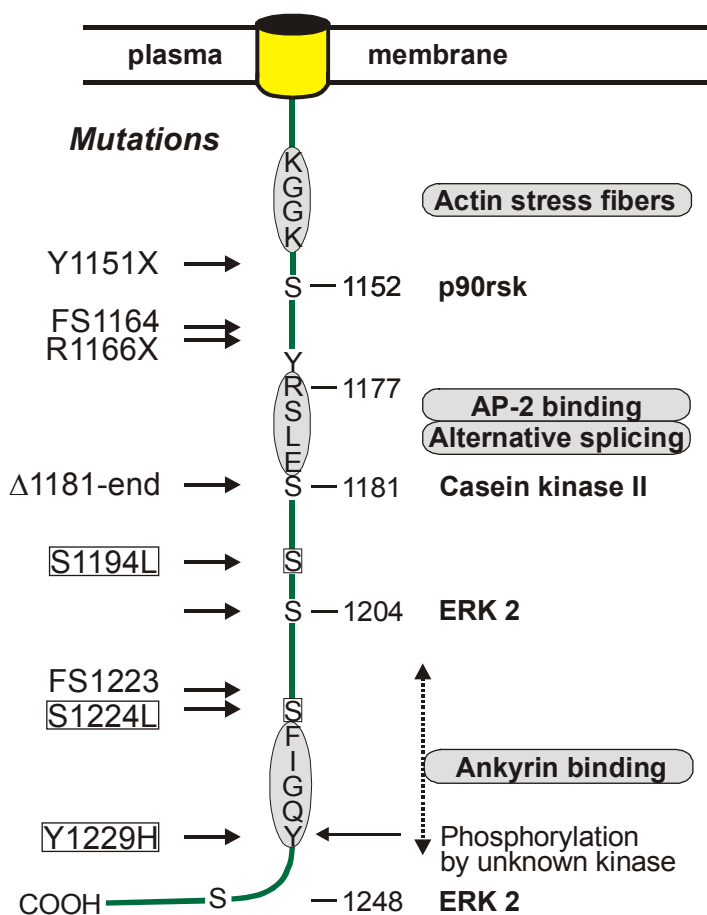


**Figure 4: Binding and phosphorylation sites within the intracellular domain of L1 in relation to the location of all known pathogenic mutations.** Gray boxes indicate binding or alternative splice sites. Missense mutations, which affect phosphorylation sites, are shown in open boxes (modified from Kenwick et al., 2000).

#### 4.5 Mutations in the L1 gene cause severe neurological disorders in humans

In 1990, the human gene encoding L1 has been located near the long arm of the X-chromosome (Djabali et al., 1990) in Xq28 (Chapman et al., 1990). Since different X-linked mental retardation syndromes have already been located to

Xq28 and the morphological abnormalities of these syndromes might result from deficits in cell migration, axonal pathfinding and fasciculation, L1 was a likely candidate gene causing these syndromes. HSAS syndrome (hydrocephalus due to stenosis of the aqueduct of Sylvius; Bickers and Adams, 1949) was first attributed to mutations in the L1 gene (Rosenthal et al., 1992). Subsequently, L1 mutations were found in patients with MASA syndrome (mental retardation, aphasia, shuffling gait and adducted thumbs; Bianchine and Lewis, 1974), X-linked complicated SP-1 (spastic paraplegia; Kenwrick et al., 1986) or ACC (agenesis of the corpus callosum; Kaplan et al., 1983) (Jouet et al., 1994; Fransen et al., 1994; Vits et al., 1994). The fact that all of these conditions are allelic disorders proved that HSAS, MASA, SP-1, and ACC represent overlapping clinical spectra of the same disease, and are therefore now summarized under the term 'L1 spectrum' (Moya et al., 2002). This term might be more widely acceptable than the previously proposed term CRASH (corpus callosum agenesis, retardation, adducted thumbs, shuffling gait, and hydrocephalus, Fransen et al., 1995).

L1 mutations account for 5 % of all cases with hydrocephalus and are the most frequent genetic cause of this pathology. The incidence of pathological L1 mutations is generally estimated to be around 1 in 30,000 male births (Halliday et al., 1986; Schrandt-Stumpel and Fryns, 1998). In general, the patients show a broad spectrum of clinical and neurological abnormalities, already reflected by the varying nomenclature. The severity of the disease varies significantly between patients with different L1 mutations and might also vary between patients carrying the same mutation (Serville et al., 1992). The most consistent features of affected patients are varying degrees of lower limb spasticity, mental retardation with IQs ranging between 20 and 50, enlarged ventricles or hydrocephalus (Fig. 5 B-D), and flexion deformities of the thumbs (Fig. 5 A). Those that develop hydrocephalus *in utero* or soon after birth have a low life expectancy and many of them die neonatally. Another striking morphological abnormality is a hypoplasia of the corticospinal tract (CST; compare Fig. 5 E and F) and the corpus callosum (Fig. 5 B-D). The CST is important for voluntary motor functions and its impaired development in affected patients might therefore be responsible for the spasticity. The corpus callosum connects the cerebral hemispheres and pathological alterations of this large commissure might contribute to mental retardation. Other brain malformations include hypoplasia of the septum pellucidum and the

cerebellar vermis, and fusion of the thalami and colliculi (Fig. 5; for review see: Wong et al., 1995b; Fransen et al., 1996 and 1997; Kenwrick et al., 2000).

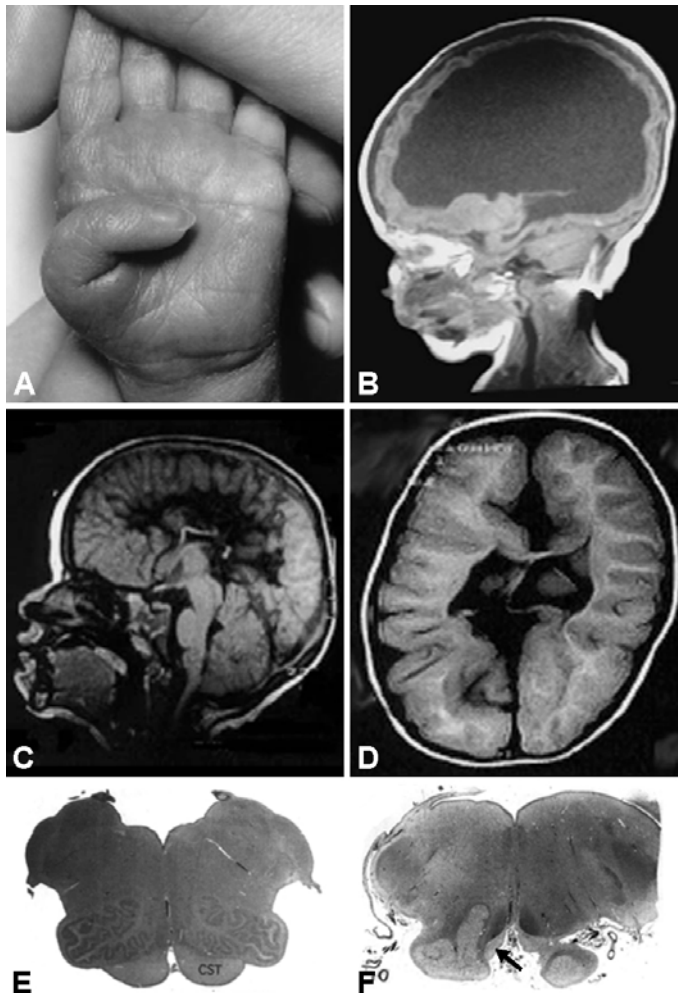


**Figure 5: Patients with syndromes of the L1 spectrum.**

**A:** Adducted thumb of an affected newborn patient. **B:** MRI scan (magnetic resonance image) of the head of same newborn as in (A), showing massive hydrocephalus. **C and D:** MRI scan of the head of a 5 year old affected child showing dysgenesis of the corpus callosum and dilated lateral ventricles. **E and F:** The corticospinal tract of an affected patient (arrow in F) is significantly reduced in size when compared to the tract of a healthy individual (CST in E). (A and B: from Schrandt-Stumpel and Fryns, 1998; C and D from Moya et al., 2002; E and F: from Wong et al., 1995b).

#### 4.6 Genotype-phenotype relationship for L1 mutations

Up to date, about 140 different pathogenic mutations have been identified in virtually all regions of the gene. Hot spots for pathogenic mutations have not been observed. The majority of mutations are restricted to single families (for a continuously updated list of L1 mutations, see the L1 mutation web page <http://dnalab-www.uia.ac.be/dnalab/l1/>; Van Camp et al., 1996). All kinds of mutations were found in human patients including missense, nonsense, and frame shift mutations, deletions, insertion, and splice site mutations with often unknown consequences for the amino acid sequence. Despite the wide range of symptoms, a certain correlation between the severity of the disease and the type and location

of the mutation has been demonstrated (Bateman et al., 1996; Fransen et al., 1998 b; Michaelis et al., 1998; Yamasaki et al., 1997). Patients carrying known L1 mutations were scored as being 'severely' or 'mildly' affected. Severely affected patients either died before the age of 2 years, were born macrocephalic, or needed shunt. Mildly affected patients had none of these three criteria.

Mutations that truncate the protein in the extracellular domain are expected to abolish cell surface expression and therefore to result in a 'loss of function' of L1-mediated interactions. Such truncations generally produce the most severe phenotypes (Yamasaki et al., 1997). Most frequent are missense mutations within the extracellular domain (35%), which in many cases cause a severe phenotype but might also result in a relatively mild phenotype. An explanation for the variable outcome of missense mutations came from computer modeling studies, which classified extracellular missense mutations into 'key' and 'surface' amino acid residues. Key residues are responsible for maintaining the conformation of L1 in its respective domains, whereas surface residues are expected to have little influence on the rest of the domain, but might be important for the finely tuned interactions of L1 with its various ligands (Bateman et al., 1996). Indeed, substitutions involving the 'key' residues produce the most severe forms of hydrocephalus and are most deleterious to infant survival (Michaelis et al., 1998; Fransen et al., 1998b). However, the reasons for the high number of different L1 missense mutations with severe consequences remain only partly understood, and appropriate animal models for such conditions are still missing. Potentially, these mutations might interfere with homophilic or heterophilic interactions of L1 or with the targeting of the protein to the cell surface (De Angelis et al., 1999 and 2002; Moulding et al., 2000).

In contrast, any kind of mutation within the cytoplasmic domain cause moderate or variable phenotypes with rare observations of severe hydrocephalus, grave mental retardation or death before the second postnatal year. These mutations are expected to interfere with intracellular signaling and interactions with the cytoskeleton, but are unlikely to disrupt L1-mediated adhesion as indicated by the observations that a deletion of large portions of the intracellular domain of L1 (Wong et al., 1995 a) or *Drosophila* neuroglian (Hortsch et al., 1995) did not affect L1-dependent homophilic cell-cell interactions.

#### **4.7 The L1-deficient mouse: an animal model for human diseases of the L1 spectrum**

To obtain a mouse model for L1 spectrum, two mouse L1 knock-out (L1ko) lines were independently generated in two laboratories by targeted disruption of the L1 gene (Dahme et al., 1997; Cohen et al., 1998). Many of the pathological features observed in human patients with L1 mutations were also seen in these L1ko mice, and their analysis provided important insights into the functions performed by L1 *in vivo* (Dahme et al., 1997; Cohen et al., 1998; Fransen et al., 1998 a; Demyanenko et al., 1999; Haney et al., 1999; Rolf et al., 2001). The phenotypes of the two independently generated L1 mutants showed many similarities. The body size of both mutants was significantly reduced when compared with wild-type littermates, the eyes were lacrimous and further back in their sockets and thus appeared smaller, and both mutants showed difficulties to use their hind legs (Cohen et al., 1998; Dahme et al., 1997). The latter observation may parallel the shuffling gait of patients with L1 spectrum. L1 mutant mice also showed a decreased sensitivity to touch and pain (Dahme et al., 1997). Although a few L1 mutants were able to breed, the vast majority of them were sterile (Cohen et al., 1998; our unpublished observations). The mortality of the mutants was increased when bred in a 129Sv mouse strain background and, even more, in a C57 genetic background. The higher mortality in the C57 strain correlated with a more severe phenotype when compared to mutants with a 129-background (see below). L1 mutants and wild-type mice were subjected to a passive avoidance-learning task, and both genotypes showed a similar learning ability (Fransen et al., 1998a). However, experiments in the Morris water maze revealed impaired spatial learning of L1 mutants compared to wild-type controls (Fransen et al., 1998a).

The L1ko mice showed diverse morphological abnormalities. The CST of L1-deficient mice was reduced in size by about 40 % (Dahme et al., 1997). The hypoplasia of the CST was shown to result from pathfinding errors of corticospinal axons (Cohen et al., 1998). In wild-type mice, the majority of these axons turns dorsally at the pyramidal decussation, located at the caudal end of the medulla oblongata, and extends into the contralateral dorsal column. In L1-deficient mice, however, the majority of axons stayed ventrally and entered the contralateral pyramid or turned dorsally, but entered the ipsilateral instead of the contralateral

dorsal column (Cohen et al., 1998). The abnormalities of the corticospinal tract might explain the locomotor deficits of L1 mutants and also of patients with L1 spectrum.

Significant hypoplasia was also reported for the corpus callosum, the major commissure of the brain (Demyanenko et al., 1999). This defect apparently resulted from a failure of callosal axons to cross the midline of the brain and is also found in patients with L1 spectrum. Other abnormalities of L1 mutants reported in the same study included abnormal morphology of septal nuclei, an approximately 30 % reduction in the number of hippocampal pyramidal and granule cells, and an abnormal orientation and undulating appearance of apical dendrites of a fraction of pyramidal cells in motor, visual, and somatosensory cortices (Demyanenko et al., 1999).

Given that anti-L1 antibodies interfere with the migration of granule cells in cerebellar explant cultures and with the elongation and fasciculation of neurites of cerebellar nerve cells, it is remarkable that the cytoarchitecture of the cerebellar cortex of L1 mutants showed no evidence for disturbed cell migration, axon outgrowth, or axon fasciculation (Dahme et al., 1997). The only abnormality reported for the cerebellum of L1 mutants was a hypoplasia of the cerebellar vermis (Fransen et al., 1998 a), a defect also frequently observed in patients with L1 spectrum (Yamasaki et al., 1995). In addition to the unexpectedly mildly affected cerebellum, axon tracts other than the CST and the corpus callosum appear to develop normal in L1-mutant mice (Cohen et al., 1998; Dahme et al., 1997). One explanation might be that other molecules, which perform similar functions as L1, might compensate for the lack of L1 and thus allow normal development of the cerebellum and of the majority of axon tracts in the mutant.

The most striking defect of L1 mutant mice is certainly the significant enlargement of the ventricular system (hydrocephalus). This abnormality is again reminiscent of pathological alterations reported for brains of patients with L1 spectrum. Massively enlarged lateral ventricles were observed in L1 mutants with a C57 genetic background, whereas only slightly ventricular dilations were found in mutants with a 129 background (Dahme et al., 1997; Fransen et al., 1998 a; Demyanenko et al., 1999). The strong dependence of this defect on the genetic

background suggests that modifier genes, together with the mutated L1 gene, determine the severity of this morphological abnormality.

In the PNS, where nonmyelinating Schwann cells express sL1, L1 deficient mice show defects in unmyelinated fibers. These morphological abnormalities include a reduced number of unmyelinated axons per nonmyelinating Schwann cell, Schwann cell processes extending into the endoneurial space, and the presence of incompletely ensheathed unmyelinated axons (Dahme et al., 1997; Haney et al., 1999). These defects demonstrate that L1 is essential for normal interactions between nerve cells and nonmyelinating Schwann cells and probably also for the long-term maintenance of unmyelinated axons.

## 5 The aim of this study

As discussed above, pathogenic missense mutations within the extracellular domain might cause severe phenotypes, but might also result in a relatively mild phenotype. Compared to the phenotypic variability of extracellular mutations, any kind of mutation within the intracellular domain causes relatively mild phenotypes. The latter fact is remarkable with regard to the high degree of conservation of the cytoplasmic domain, which is generally considered as a hint for functional importance. Thus, for missense mutations or short in frame deletions and insertions, the disease-causing nature of the mutation is not directly evident and, despite same *in vitro* studies on L1 missense mutations, only partly understood. To obtain insights into consequences of L1 mutations concerning hetero- or homophilic interactions, posttranslational processing or protein trafficking, we addressed a detailed characterization of different L1 mutations *in vitro*: The following mutations were analyzed:

1. The pathogenic L1 missense mutation C264Y within the third Ig domain is known to cause a severe syndrome in humans, called HSAS (Jouet et al., 1993).
2. The putative 14 amino acid homophilic binding site within the second Ig domain (Zhao et al., 1998) was chosen for deletion. This sequence contains three pathogenic missense mutations: I179S, R184W and R184Q (Ruiz et al., 1995; Fransen et al., 1996; Jouet et al., 1994).

3. Intracellularly truncated L1 was studied to obtain insights into the functional consequences of pathogenic mutations within the intracellular domain.
4. Short L1 variants with deletion of exon 2 and/or exon 27 were included, in which the extra- and/or the intracellular domain is affected. Deletion of exon 2 possibly mimics a pathogenic mutation within the donor splice site located in intron 1 which is predicted to result in skipping of exon 2 (Jouet et al., 1995; Jouet and Kenwrick, 1995).

The L1-deficient mouse displays many of the pathological features of patients with L1 mutations. However, in humans the majority of pathogenic L1 mutations have been identified as small deletions or insertions and missense mutations rather than null mutations. Since many of these mutations might affect only single L1 functions or lead to gain of functions, the question of how these mutations affect the development of the nervous system cannot be answered by the analysis of the L1-deficient mouse. Therefore, we generated and analyzed a transgenic mouse line, which expresses the human pathogenic L1C264Y missense mutation under the control of the L1 promoter in a L1-deficient background.

## II Materials and Methods

### 1 Materials

#### 1.1 Chemicals

All chemicals were obtained from the following companies in p.a. quality: GibcoBRL (Life Technologies, Karlsruhe, Germany), Macherey-Nagel (Düren, Germany), Merck (Darmstadt, Germany), Serva (Heidelberg, Germany) and Sigma-Aldrich (Deisenhofen, Germany).

Restriction enzymes were obtained from New England Biolabs (Frankfurt am Main, Germany) and MBI Fermentas (St. Leon-Rot, Germany), molecular weight standards were obtained from GibcoBRL. DNA purification kits were purchased from Life Technologies, Pharmacia Biotech (Freiburg, Germany), Macherey & Nagel and Qiagen (Hilden, Germany). Plasmids and molecular cloning reagents were obtained from Clontech, Invitrogen, Pharmacia Biotech, Promega, Qiagen and Stratagene. Oligonucleotides were ordered from metabion (Munich, Germany). All oligonucleotides used are listed in the appendix. Cell culture material was ordered from Nunc or Life Technologies.

#### 1.2 Solutions and buffers

(in alphabetical order)

Blotting buffer, pH 8.3 ( <i>Western Blot</i> )	25 mM	Tris-HCl
	190 mM	Glycin
	0.01 %	SDS
	10 %	Methanol
Boston buffer ( <i>Lysis of tail cuts</i> )	50 mM	Tris-HCl, pH 8.0
	50 mM	KCl
	2.5 mM	EDTA
	0.45 %	NP-40
	0.45 %	Tween 20

Citrate buffer (2x) ( <i>Endo H digestion</i> )	75 mM	Sodium citrate, pH 5.5
Complete™ (25x)	Protease-inhibitors pills; 1 tablet resuspended in 2 ml solution results in a 25xstock solution	
Denhardts (50x) ( <i>Southern Blotting</i> )	1 %	BSA
	1 %	Ficoll
	1 %	polyvinylpyrrolidon
DNA-sample buffer (5x) ( <i>DNA-gels</i> )	20 % (w/v)	glycerol in TAE buffer
	0,025 % (w/v)	orange G or bromophenol blue
dNTP-stock solutions ( <i>PCR</i> )	25 mM	each dATP, dCTP, dGTP, dTTP
Ethidiumbromide-staining solution ( <i>DNA-gels</i> )	10 µg/ml	ethidiumbromide in 1xTAE
Lysis buffer I ( <i>lysis of brain</i> )	20 mM	Tris-HCl, pH 7.5
	150 mM	NaCl
	1 mM	EDTA
	1 mM	EGTA
	1 x	complete™ (directly before use)
Lysis buffer II ( <i>lysis of brain</i> )	20 mM	Tris-HCl, pH 7.5
	150 mM	NaCl
	1 mM	EDTA
	1 mM	EGTA
	1 % (w/v)	NP-40
	1 x	complete™ (directly before use)
MOPS (10x) ( <i>PBS-CM</i> )	220 mM	MOPS, pH 7.4
	50 mM	Na-acetate
	10 mM	EDTA
Phosphate buffered saline ( <i>PBS, biochemistry</i> )	150 mM	NaCl
	8.1 mM	Na <sub>2</sub> HPO <sub>4</sub> ,
	1.7 mM	NaH <sub>2</sub> PO <sub>4</sub> pH 7.4
(PBS, morphology)	270 mM	NaCl
	19 mM	Na <sub>2</sub> HPO <sub>4</sub>
	5 mM	KCl
	3.4 mM	KH <sub>2</sub> PO <sub>4</sub> pH 7.4

PBS with Ca <sup>2+</sup> , Mg <sup>2+</sup> (PBS-CM)	150 mM	NaCl
	20 mM	Na <sub>3</sub> PO <sub>4</sub> , pH 7.4
	0.2 mM	CaCl <sub>2</sub>
	2 mM	MgCl <sub>2</sub>
RIPA-buffer (cell lysis)	50 mM	Tris-HCl, pH 7.4
	150 mM	NaCl
	1 % (w/v)	NP-40
	1 mM	EDTA
	1x	complete™ proteinase inhibitor cocktail
Running Gel 8.0 % (protein gels)	4.89 ml	deionized water
	5.26 ml	1 M Tris-HCl, pH 8.8
	0.14 ml	10 % SDS
	3.73 ml	30 % Acrylamide – Bis 29:1
	70.0 µl	10 % APS
	7.00 µl	TEMED
SDS sample buffer (5x) (protein gels)	62.5 mM	Tris-HCl, pH 6.8
	2 % (w/v)	SDS
	5 % (w/v)	β-mercaptoethanol
	20 % (v/v)	Glycerol
	0.04 % (w/v)	bromphenolblue
SDS running buffer (10x) (protein gels)	0.25 M	Tris-HCl
	1.90 M	glycine
	1 % (w/v)	SDS
	10 %	methanol, pH 8.3
SSC (20x)	3 M	NaCl
	0.3 M	Na <sub>3</sub> -citrate, pH 7.5
SSPE (20x)	3.6 M	NaCl
	0.2 M	sodium phosphate
	0.02 M	EDTA, pH 7.7
Stacking Gel 5 % (protein gels)	3.77 ml	deionized water
	0.32 ml	1 M Tris-HCl, pH 6.8
	0.05 ml	10 % SDS
	0.83 ml	30 % Acrylamide – Bis 29:1
	25.0 µl	10 % APS
	7.00 µl	TEMED

Stripping buffer	0.5 M	NaCl
(Western blots)	0.5 M	acetic acid
TAE (50x)	2 M	Tris-Acetat, pH 8,0
(DNA-gels)	100 mM	EDTA
TE (10x)	0,1 M	Tris-HCl, pH 8.0
	10 mM	EDTA

### 1.3 Bacterial and cell culture media

Bacterial media were autoclaved and antibiotics were supplemented prior to use. Cell culture media were prepared from a 10x stock solution purchased from Gibco GBL and were sterile filtered.

DMEM (for TE761 cells)	Dulbecco MEM, high glucose (4500 mg/l)	
	supplemented with	
	5 % (v/v)	fetal calf serum (FCS)
	1x	non-essential amino acids
	50 U/ml	penicilline/streptomycine (P/S)
	1 mM	pyruvate
	4 mM	L-glutamine
GMEM (for CHO cells)	Glasgow MEM (with nucleotides; L-glutamine)	
	supplemented with	
	10 % (v/v)	fetal calf serum (FCS)
	1x	non-essential amino acids
	50 U/ml	penicilline/streptomycine
	1 mM	pyruvate
	4 mM	L-glutamine
LB-agar	20 g/l	agar LB-medium
LB-medium	10 g/l	bacto-tryptone
	10 g/l	NaCl
	5 g/l	yeast extract, pH 7.4
Antibiotic- and X-Gal-concentrations	150 mg/l	ampicillin (Amp)
(in medium or agar)	50 mg/l	chloramphenicol (Cm)
	25 mg/l	kanamycin (Kan)
	25 mg/l	X-Gal
Versene	Gibco GBL	

## 1.4 Bacterial strains and cell lines

CHO-K1	<i>Chinese Hamster Ovary</i>
TE671	human fibroblast cell line
<i>Escherichia coli</i> DH5 $\alpha$	F <sup>-</sup> , <i>supE44</i> , <i>DlacU169</i> , [ $\Phi$ 80 <i>lacZDM15</i> ], <i>hsdR17</i> , <i>recA1</i> , <i>endA1</i> , <i>gyrA96</i> , <i>thi-1</i> , <i>relA1</i> , ( <i>res</i> <sup>-</sup> , <i>mod</i> <sup>+</sup> ), <i>deoR</i> ; NEB
<i>Escherichia coli</i> XL1-Blue	<i>recA1</i> , <i>end A1</i> , <i>gyrA96</i> , <i>thi-1</i> , <i>hsdR17</i> , <i>supE44</i> , <i>relA1</i> , <i>lac[F'proAB lac<sup>f</sup>Z<math>\Delta</math>M15Tn10(Tet<sup>r</sup>)]</i> ; Stratagene

## 1.5 Plasmids

pBlueCm SK (+)	cloning vector; <i>lacZ<math>\alpha</math></i> ; Cm-resistance (r) (Stratagene)
pcDNA3	mammalian expression vector; Amp-r (Invitrogen)
pCRuni-3.1uni	mammalian expression vector; Amp-r (Stratagene)
pK19	pUC19, replacement of Amp-r to Km-r, <i>lacZ<math>\alpha</math></i> ; (Pridmore, 1987)
pGEM2	cloning vector; Amp-resistance (Promega)

## 1.6 Antibodies

### 1.6.1 Primary antibodies

mc- $\alpha$ L1-555	monoclonal rat anti-mouse L1 antibody, supernatant of rat hybridoma cell line (produced in the lab of M. Schachner; Appel et al., 1995) immunoblot: 1:8 in 2 % M-PBS immunocytochemistry: undiluted.
pc- $\alpha$ L1-a:	polyclonal rabbit anti-mouse L1 antibody, purified blood serum (Dr. F. Plöger, ZMNH) Immunoblot: 1:8000 in 2 % M-PBS
pc- $\alpha$ L1-b	polyclonal rabbit anti-mouse L1 antibody, purified rabbit blood serum (Fraissner et al., 1985) Immunohistochemistry: 1:500 in PBS

### 1.6.2 Secondary antibodies

All horseradish-coupled secondary antibodies were purchased from dianova and used for immunoblot analysis in a dilution of 1:10,000.

For immunocytochemistry and -histochemistry, Cy3, and FITC -labeled secondary antibodies were obtained from dianova and used in a dilution of 1:500.

## 2 Methods

### 2.1 Molecular biological methods

#### 2.1.1 Maintenance of bacterial strains

(Sambrook et al., 1989)

Strains were stored as glycerol stocks (LB-medium, 25 % (v/v) glycerol) at  $-70^{\circ}\text{C}$ . An aliquot of the stock was streaked on an LB-plate containing the appropriate antibiotics and incubated overnight at  $37^{\circ}\text{C}$ . Plates were stored for up to 6 weeks at  $4^{\circ}\text{C}$ .

#### 2.1.2 Production of competent bacteria

(Inoue et al., 1990)

DH5 $\alpha$  bacteria were streaked on LB-plates and grown overnight at  $37^{\circ}\text{C}$ . 50 ml of LB-medium was inoculated with 5 colonies and grown at  $37^{\circ}\text{C}$  until the culture had reached an optical density ( $\text{OD}_{600}$ ) of 0.3-0.5. Cells were pelleted at 3,000 rpm and  $4^{\circ}\text{C}$  and resuspended in 30 ml cold TFBI-buffer (30 mM KAc, 50 mM  $\text{MnCl}_2 \cdot 4 \text{H}_2\text{O}$ , 100 mM RbCl, 10 mM  $\text{CaCl}_2$ , 15 % glycin, adjusted to pH 5.8 with 0.2 N acetic acid, ad to 500 ml with ddH $_2\text{O}$  and sterile filtered). After incubation for 10 min on ice, cells were pelleted at 3,000 rpm and  $4^{\circ}\text{C}$  for 10 min and resuspended in 4 ml TFBII-buffer (10 mM MOPS, 75 mM  $\text{CaCl}_2$ , 10 mM RbCl, 15 % glycin, adjusted to pH 5.8 with 0.2 N acetic acid, ad to 500 ml with ddH $_2\text{O}$  and sterile filtered). Aliquots of 100  $\mu\text{l}$  were stored at  $-80^{\circ}\text{C}$ .

### 2.1.3 Transformation of bacteria

(Sambrook et al., 1989)

To 100  $\mu$ l of competent DH5 $\alpha$  either 50-100 ng of plasmid DNA or 20  $\mu$ l of ligation mixture were added and incubated for 30 min on ice. After a heat shock (2 min, 42°C) and successive incubation on ice (3 min), 800  $\mu$ l of LB-medium were added to the bacteria and incubated at 37°C for 30 min. Cells were then centrifuged (10,000 x g, 1 min, RT) and the supernatant removed. Cells were resuspended in 100  $\mu$ l LB medium and plated on LB plates containing the appropriate antibiotics. Plates were incubated at 37°C overnight.

### 2.1.4 Plasmid isolation of E. coli

#### 2.1.4.1 Plasmid isolation from 3 ml cultures (Minipreps)

(Sambrook et al., 1989; *Amersham Pharmacia Mini preparation kit*)

3 ml LB/Amp- or /Cm-medium were inoculated with a single colony and incubated over night at 37°C with constant agitation. Cultures were transferred into 2 ml Eppendorf tubes and cells were pelleted by centrifugation (12,000 rpm, 1 min, RT). Plasmids were isolated from the bacteria according to the manufactures protocol. The DNA was eluted from the columns by addition of 50  $\mu$ l Tris-HCl (10 mM, pH 8.0) with subsequent centrifugation (12,000 rpm, 2 min, RT).

#### 2.1.4.2 Plasmid isolation from 15 ml-cultures

(*Macherey-Nagel Nucleospin kit*)

To obtain rapidly higher amounts of DNA, the Macherey-Nagel Nucleospin kit was used. 15 ml LB/Amp- or /Cm-medium were inoculated with a single colony and incubated over night at 37°C with constant agitation. Cultures were transferred into 15 ml Falcon tubes and cells were pelleted by centrifugation (12,000 rpm, 1 min, RT) in a eppendorf centrifuge. Plasmids were isolated from the bacteria according to the manufactures protocol with the exception that twice the suggested amount of buffers were used. DNA was eluted from the columns by adding twice 50  $\mu$ l of prewarmed (65°C) Tris-HCl (10 mM, pH 8.0) with subsequent centrifugation (12,000 rpm, 2 min, RT). Finally, the concentration was determined.

### **2.1.4.3 Plasmid isolation from 500 ml-cultures (Maxipreps)**

(Quiagen Maxiprep kit)

For preparation of large quantities of DNA, the Qiagen Maxiprep kit was used. A single colony was inoculated in 2 ml LB/Amp- or /Cm- medium and grown at 37°C for 8 h with constant agitation. Afterwards, this culture was added to 500 ml LB/amp- or /Cm- medium and the culture was incubated at 37°C with constant agitation overnight. Cells were pelleted in a Beckmann centrifuge (6,000 x g, 15 min, 4°C) and DNA was isolated as described in the manufactures protocol. Finally, the DNA pellet was resuspended in 600 µl of prewarmed (70°C) Tris-HCl (10 mM, pH 8.0) and the DNA concentration was determined.

## **2.1.5 Enzymatic modification of DNA**

### **2.1.5.1 Digestion of DNA**

(Sambrook et al., 1989)

For restriction, the DNA was incubated with twice the recommended amount of appropriate enzymes in the recommended buffer for 2 h. If two enzymes were incompatible with each other, the DNA was digested successively with the enzymes. The DNA was purified between the two digestions using the rapid purification kit (Life technologies). Restriction was terminated by addition of sample buffer and applied on a agarose gel.

### **2.1.5.2 Dephosphorylation of Plasmid-DNA**

(Sambrook et al., 1989)

After restriction, the plasmid DNA was purified and SAP buffer (Boehringer Ingelheim) and 1 U SAP (scrimps alkaline phosphatase) per 100 ng plasmid DNA was added. The reaction was incubated at 37°C for 2 h and terminated by incubation at 70°C for 10 min. The plasmid DNA was used for ligation without further purification.

### **2.1.5.3 Ligation of DNA-fragments**

(Sambrook et al., 1989)

Ligation of DNA fragments was performed by mixing 50 ng vector DNA with the fivefold molar excess of insert DNA. 1  $\mu$ l of T4-ligase and 2  $\mu$ l of ligation buffer (both Boehringer Ingelheim) were added and the reaction mix was brought to a final volume of 20  $\mu$ l. The reaction was incubated either for 2 h at room temperature or overnight at 16°C. The reaction mixture was used directly for transformation without any further purification.

### **2.1.6 DNA Gel-electrophoresis**

(Sambrook et al., 1989)

DNA fragments were separated by horizontal electrophoresis chambers (BioRad) using agarose gels. Agarose gels were prepared by heating 1-2.5 % (w/v) agarose (Gibco) in 1xTAE buffer, depending on the size of DNA fragments. The gel was covered with 1xTAE buffer and the DNA samples were pipetted in the sample pockets. DNA sample buffer was added to the probes and the gel was run at constant voltage (10 V/cm gel length). Afterwards, the gel was stained in an ethidiumbromide staining solution for 20 min. Finally gels were documented using a UV-light imaging system.

### **2.1.7 Extraction of DNA fragments from agarose gels**

(Rapid gel extraction kit, Life technologies)

For isolation and purification of DNA fragments from agarose gels, ethidiumbromide-stained gels were illuminated with UV-light and the appropriate DNA band was excised from the gel with a clean scalpel and transferred into an Eppendorf tube. The fragment was isolated following the manufactures protocol. The fragment was eluted from the column by addition of 50  $\mu$ l prewarmed (70°C) Tris-HCl (10 mM, pH 8.0). The DNA-concentration was determined using the undiluted eluate.

### 2.1.8 Purification of DNA fragments

(Rapid PCR Purification kit, Life technologies)

For purification of DNA fragments the Rapid PCR Purification kit was used according to the manufactures protocol. The DNA was eluted from the column by addition of 50  $\mu$ l prewarmed (70°C) Tris-HCl (10 mM, pH 8.0). The DNA-concentration was determined using the undiluted eluate.

### 2.1.9 Determination of DNA concentrations

DNA concentrations were determined spectroscopically using an Amersham-Pharmacia spectrometer. The absolute volume necessary for measurement was 50  $\mu$ l. For determining the concentration of DNA preparations, the eluate was diluted 1:50 with water and the solution was pipetted into a 50  $\mu$ l cuvette. Concentration was determined by measuring the absorbance at 260 nm, 280 nm and 320 nm. Absorbance at 260 nm had to be higher than 0.1 but less than 0.6 for reliable determinations. A ratio of  $A_{260}/A_{280}$  between 1,8 and 2 monitored a sufficient purity of the DNA preparation.

### 2.1.10 DNA Sequencing

(Step-by-Step protocols for DNA-sequencing with Sequenase-Version 2.0, 5<sup>th</sup> ed., USB, 1990)

DNA sequencing was performed by the sequencing facility of the ZMNH. For preparation, 1  $\mu$ g of DNA was diluted in 7  $\mu$ l ddH<sub>2</sub>O and 1  $\mu$ l of the appropriate sequencing primer (10 pM) was added.

### 2.1.11 Mutagenesis via PCR

(*Seamless® PCR cloning Kit*; Stratagene)

For investigation of different mutated L1 variants in cell culture and for generation of the L1C264Y mouse line, the Seamless PCR cloning Kit (Stratagene) was used to delete several nucleotides or to exchange a single base pair within the mouse L1cDNA. This kit allows cloning of large DNA fragments without introducing

additional restriction sites by combination of higher-fidelity PCR (*Pfu* DNA polymerase) with the activity of the type IIS restriction endonuclease Eam 1104 I that cleaves at a defined distance downstream of its recognition sequence. For detailed information, see the manufactures instruction.

In brief, the whole vector pGEM2-L1 (mouse L1cDNA cloned into the EcoRI site of pGEM2) was amplified using primers designed such that:

1. they contain 4 variable bases followed by the recognition side for Eam1160I and one additional variable base at the 5' end,
2. the following bases directly flanks the region for deletion or contain the desired mutation with at least 20 bases homologue to the sequence at the 3' end.

The reaction mixture was prepared as followed with 4 different primer sets:

template (pGEM2-L1)	20 ng
Mutation-Primer 1 (10 pM)	100 ng
Mutation-Primer 2 (10 pM)	100 ng
nucleotides (dNTPs, 40 mM)	1 $\mu$ l
10x <i>pfu</i> -polymerase buffer	5 $\mu$ l
cloned <i>pfu</i> -DNA-polymerase	1 $\mu$ l (2.5 U)
ddH <sub>2</sub> O	ad 50 $\mu$ l

The following step gradient was applied for mutagenesis:

cycle 1:	1) Denaturing	95°C	3 min
	2) Annealing	63°C	1 min
	3) Synthesis	72°C	13.5 min
cycle 2-10 and 11-15:	1) Denaturing	95°C	45 sec
	2) Annealing	63°C	35 sec
	3) Synthesis	72°C	13.5 min

After the 10<sup>th</sup> PCR-cycle, to the reaction mixture were added:

5-methyl dCTP, dA/T/GTPmix (40mM)	1 $\mu$ l
10x <i>pfu</i> -polymerase buffer	5 $\mu$ l
ddH <sub>2</sub> O	44 $\mu$ l

The introduction of 5-methyl dCTP during the last 5 PCR-cycles protects internal Eam 1104I recognition sites of the amplified DNA from cleavage with Eam 1104I,

whereas the Eam 1104I restriction sites contained in the primers stay Eam 1104I sensitive.

The PCR-product was purified and digested with Eam 1104I in the following digestion mixture for 1 h at 37°C:

PCR-product	0.7 µg
10x universal buffer	5 µl
Eam 1104I	4 µl
ddH <sub>2</sub> O	ad 50 µl

The Eam 1104I digested DNA-fragment was ligated in the following mixture for 30 min at 37°C:

digestion mixture	6 µl
10x ligase buffer	2 µl
T4-DNA-ligase (1:16)	1 µl
Eam 1104I	1 µl
10 mM ATP	2 µl
ddH <sub>2</sub> O	8 µl

Afterwards, the ligation reaction was transformed into XL1-Blue MRF<sup>+</sup> supercompetent cells (strain that accepts methylated DNA) as described. Single colonies were picked from the plate and inoculated into 3 ml cultures. Plasmid DNA was prepared and mutation was verified by restriction analysis. The L1cDNA was sequenced to exclude introductions of undesired mutations during PCR.

For expression in cell culture the mutated L1cDNAs were cloned into the eucaryotic expression vector pcDNA3 via EcoRI.

## **2.1.12 Generation of the L1C264Y transgenic mouse line**

### **2.1.12.1 Construction and preparation of the transgene**

The L1lacZ vector, containing the L1 promoter, a lacZ gene and the NRSE sequence (kind gift of P. Kallunki; Kallunki et al., 1997 and 1998; Meech et al., 1997) was modified to generate a mouse line, expressing the pathogenic missense mutation L1C264Y under the control of the L1 promoter. An EcoRI-PvuI-fragment of the pcDNA3-L1C264Y containing the mouse L1cDNA with the C264Y

mutation was initially cloned into the EcoRI-opened vector pBlueCAM-SK(+). The lacZ gene was removed from vector L1lacZ by digestion with NotI and XhoI and replaced with L1C264Y.

The 22 kb-transgenic construct was excised from the plasmid by digestion with PvuI and SnaBI and separated by gel-electrophoresis. The DNA was extracted from the gel by electroelution. Therefore the excised gel was placed into a dialysis tube with 2 ml TAE which then was laid in a horizontal electrophoresis chamber (BioRad). The tube was covered with 1x TAE buffer and fixed with a glass plate and run at constant voltage of 75 V for 120 min. The DNA in the TAE of the tube was precipitated and washed with ethanol.

#### **2.1.12.2 Microinjection of the transgenic construct into zygotes**

The linear 22 kb-transgenic fragment was microinjected into DBA-C57BL/6J-hybrid zygotes and transplanted into pseudopregnant nurse females using standard techniques (Hogan et al., 1994). The microinjections were done in the service facility of the ZMBH in Heidelberg. Founder mice were identified by PCR and Southern Blot analysis.

#### **2.1.12.3 Breeding of mice**

To verify the expression of each founder line at the protein level, the F1 generation of five founders was crossed with heterozygous L1 knock-out (L1ko) females (Dahme et al., 1997) to obtain double mutants. For all further investigations transgenic males of two founder lines were mated with heterozygous L1 knock-in (L1ki) females (L1-deficient mice, generated by insertion of thymidine kinase and neomycine-resistance genes into the ninth exon of the L1 gene; 129/SvJ-F6; Rolf et al., 2001). Heterozygous L1ki and transgenic females were also crossed with 129/SvJ wt males. Animals from the second to fifth generation of such crosses were used for analysis.

### 2.1.13 Methods for genotyping of mice

#### 2.1.13.1 Preparation of genomic DNA for genotyping by PCR and Southern Blot

About 3 mm of tail segments were incubated overnight in 250-300  $\mu$ l Boston buffer (supplemented with 150  $\mu$ g/ml proteinase K) at 56°C. After centrifugation (5 min, 14,000 rpm) a 1  $\mu$ l probe of the supernatant was used as template for PCR.

For Southern Blot analysis the genomic DNA was purified by chloroform extraction. 1/6 vol 8 M potassium acetate and 1 vol chloroform was added to the lysated tail cut sample and incubated 30 min on ice. After centrifugation (13,000 x g, 5 min) the DNA in the upper phase was precipitated by adding 1 ml ethanol (absolute) and pelleted by centrifugation (13,000 x g, 10 min). The DNA was washed with ethanol (absolute, -20 °C) and 70 % ethanol (-20 °C) and resolved in 100  $\mu$ l Tris-HCl, pH 7.0. The purified genomic DNA was digested with BamHI.

#### 2.1.13.2 Genotyping by PCR

For the genotyping of mice from crosses of heterozygous L1 knock out (L1ko; Dahme et al., 1997) with L1C264Y transgenic males two different multiplex PCRs (PCR-L1ko and PCR-L1tg) were used to identify the L1ko allele and the L1C264Y transgene, respectively, in addition to the endogenous L1wt allele as an internal control. The following reaction mixtures were used (for step gradient see PCR-L1tg-ki below):

<u>PCR-L1ko:</u>		<u>PCR-L1tg :</u>	
template	1 $\mu$ l	template	1 $\mu$ l
Primer L1-A'	1.5 $\mu$ l	Primer L1-292	1 $\mu$ l
Primer L1-D	1.5 $\mu$ l	Primer L1-709	1 $\mu$ l
Primer L1-C	3 $\mu$ l	Primer L1-C	4 $\mu$ l
dNTPs (20 mM)	1 $\mu$ l	Primer L1-D	4 $\mu$ l
10x PCR buffer	3 $\mu$ l	dNTPs (20mM)	1 $\mu$ l
MgCl <sub>2</sub> (50 mM)	1.5 $\mu$ l	10x PCR buffer	5 $\mu$ l
Taq-polymerase	1 $\mu$ l	MgCl <sub>2</sub> (50 nM)	2 $\mu$ l
ddH <sub>2</sub> O	ad 30 $\mu$ l	Taq-polymerase	1 $\mu$ l
		ddH <sub>2</sub> O	ad 50 $\mu$ l

For genotyping of animal obtained from crosses of parents with a L1 knock-in allele (Rolf et al., 2001) and the L1C264Y transgene, a multiplex PCR was established (PCR-L1ki-tg) to identify the L1 knock-in allele the L1C264Y-transgene as well as the endogenous L1 gene(s) as an internal control. The following mixture and step gradient was used:

<u>PCR-L1ki-tg :</u>		Step gradient (for all PCR-genotypings):	
template	1 $\mu$ l	1) Initial denaturing	95°C 2 min
Primer L1-ki	1 $\mu$ l	cycles 1-30:	
Primer L1-arm	1 $\mu$ l	2) Denaturing	95°C 45 sec
Primer L1 5'up	4 $\mu$ l	3) Annealing	68°C 1.5 min
dNTPs (20mM)	1 $\mu$ l	4) Synthesis	72°C 1.5 min
10x PCR buffer	3 $\mu$ l	5) Termination	72°C 10 min
MgCl <sub>2</sub> (50 nM)	1.5 $\mu$ l	6) Cooling	4°C
<i>Taq</i> -polymerase	1 $\mu$ l		
ddH <sub>2</sub> O	ad 50 $\mu$ l		

#### 2.1.14 Southern Blot analysis

For identification of founder animals, in which the L1C264Y transgene has integrated into the genome, Southern Blot analysis were performed in addition to a genotyping by PCR.

##### 2.1.14.1 PCR-amplification and labeling of probe

A 550 bp-probe which binds exclusively to the L1 transgenic construct was amplified by PCR for Southern Blot analysis. The following mixture was prepared:

Primer SBtgL1-A	4 $\mu$ l
Primer SBtgL1-B	4 $\mu$ l
dNTP (25 mM)	1.5 $\mu$ l
10x PCR-buffer	5 $\mu$ l
MgCl <sub>2</sub> (50 mM)	3 $\mu$ l
<i>Taq</i> -polymerase	1 $\mu$ l
ddH <sub>2</sub> O	ad 50 $\mu$ l

Amplification was performed in a MWG-PCR cycler with the following step

gradient:	1) Initial denaturing	95°C	4 min
cycle 1-30:	2) Denaturing	95°C	1 min
	3) Annealing	55°C	1 min
	4) Synthesis	72°C	1 min
	5) Termination	72°C	5 min
	6) Cooling	4°C	

The probe was isolated and purified by gel-electrophoresis and gel-extraction. The radioactive labeling was performed in accordance to Sambrook et al. (1989).

#### **2.1.14.2 Gel-electrophoresis and Vacuum-Transfer**

The BamHI-digested genomic DNA was subjected to gel-electrophoresis (1 % agarose, 24 cm in length). The gel was denatured in 2 % HCl for 25 min, washed with dH<sub>2</sub>O, and neutralized in 0.4 M NaOH. The DNA was transferred from the gel on a nitrocellulose membrane (Hybond N Plus) using a Vacuum-Blot-apparatus (BioRad). The blotting sandwich was assembled as described in the manufactures protocol. DNA was transferred by applying a vacuum of 300-350 mbar for 90 min.

#### **2.1.14.3 Radioactive detection of DNA on nitrocellulose membrane**

The nitrocellulose membrane was incubated in prehybridization buffer (5x Denhardtts, 5x SSPE, 0.5 % SDS) over night at 65 °C in a rotator, followed by an incubation in hybridization mix (5x Denhardtts, 5x SSPE, 0.5 % SDS) over night at 65 °C. The membrane was washed two times for 30 min in 2x SSC containing 0.1 % SDS, one time with 1x SSC containing 0.1 % SDS and finally two times by 0.1x SSC containing 0.1 % SDS. The membrane was exposed to X-ray film (Biomax-MR, Kodak) for 3 days.

## 2.2 Protein-biochemical methods

### 2.2.1 SDS-poly-acrylamide gel electrophoresis

(Laemmli, 1970)

Separation of proteins was performed by means of the discontinuous SDS-polyacrylamide gel electrophoresis (SDS-PAGE) using the Mini-Protean III system (Bio-Rad). The size of the running and stacking gels were as follows:

Running gel: height 4.5 cm, thickness 1 mm

8 % acrylamide solution

Stacking gel: height 0.8 cm, thickness 1 mm

5 % (v/v) acrylamide solution

15-well combs

After complete polymerization of the gel, the chamber was assembled as described by the manufactures protocol. Up to 25  $\mu$ l sample were loaded in the pockets and the gel was run at constant voltage at 80 V for 10 min and then for the remaining time at 140V. The gel run was stopped when the bromphenolblue line has passed the end of the gel. Gels were then either stained or subjected to Western blotting.

### 2.2.2 Western Blot-analysis

#### 2.2.2.1 Electrophoretic transfer

(Towbin et al., 1979)

Proteins were transferred from the SDS-gel on a nitrocellulose membrane (Protran Nitrocellulose BA 85, 0.45  $\mu$ m, Schleicher & Schüll) using a MINI TRANSBLOT-apparatus (BioRad). After equilibration of the SDS-PAGE in blot buffer for 5 min, the blotting sandwich was assembled as described in the manufactures protocol. Proteins were transferred electrophoretically at 4°C in blot buffer at constant voltage (70 V for 150 min or 35 V overnight). The prestained marker BenchMark™ (Gibco BRL) was used as a molecular weight marker and to monitor electrophoretic transfer.

### **2.2.2.2 Immunological detection of proteins on Nitrocellulose membranes**

(Ausubel, 1996)

After electrophoretic transfer, the membranes were placed protein-binding side up in glass vessels. Membranes were incubated in 8 ml blocking buffer for 1.5 h at room temperature. Afterwards, the primary antibody was added in the appropriate dilution overnight at 4°C. The primary antibody was removed by washing the membrane 5 x 5 min with PBS-0.05 % Tween. The appropriate secondary antibody was applied for 2 h at RT. The membrane was washed again 5 x 5 min with PBS-0.05 % Tween and immunoreactive bands were visualized using the enhanced chemiluminescence detection system (Pierce). The membrane was soaked for 1 min in detection solution (1:1 mixture of solutions I and II). The solution was removed and the blot was placed between two saran warp foils. The membrane was exposed to X-ray film (Biomax-MR, Kodak) for diverse time periods.

### **2.2.2.3 Densitometric evaluation of band intensity**

Band densities were quantified using the image processing software *Scion Image* (Scion Corporation, Frederick, MD, USA). The developed film was scanned and the digitized picture was exported to *Scion Image*. Band densities were evaluated using the “Gelplot2”-macro according to the manual.

### **2.2.3 Lysis of CHO-cells**

After maintenance of CHO cells in 35 mm-culture dishes, the medium was removed and cells were lysed in 400 µl RIPA buffer per 35 mm well with constant agitation (1 h, 4°C). Cells were scraped of the wells and transferred into a 1.5 ml Eppendorf tube. Debris was removed by centrifugation (15,000 x g, 4°C, 10 min) and the supernatant was stored at -20°C.

#### **2.2.4 Preparation of crude brain homogenates**

The brains of embryonic (17.5-day-old, n = 2 per genotype) or adult (3-month-old, n = 2 per genotype) mice were homogenized in 300  $\mu$ l or 1 ml lysis buffer LB2 (20 mM Tris-HCl, pH 7.5, 150 mM NaCl, 1 mM EDTA, 1 mM EGTA, 1% NP-40, 1x COMPLETE protease inhibitor cocktail), respectively, with a potter (Kinematica, Luzern) and incubated for 30 min at 4°. The homogenates were cleared by centrifugation three times at 12,000 x g for 20 min at 4°C.

#### **2.2.5 Fractioned preparation of brain homogenates**

The brains of 12 129SvEv mice of the 5<sup>th</sup> postnatal day were homogenized in 5 ml lysis buffer LB1 (20 mM Tris-HCl, pH 7.5, 150 mM NaCl, 1 mM EDTA, 1 mM EGTA, 1x COMPLETE protease inhibitor cocktail). The cell nuclei were pelleted at 1000 x g for 10 min at 4°C and resuspended in 2.9 ml LB1. To further purify the nuclei fraction, the centrifugation step was repeated three times and it was finally solubilized in 3 ml LB2 (LB1 containing 1% NP-40). The collected and united supernatants were ultra-centrifuged at 100,000 x g for 1 h at 4°C. The pellet was washed three times with LB1 and washing steps were performed in a head-over-roller for 20 min at 4°C. The collected supernatants represented the cytosolic fraction. The pellet was solubilized over night in 3.6 ml LB2. After centrifugation at 100,000 x g for 1 h at 4°C the supernatant containing the membrane fraction was separated from the pellet. The pellet was washed three times for 20 min in LB2 and finally resuspended in 2 ml LB3 (12.5 mM Tris-HCl, pH 7.5, 0.4 % SDS, 1x COMPLETE protease inhibitor cocktail) and solubilized at 95°C for 1 h. After a final centrifugation at 20,000 x g for 15 min at RT the supernatant contained cytoskeletal proteins.

#### **2.2.6 Endoglycosidase H digestion of CHO cell lysates and brain homogenates**

Cell lysates or brain homogenates were diluted with 2x citrate buffer (75 mM sodium-citrate, pH 5.5) and after addition of 0.1 U endoglycosidase H (endo H, Roche Diagnostics) lysates were incubated at 37°C overnight. Controls were

treated identically without addition of endo H. Lysates were subjected to SDS-PAGE and probed with mc-anti-L1-555 or pc-anti-L1-b.

### **2.2.7 Determination of protein concentration (BCA)**

(Ausrubel, 1996)

The protein concentration of cell lysates or brain homogenates was determined using the BCA kit (Pierce). For preparation of the BCA solution, solution A and B were mixed in a ratio of 1:50. 20  $\mu$ l of the cell lysate were mixed with 200  $\mu$ l BCA solution in microtiter plates and incubated for 30 min at 37°C. A BSA standard curve was co-incubated ranging from 100  $\mu$ g/ml to 2 mg/ml. The extinction of the samples was determined at 568 nm in a microtiter plate reader.

## **2.3 Cell culture**

### **2.3.1 CHO and TE671 cell culture**

CHO and TE671 cells were either cultured in GMEM or DMEM, respectively, at 37°C, 5 % CO<sub>2</sub> and 90 % relative humidity in 80 cm<sup>2</sup> flasks (Nunc) with 15 ml medium or in six-well plates (d = 35 mm; area = 9,69 cm<sup>2</sup>) with 2 ml medium. Cells were passaged when they were confluent (usually after 3-4 days). Medium was removed and cells were detached by incubation with 4 ml versene for 5 min at 37°C. Cells were centrifuged (200 x g, 5 min, RT) and the pellet was resuspended in 10 ml fresh medium. Cells were split 1:10 for maintenance or seeded in six-well plates for transfection (300  $\mu$ l per well).

For immunocytochemistry, cells were seeded on poly-L-lysine coated coverslips (d = 14 mm). Coverslips were first cleaned by extensive washing with acetone and then air-dried. Coverslips were coated with poly-L-lysine by constant agitation at 4°C overnight in a poly-L-lysine solution (50  $\mu$ g/ml in PBS). Finally, they were washed twice with ddH<sub>2</sub>O and dried under a sterile hood. Two coverslips were placed per 35 mm dish and cells were seeded with a density of 30 % confluency 24 h before use.

### 2.3.2 Transient transfection of CHO and TE671 cells

*(Lipofectamine Plus manual, Life technologies)*

For transfection of CHO or TE671 cells, the Lipofectamine Plus kit (Life Technologies) was used and performed as described in the manufactures protocol. One day before transfection,  $2 \times 10^5$  cells were seeded per 35 mm dish. When cell density had reached 80-90 % (usually after 18-24 h) the cells were washed with GMEM/DMEM Ø FCS and antibiotics and transfected with 2 µg total DNA per 35 mm well. 6 µl Plus reagent and 4 µl Lipofectamine were used per well. Transfection was terminated after 3 h by addition of an equal volume of GMEM/DMEM with 20 % FCS, 2 % P/S. 18 h after transfection, cells were detached with 500 µl versene per well and splitted for biochemical analysis and/or splitted on coverslips for immunocytochemistry.

### 2.3.3 Stable transfection of CHO cells

The transfection was carried out as described (see above). To obtain clonal transfected cells, constructs of the pcDNA3 vector containing different mutated L1 or L1wt cDNA were transfected. The pcDNA3 vector encodes a geneticin (G418; Life Technologies) resistance. 24 h after transfection the cells were passaged into two 90 mm wells and maintained in selection medium (DMEM, 10 % FCS) containing 800 µg/µl G418 and the medium was exchanged every second day to remove dead cells. After two weeks of selection single colonies have grown and were isolated. Cells were washed two times with HBSS and sterile cloning rings covered with silicon fat at the bottom were placed on single clones. The cells within the ring were detached with 10 µl versene for 5 min, resuspended after adding 60 µl GMEM-10 % FCS, and plated in 12 mm wells. The cell clones were cultivated until they had grown to confluency in a 80 cm<sup>2</sup> flasks (4<sup>th</sup> passage, after 3 weeks). From now on, the cells were maintained in DMEM-10 % FCS containing 300 µg/ml G418 and aliquots of the clones were frozen from the 5<sup>th</sup> to the 9<sup>th</sup> passage.

### **2.3.4 Surface biotinylation of transfected CHO cells**

Surface biotinylation were essentially carried out as described by Schmidt et al. (1997). In brief, 48 or 72 h after transfection, cells were washed twice with ice-cold PBS-CM. Surface proteins were biotinylated by incubating cells with 0.5 mg/ml Sulfo-NHS-SS-biotin (Pierce, Rockford, IL, USA) in PBS-CM for 10 min at 4°C. Biotinylation was terminated by incubation with 20 mM glycine in PBS-CM at 4°C for 10 min followed by extensive washing with PBS-CM. Biotinylated cells were then lysed directly in RIPA-buffer. The biotinylated proteins were precipitated with streptavidin-coupled agarose beads (Pierce) at 4°C overnight. Agarose beads were pelleted by centrifugation and washed twice with RIPA-buffer. Precipitated proteins were solubilized by addition of 5x SDS-sample buffer to the agarose beads. Proteins were separated by SDS-PAGE and proteins were quantified by immunoblot analysis using mc-anti-L1-555.

## **2.4 Immunocytochemistry**

### **2.4.1 Immunocytochemistry of living cells**

Coverslips with the attached cells were washed with PBS-5 % FCS and placed on parafilm (American National Can, Menasha, WI, USA) in a humid chamber. 80 µl of mc-αL1-555 were added on the coverslips and incubated at 4°C for 30 min. Coverslips were put into 12-well dishes and washed three times with PBS-5 % FCS. Then coverslips were put on parafilm again, covered with 80 µl PBS-5 % FCS containing the fluorescent dye-coupled secondary antibody in a 1:200 dilution, and incubated at 4°C for 20 min in the dark. Finally, coverslips were washed twice with PBS-5 % FCS, fixed with 4 % PA in PBS, washed with PBS and mounted on slides with Aqua Poly-Mount medium (Polysciences Inc).

### **2.4.2 Immunocytochemistry of fixed cells**

The medium was removed from the coverslips and cells were fixed with 1 ml of 4 % PA in PBS for 15 min at 4°C and washed twice with PBS. Coverslips were placed on parafilm in a humid chamber and incubated with 80 µl 1 % BSA in PBS

for 1 h at RT. The blocking buffer was removed by aspiration and the coverslips were covered and incubated with 80  $\mu$ l of mc- $\alpha$ L1 555 overnight at 4°C in a humid chamber. Coverslips were washed three times with 0.1 % BSA in PBS and incubated with 100  $\mu$ l antibody solution containing the fluorescent dye-labeled secondary antibody (Cy3, Cy5, FITC) for 1 h at room temperature in the dark. Finally, cells were washed three times with PBS and mounted on objectives with Aqua Poly-Mount medium (Polysciences Inc).

### **2.4.3 FACS (fluorescence activated cell sorting)**

Confluent stably transfected cells in a 80 cm<sup>2</sup> flask were washed with HBSS, detached with versene, and resuspended in 1 ml buffer (5 % FCS in PBS). After centrifugation (300 rpm) the cells were incubated with undiluted mc- $\alpha$ L1 555 for 30 min at 4°C. Cells were washed twice in 5 ml buffer and incubated with goat anti-rat IgG conjugated with Cy2 (1:300 in buffer) for 20 min at 4°C. After washing three times with 1 ml buffer, cells were fixed in 2 % PA for 5 min and washed again in PBS. Finally the cells were resuspended in PBS. Flow cytometric analysis was performed using a FACSCalibur System according to the manufactures protocol (Becton Dickinson, Heidelberg, Germany).

## **2.5 Morphological methods**

### **2.5.1 Immunostaining of Tissue Sections**

4-week- and 10-week-old animals were deeply anaesthetized by an intraperitoneal injection of 4  $\mu$ l narcorene per g body weight and perfused through the left heart ventricle with 4 % PA in PBS for 20 min. The brains were prepared and post-fixed over night in the same fixative. Vibratome sections, 25-30  $\mu$ m in thickness, were blocked in PBS containing 1% BSA and 0.5% Triton X-100 for 1.5 h, and incubated overnight at 4°C with polyclonal L1 antibodies. After washing 5 times with PBS containing 0.1 % BSA, primary antibodies were visualized with Cy3-conjugated secondary antibodies. The sections were washed 3 times with PBS and analyzed using an Axiophot (Zeiss).

### 2.5.2 Light and electron microscopy

70- to 75-day-old mice were deeply anaesthetized with 4  $\mu$ l narcorene per g body weight and perfused with 4 % PA and 3 % glutaraldehyde in PBS for 40 min. Brains and sciatic nerves were prepared and post-fixed for 2 to 4 weeks. Frontal vibratome sections of the brainstem, 400  $\mu$ m in thickness, and whole sciatic nerves were immersed in 2% OsO<sub>4</sub> for 2 h, dehydrated in an ascending series of methanol and embedded in Epon resin.

For light microscopic analysis of the corticospinal tract (CST), semithin sections, 4  $\mu$ m in thickness, were prepared from caudal levels of the medulla and stained with 0.1 % toluidine blue and 0.1 % methylene blue in 4 % Na<sub>2</sub>CO<sub>3</sub> in H<sub>2</sub>O. The area of the CST was measured at caudal levels of the medulla immediately rostral to the pyramidal decussation using a computer-assisted image analysis system (NeuroLucida, MicroBrightfield, Colchester, UK).

For electron microscopic analysis of the peripheral nervous system, ultrathin sections were prepared from sciatic nerves and counterstained with lead citrate. Micrographs from randomly selected unmyelinated fibers were taken at a magnification of 8,000 x with a Zeiss EM10 electron microscope. For each animal 25–35 unmyelinated fibers were quantified.

### 2.5.3 Tracing of the corticospinal tract

Three injections of the lipophilic fluorescent dye 1,1'-dioctadecyl-3,3,3',3'-tetramethylindocarbocyanine perchlorate (DiI, dissolved in dimethylformamide (Sigma, Deisenhofen, Germany) were made unilaterally into the motor cortex of deeply anaesthetized mice at postnatal day one or two with a multi-channel picospritzer (General Valve, Fairfield, NJ, USA). After 1–2 days (at P3–4), brains were removed and immersion-fixed in PBS, pH 7.4 containing 4 % PA for 3–5 days. Frontal vibratome sections, 50  $\mu$ m in thickness, were prepared starting at rostral levels of the medulla and ending at cervical levels of the spinal cord. Only animals with unilateral tracing of corticospinal axons were analyzed.

## III Results

### 1 Part I: Cell culture experiments

#### 1.1 Mutagenesis of mouse L1cDNA

Five different mutant variants of murine L1cDNA were constructed (Fig. 6): L1 lacking exon 2 ( $\Delta E2$ ; deletion of bp 77–91) or exon 27 ( $\Delta E27$ ; deletion of bp 3540–3551), or both (sL1); L1 lacking the putative homophilic binding side of 14 amino acids from residue His177 to Gly190 (L1 $\Delta$ hbs; deletion of bp 529–570; Zhao et al., 1998), and L1 with the pathogenic missense mutation C264Y (L1C264Y; G to A substitution of bp 788, Jouet et al., 1993). In addition, a L1 construct containing the extracellular, transmembrane and the first nine amino acids of the intracellular domain (aa 1–1152) in fusion with a HA-tag (kind gift of P. Kallunki) was used.

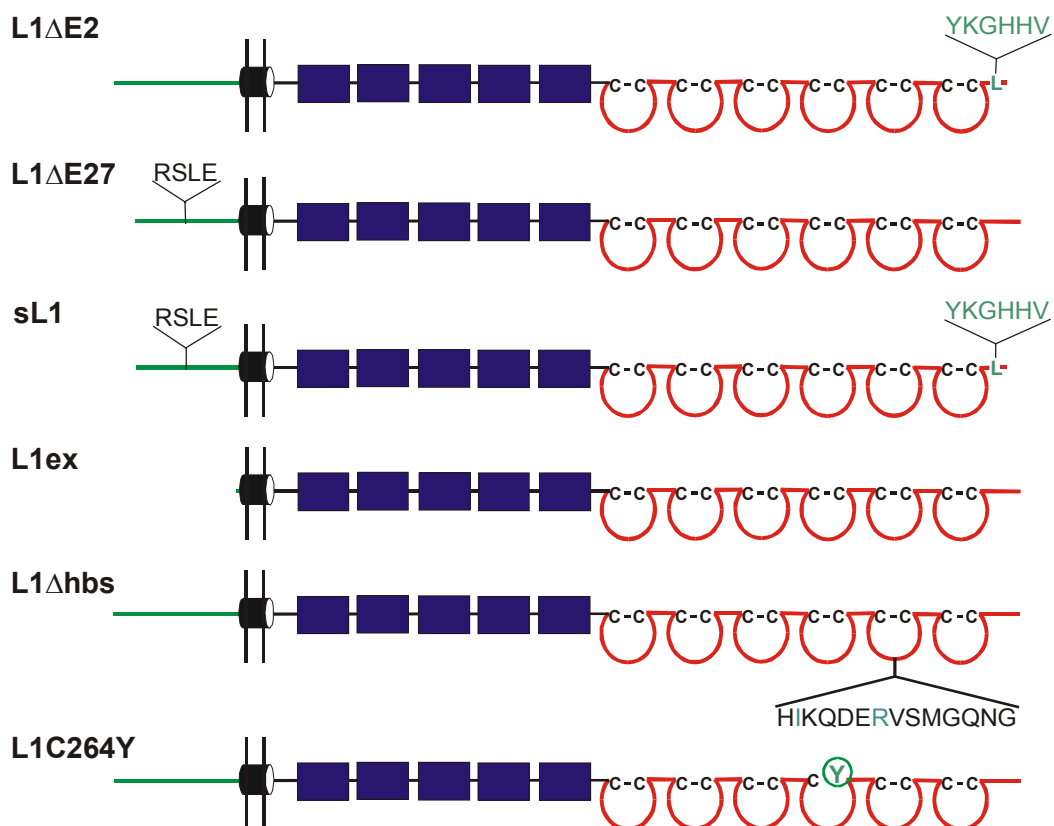


**Figure 6: Location and type of mutations in L1 variants investigated in cell culture experiments.** Deletion of amino acids are indicated by Y-shaped lines; the single amino acid exchange (C264Y) is marked by a circle. Affected amino acid residues with pathological relevance are shown in green.

## 1.2 Cell surface expression of L1 $\Delta$ hbs and L1C264Y is strongly reduced

The localization of L1wt, sL1, L1 $\Delta$ E2, L1 $\Delta$ E27, L1ex, L1 $\Delta$ hbs, and L1C264Y on the surface of CHO cells was investigated by immunostaining of live cells 36, 48 and 72 h after transfection with the different constructs (Fig. 7: 36 h). A high percentage of L1 immunopositive cells (about 70-80 %) was found in cultures 36 h after transfection with L1wt, L1 $\Delta$ E27, and L1ex. Cultures transfected with L1 $\Delta$ E2 and sL1 contained slightly fewer immunoreactive cells (40-60 %). In contrast, the percentage of L1-immunopositive CHO cells expressing L1 $\Delta$ hbs and L1C264Y was very low (about 10-20 %), particularly for L1C264Y-transfected cultures. The variability in labeling intensities of L1wt-, sL1-, L1 $\Delta$ E2-, L1 $\Delta$ E27-, and L1ex-transfected cells was very broad, ranging from weakly to intensely stained cells. In comparison, only strongly labeled cells were found in cultures transfected with L1 $\Delta$ hbs and L1C264Y.

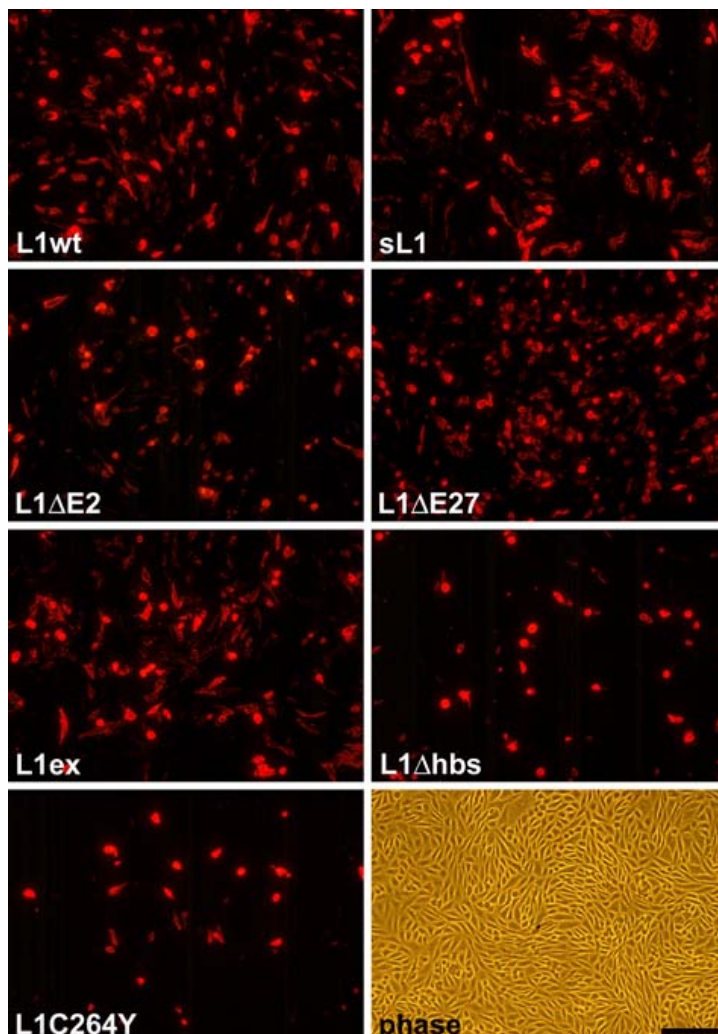


**Figure 7: L1 immunocytochemistry of live CHO cells 36 h after transient transfection with L1wt and mutated L1 (as indicated).** The majority of cells in cultures transfected with L1wt, sL1, L1 $\Delta$ E2, L1 $\Delta$ E27, and L1ex is L1 immunoreactive. In contrast, only a few L1-positive cells are detectable in cultures transfected with L1 $\Delta$ hbs or L1C264Y. phase: Representative phase contrast photomicrograph of a culture transfected with L1C264Y. Bar in phase (for all images): 100  $\mu$ m.

L1 immunostainings 48 and 72 h post-transfection showed an even stronger decrease in the number of L1 $\Delta$ hbs- and L1C264Y-immunopositive cells when compared to cultures transfected with L1wt, L1 $\Delta$ E2, L1 $\Delta$ E27, sL1 or L1ex (data not shown). In fact, in L1C264Y-transfected cultures, labeled cells were virtually absent 72 h after transfection. The number of sL1- and L1 $\Delta$ E2-transfected cells with cell surface expression of L1 did not decrease in relation to L1wt. Similar results were obtained from TE671 cells transfected with the different L1cDNA constructs.

For analysis of long-term expression, CHO cells were stably transfected with L1wt, L1 $\Delta$ E2, L1 $\Delta$ E27, L1ex, L1 $\Delta$ hbs, and L1C264Y. For each construct, six clones were stained as live cells with anti-L1 antibodies and analyzed by FACS to determine the number of positive cells. The percentage of L1-positive cells in the clonal cultures was estimated for all L1 mutations and related to L1wt (set to  $100 \pm 9.7$  %; Fig. 8). The percentage of cells expressing L1ex ( $88.6 \pm 30.0$  %) or L1 $\Delta$ E27 ( $92.5 \pm 31.6$  %) on their surface was similar to that of L1wt cells. In contrast, only 9.5 % ( $\pm 6.7$  %) of cells were labeled in L1 $\Delta$ hbs-transfected cultures. The percentage of positive cells in L1C264Y-transfected cultures ( $3.5 \pm 1.3$  %) was in

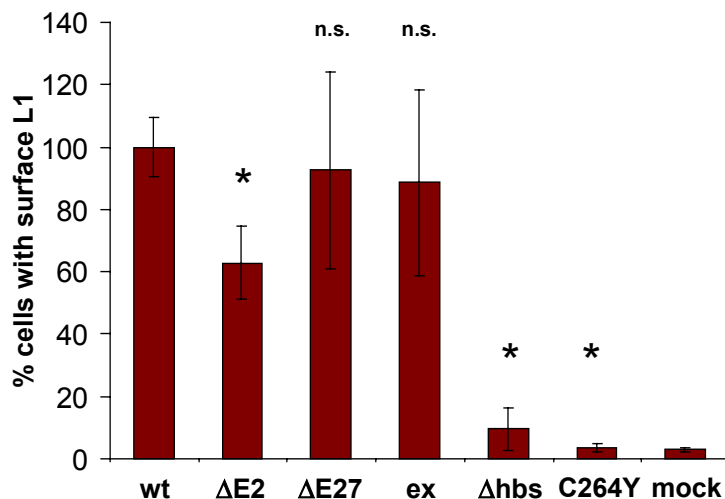


**Figure 8: The percentage of CHO cells with cell surface expression of L1 after stable transfection with different L1 constructs.** CHO cells were stably transfected with L1wt, L1 $\Delta$ E2, L1 $\Delta$ E27, L1ex, L1 $\Delta$ hbs, and L1C264Y and the percentage of cells expressing L1 on their surface was determined using FACS analysis (the percentage of L1-immunoreactive cells in cultures transfected with L1wt

was set to 100 %). A similar percentage of cells with surface expression of L1 is present in cultures transfected with L1wt, L1 $\Delta$ E27, and L1ex. In comparison, L1-positive cells are hardly detectable in cultures transfected with L1 $\Delta$ hbs or L1C264Y. The number of positive cells transfected with L1 $\Delta$ E2 is significantly reduced. Mock-transfected CHO cells served as a negative control. Bars represent mean values  $\pm$  SD of six independent experiments for each construct. n.s.: not significantly different from L1wt; \*: significantly different from L1wt ( $p < 0.01$ ; Mann-Whitney-test).

the range of mock-transfected cells ( $3.0 \pm 0.8$  %). A substantial but in comparison to L1wt significantly reduced percentage amount of L1 $\Delta$ E2-transfected cells showed L1 surface staining. These findings confirm the qualitative data obtained by immunostaining of transiently transfected cells (see above).

The percentage of L1-immunoreactive cells in L1 $\Delta$ hbs- or L1C264Y-transfected cultures was significantly increased when cells were permeabilized prior to immunostaining (data not shown). This observation argues against the possibility that the low number of L1 $\Delta$ hbs- or L1C264Y-transfected cells with surface expression is due to low expression levels or poor transfection efficiency.

### **1.3 L1 $\Delta$ hbs and L1C264Y are expressed as a protein variant with a reduced molecular weight of 190 kD**

To further analyze the expression levels and post-translational modifications of the different L1 mutations, CHO cells were subjected to immunoblot analysis (Fig. 9; 10 B and D). At all time points after transient transfection (36, 48 and 72 h) total lysates of these cells contained similar amount of L1 protein, irrespective of the L1 construct that was used for transfection. This observation argues against different L1 expression rates or transfection efficiencies as a reason for the observed differences in cell surface localization of the different L1 variants. 36 h post-transfection (Fig. 9 A), two bands of 220 and 190 kD, characteristic for L1 expressed in cell culture, were identified for L1wt and all L1 mutations. For the L1ex mutation, both bands had a reduced molecular weight (about 200 and 170 kD) due to the lack of the intracellular domain. The upper 220 kD band corresponds to the full length and fully glycosylated form of L1 located at the cell surface (Zisch et al., 1997). In cultures transfected with L1wt, sL1, and L1ex, the 220 kD band had the same intensity as the 190 kD band. In contrast, in L1 $\Delta$ hbs- and L1C264Y-transfected cultures, the 220 kD signal was much weaker than that of the 190 kD band. After longer time periods post-transfection (48 h: Fig. 10 B; 72 h: Fig. 10 D), the ratio between the intensity of the 220 and 190 kD band shifted slightly in favor of the lower one for all constructs. As a result, the 220 kD band was very faint in L1 $\Delta$ hbs-transfected cultures and almost absent for L1C264Y-transfected cultures 72 h after transfection.

Similar results were obtained for CHO cells stably transfected with L1wt, L1 $\Delta$ E2, L1 $\Delta$ E27, L1ex, L1 $\Delta$ hbs, L1C264Y and L1ex (Fig. 9 B). Both, the 220 and the 190 kD band were present in lysates of L1wt-, L1 $\Delta$ E2-, L1 $\Delta$ E27-, and L1ex-transfected cells. In L1 $\Delta$ hbs- and L1C264Y-transfected cultures, only one single band at 190 kD was detectable. Interestingly, in lysates of L1ex-transfected cell clones a more intense 140 kD band was detectable compared e.g. to L1wt, which indicates an increased proteolytic cleavage (Fig. 9B).

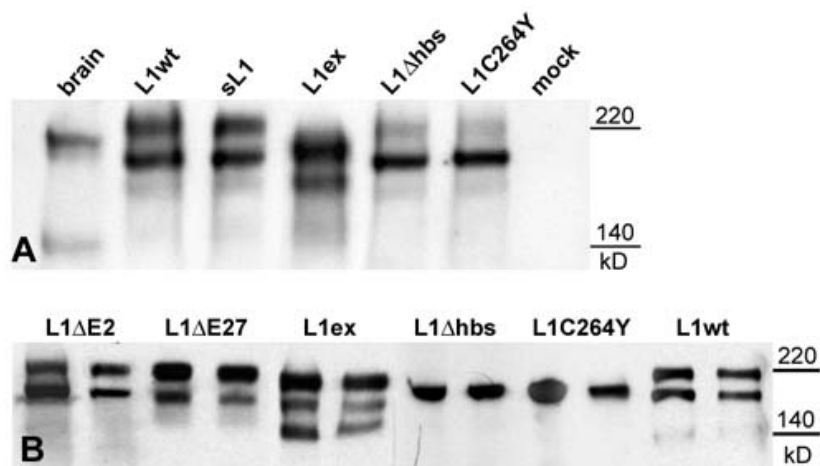


**Figure 9: L1 immunoblot analysis of lysates from transiently (A; 36 h after transfection) and stably (B) transfected cells.** L1-immunoreactive bands at 220 and 190 kD are detectable in cultures transfected with L1wt, sL1, and L1ex (A). The reduced molecular weights in cells transfected with L1ex are related to the lack of the intracellular domain. In cultures transiently transfected with L1 $\Delta$ hbs or L1C264Y (A), the 190 kD form of L1 is strongly expressed whereas the 220 kD form is hardly detectable. The 220 and 190 kD form of L1 are expressed in cultures stably transfected with L1 $\Delta$ E2, L1 $\Delta$ E27, L1ex and L1wt (B), while only the 190kD band is detectable in cultures stably transfected with L1 $\Delta$ hbs or L1C264Y (shown are results from 2 out of 8 independent experiments for each construct). Mouse brain homogenates (brain) served as an internal control and mock-transfected CHO cells as a negative control (only shown in A).

#### 1.4 L1 with a molecular weight of 190 kD is not expressed on the cell surface

Mutations L1 $\Delta$ hbs and L1C264 showed a decrease in cell surface location and in the amount of the 220 kD form with increasing time intervals after transfection. Therefore, it is conceivable that the 190 kD band represents a protein not expressed at the cell surface. To investigate this hypothesis, protein on the cell

surface of transfected CHO cells was biotinylated 48 and 72 h after transfection. The biotinylated protein was extracted and analyzed by L1 immunoblotting (Fig. 10 A and C; B and D show whole cell lysates before extraction of biotinylated protein).

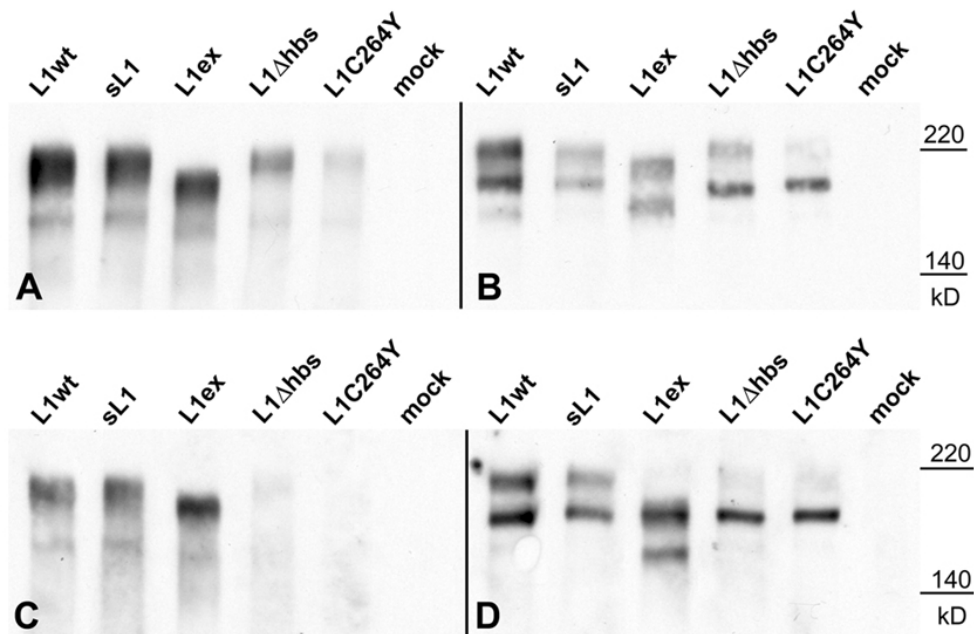


**Figure 10: Cell surface biotinylation.** Extracted biotinylated cell surface proteins (A and C) and whole cell lysates (B and D) from transiently transfected CHO cells (A and B: 48 h after transfection; C and D: 72 h after transfection) were subjected to L1 immunoblot analysis. Analysis of biotinylated proteins from CHO cells transfected with L1wt, sL1 and L1ex reveals a prominent band at 220 kD at both time points after transfection (A and C). In cultures transfected with L1Δhbs and L1C264Y, in comparison, the 220 kD form of L1 is only weakly expressed 48 h (A) and hardly detectable 72 h (C) after transfection. Note that the 190 kD form of L1 is absent from biotinylated protein extracts of all transfectants (compare A and B, C and D).

The intensity of the 220 kD band was measured and related to L1wt (100 %; Fig. 11). Cells transfected with sL1 (48 h: 89.2 %; 72 h: 92.6 %) and L1ex (48 h: 84,6 %; 72 h: 105.1 %) expressed similar amounts of the 220 kD form of L1 at the cell surface. In comparison, levels of cell surface-associated protein were significantly reduced 48 h (45.0 % and 20.4 %) and 72 h (20.4 % and 8.5 %) post-transfection in L1Δhbs- and L1C264Y-transfected cultures, respectively. Thus, for these two mutations, a decrease in L1 expression of about 50 % was observed between the two investigated time points. This finding fits well with the decline of L1-immunopositive live cells with time after transfection. Remarkably, the amount of surface labeled protein of the sL1-transfected cells was not reduced in relation

to L1wt. This is in contrast to the immunocytochemical data of transient sL1 and L1 $\Delta$ E2- or stably L1 $\Delta$ E2-transfected cells which showed a reduced number of cells with surface L1.

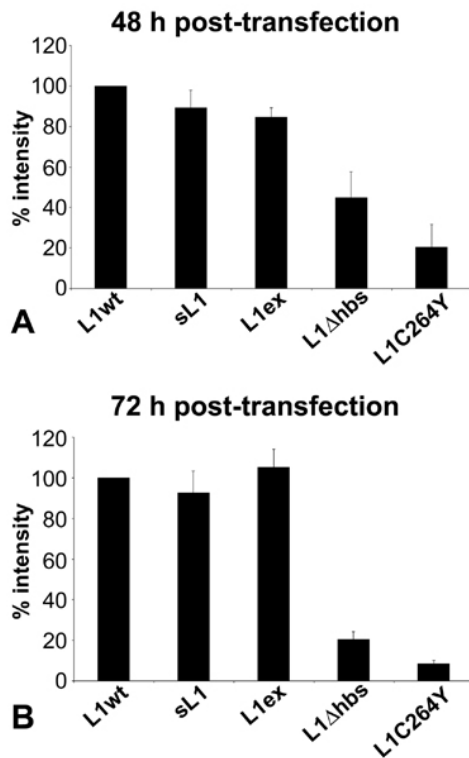


**Figure 11: The amount of mutated L1 proteins and L1wt at the cell surface of transfected CHO cells.** The intensities of immunoreactive bands of biotinylated proteins (Fig. 10 A and C) were determined and related to L1wt (set to 100 % in each blot) for two time points after transfection (A and B). In relation to L1wt, the amount of surface L1 was clearly reduced in L1 $\Delta$ hbs- and L1C264Y-transfected cells 48 h and 72 h after transfection and, moreover, decreased for both mutations by approximately 50 % between both time points (compare A and B). Bars in A and B represent the mean values  $\pm$  SD of two independent experiments.

Biotinylation of live cells and subsequent immunoblot analysis identified the 220 kD form of L1 as the major protein form of L1 at the cell surface of transfected CHO cells (Fig. 10 A and C). In addition, a faint 160 kD band was found, most probably corresponding to the 140 kD proteolytic cleavage fragment of L1 observed in mouse brain. The broad band at 220 kD might contain an additional band, known as the 180 kD proteolytic fragment of L1 from mouse brain (Sadoul et al., 1988 and 1989), which is expressed to have a molecular weight of about 200 kD in this cell line. In contrast, the 190 kD protein form, present in lysates of CHO cells transfected with L1wt and the different L1 variants, was not labeled at the cell surface, indicating that it is not transported to the plasma membrane, but is instead located inside the cell.

### 1.5 L1 $\Delta$ hbs and L1C264Y are not located at the cell surface, but within the endoplasmic reticulum

The most likely explanation for the reduced molecular weight of the L1 $\Delta$ hbs- and L1C264Y-variants of L1 is a change in the glycosylation pattern, probably resulting from impaired protein transport within the cell. To investigate this hypothesis, CHO cells were lysated 72 h after transfection and the protein was digested with endoglycosidase H (endo H; Fig. 12). The enzyme removes N-linked glycans with terminal mannose residues, characteristic for glycoproteins located in the endoplasmic reticulum and early *cis*-Golgi apparatus during oligosaccharide processing (for review see: Helenius and Aebi, 2001; Parodi, 2000a, b). After endo H treatment, the 190 kD protein form of L1 $\Delta$ hbs and L1C264Y shifted to a 150 kD band, the estimated molecular weight of deglycosylated L1 protein. The same shift in molecular weight was observed for the 190 kD band in cultures transfected with L1wt, sL1 and L1ex. Therefore, the 190 kD form of L1 has undergone a complete cleavage of its glycans by endo H, indicating that it is located within the endoplasmic reticulum and, in the case of L1 $\Delta$ hbs and L1C264Y, is not further transported through the Golgi network to the cell surface.

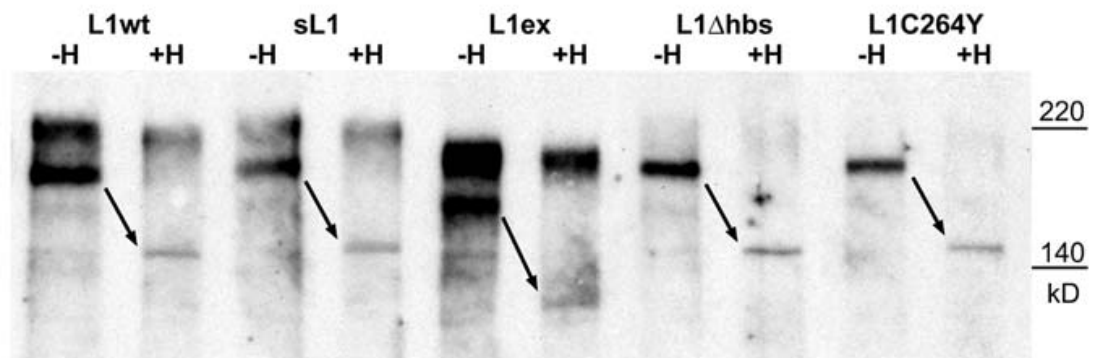


**Figure 12: Deglycosylation of L1wt and mutated L1 by endo H.** L1 immunoblot analysis of transiently transfected CHO cells (72 h after transfection) either without (-H) or after (+H) digestion with endo H. Treatment with endo H does not alter the molecular weight of the 220 kD form of L1, while it reduces the molecular weight of the 190 kD form to 150 kD.

## 2 Part II: The L1C264Y transgenic mouse

### 2.1 Generation of L1C264Y transgenic mice

Transgenic mice with an expression of L1C264Y under the control of the L1 promoter (Kallunki et al., 1998) were generated to establish an animal model for this pathogenic missense mutation (Fig. 13).

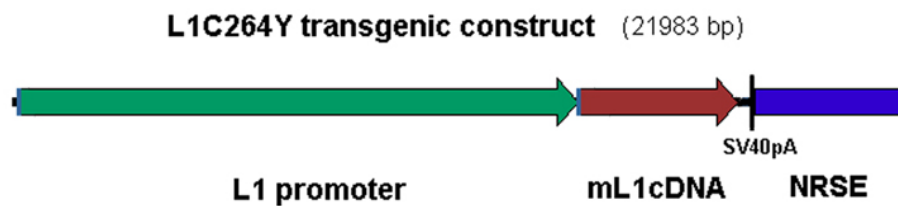


**Figure 13: Construct for the generation of L1C264Y mice.** This construct comprises the regulatory elements of the gene, i.e. the L1 promoter and the NRSE sequence (neural restrictive silencer element; kind gift of Pekka Kallunki; Kallunki et al., 1998), the cDNA encoding L1C264Y, and the SV40 polyadenylation site. The entire transgenic construct has a length of about 22 kb.

After microinjection of the transgene into 150 zygotes (second generation of crosses between C57B6 and DBA mouse strains) and their implantation into the nurse female, 72 mice were born. Out of this animals, five founders carrying the transgene were identified by PCR and Southern blot analysis (Fig. 14), four females and one male founder. For the male founder, further breeding identified the Y-chromosome as the integration site of the transgene.

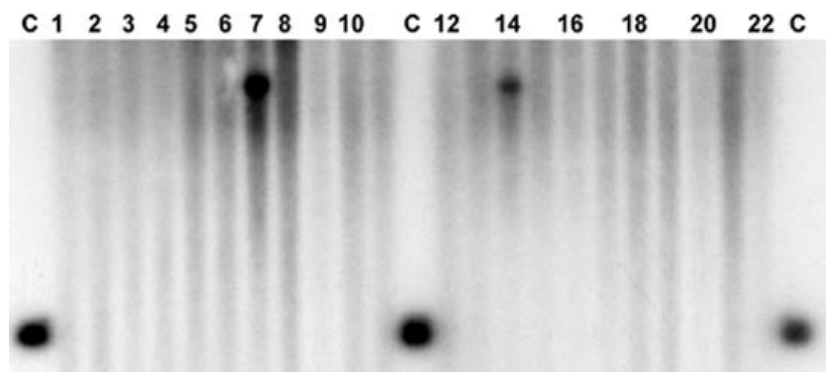


**Figure 14: Southern Blot analysis for identification of transgenic founders.** The Southern Blot reveals a positive signals for animals '7' and '14', which identify them as transgenic founders. These founders gave rise to the founder lines L1C264Y-III and -IV. C: control marker.

To confirm the expression of the transgenic L1C264Y protein, transgenic mice were crossed into a L1-deficient background by breeding males of the first generation (into the C57BL/6J mouse strain; L1+/y\_C264Y) with C57BL/6J heterozygous L1 knock-out females (L1+/-; Dahme et al., 1997). Wild-type (wt), L1-deficient (L1-/y), L1+/-, and L1C264Y transgenic male embryos (L1-/y\_L1C264Y; further termed L1C264Y) at embryonic day 17.5 were used for L1 immunoblot analysis (Fig. 15). Substantial amounts of L1C264Y protein were expressed in founder line IV (Fig. 15 A) and at lower levels in line III, whereas in lines I, II (Fig. 15), and V no L1C264Y protein was detectable.

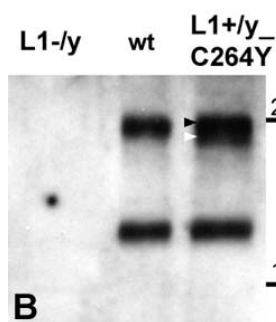
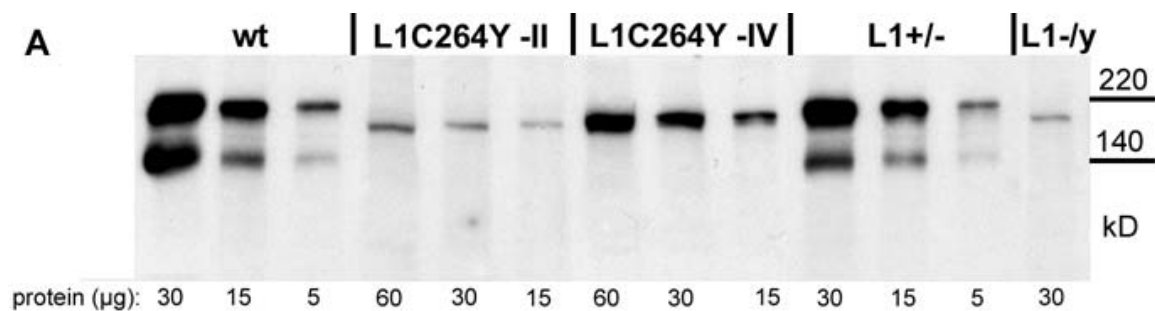


**Figure 15: Amount of L1 protein in brain homogenates from mouse embryos (at E17.5) of different genotypes (A).** In comparison to wild-type (wt) mice, the homogenate of the L1C264Y transgenic mouse of the founder line IV (L1C264Y -IV) contains reduced but substantial amounts of transgenic protein whereas that of founder line II (L1C264Y -II) shows no expression of transgenic L1C264Y protein (compare to L1-/y; the band detected in L1-/y corresponds to residual L1-immunoreactivity, described for this L1 knock-out line (Dahme et al., 1997)). Note that the L1C264Y protein has a molecular weight of 190 kD, instead of 200 and 140 kD as detectable in wt. The amount of L1 in L1+/- is slightly reduced compared to wt brains. **(B)** In brain homogenates of L1+/y\_C264Y mice of line IV (expression L1C264Y in addition to endogenous L1) the 190 kD protein (white arrowhead) is visible in addition to the 200 kD (black arrowhead) and 140 kD protein of endogenous L1 wt. L1-deficient (L1-/y) mice of the L1 knock-in mouse line (Rolf et al., 2001) showed no residual L1-immunoreactivity. All used animals in (B) were 6 weeks of age.

Note that the L1C264Y protein has a molecular weight of 190 kD, instead of 200 and 140 kD as detectable in wt. The amount of L1 in L1+/- is slightly reduced compared to wt brains. **(B)** In brain homogenates of L1+/y\_C264Y mice of line IV (expression L1C264Y in addition to endogenous L1) the 190 kD protein (white arrowhead) is visible in addition to the 200 kD (black arrowhead) and 140 kD protein of endogenous L1 wt. L1-deficient (L1-/y) mice of the L1 knock-in mouse line (Rolf et al., 2001) showed no residual L1-immunoreactivity. All used animals in (B) were 6 weeks of age.

The amount of L1 in transgenic lines III and IV was estimated by quantification of band intensities on immunoblots, and was related to L1 levels in wt mice (Fig. 16). The founder line IV expressed the highest level of L1C264Y protein (34 % compared to L1 in wt mice), whereas expression of transgenic L1 in line III was significantly lower (11 % compared to L1 in wt mice). Therefore, the founder line IV

was chosen for all further investigations (now termed L1C264Y without indication of the line), and were crossed into the L1-deficient background by cross-breeding with L1 knock-in mice (Rolf et al., 2001), in which the L1-/- males showed no residual L1 protein (Fig. 15 B).

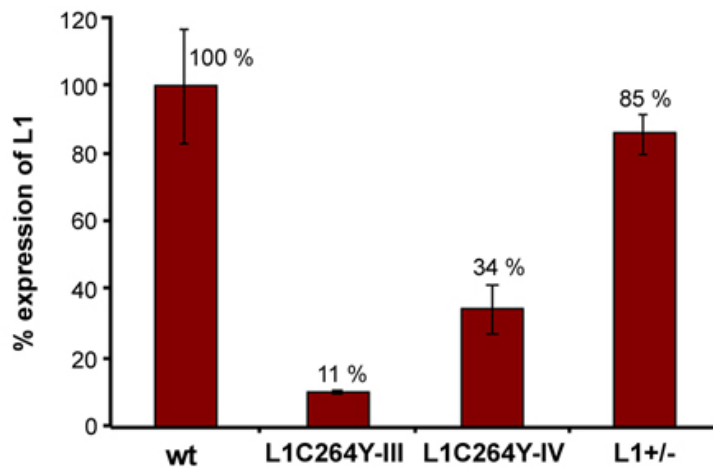


**Figure 16: Amount of L1 in wt males, heterozygous L1ko (L1+/-) females and L1C264Y transgenic mice of founder lines III and IV as revealed by quantification of band intensities of L1 immunoblots (an example is shown in Fig. 15). For every genotype or transgenic mouse line, the bands of three different protein concentration**

concentrations per blot and two different blots were quantified and related to wt. Bars represent mean values  $\pm$  SD of two independent experiments.

## 2.2 L1C264Y expressed *in vivo* is endo H-sensitive

Immunoblot analysis of brain tissue from 17.5-day-old L1C264Y mouse embryos revealed a single L1-immunoreactive band of about 190 kD instead of the characteristic 200 kD (full length) and 140 kD (proteolytic cleavage product) bands found in brain homogenates of wt mice (Fig. 15 A). In brain homogenates of L1+/Y\_C264Y animals (expressing L1C264Y in addition to endogenous L1) a 190 kD in addition to a 200 and 140 kD L1 protein form were found (Fig. 15 B).

Treatment of brain homogenates from L1C264Y males with endo H resulted in a shift of the 190 kD band to a 150 kD band (Fig. 17). Molecular weights of L1-immunoreactive bands in wt homogenates, in contrast, were not altered by endo H treatment (Fig. 17). This observation indicates that the 190 kD variant of L1 expressed in L1C264Y mice represents a not fully glycosylated protein. The same results were obtained with brain homogenates of 3-month-old mice (data not shown).

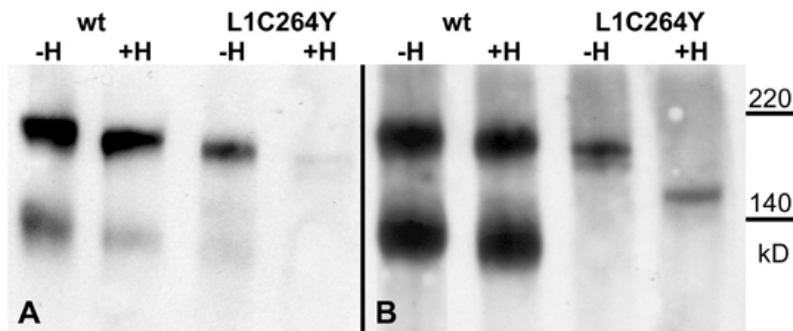


**Figure 17:** Brain homogenates from 17.5-day-old wt and L1C264Y transgenic mouse embryos were subjected to L1 immunoblot analysis either without (-H) or after (+H) digestion with endo H. The two antibodies mc- $\alpha$ L1-555

(A) and pc- $\alpha$ L1a (B) were used. In undigested samples of wt mice (-H in A and B), the characteristic L1-immunoreactive bands at 200 and 140 kD (a proteolytic cleavage product of L1) are detectable. These L1wt protein is insensitive to endo H treatment (+H in A and B). In comparison, homogenates from L1C264Y transgenic mice contain a 190 kD instead of a 200 kD band and lack the 140 kD proteolytic cleavage product of L1 (-H in A and B), and endo H digestion results in a shift of the 190 kD band to 150 kD (+H in B). Note that the mc- $\alpha$ L1-555 (A) does not recognize the deglycosylated 150 kD protein in samples of L1C264Y mice

### 2.3 Expression of L1C264Y protein is restricted to cell bodies of neurons

To study the expression pattern and the localization of L1C264Y protein in brain tissue by immunohistochemistry, wt, L1C264Y, L1-*y*, and L1+*y*\_C264Y mice were perfused and 25  $\mu$ m thick vibratome sections of diverse regions of the CNS were stained with L1 antibodies (Fig. 18 and 19). In wt mice, intense and homogeneously distributed L1-immunoreactivity was observed in the molecular layer of the cerebellar cortex (Fig. 18 A), in the fiber-rich layers of the hippocampus (alveus, strata lacunosum moleculare, radiatum, and oriens; Fig. 19 A, C, E, F), in the nerve fiber layer and inner and outer plexiform layers of the retina (Fig. 18 F), and in the molecular layer of the olfactory bulb (data not shown). In contrast, L1-immunostaining in L1C264Y mice was restricted to the somata of neurons normally extending L1-positive processes, including Golgi, granule, basket, and stellate cells in the cerebellum (Fig. 18 B and E); pyramidal cells (Fig. 19 B and D), granule cells, and hilar interneurons (Fig. 19 B, F, H) in the hippocampus; ganglion, amacrine, and horizontal cells in the retina (Fig. 18 G), and mitral cells in the olfactory bulb (data not shown). L1-immunopositive fibers were not detectable in the CNS of L1C264Y transgenic mice. In L1+*y*\_C264Y mice, intense L1-immunoreactivity was found in fiber-rich mice brain regions and

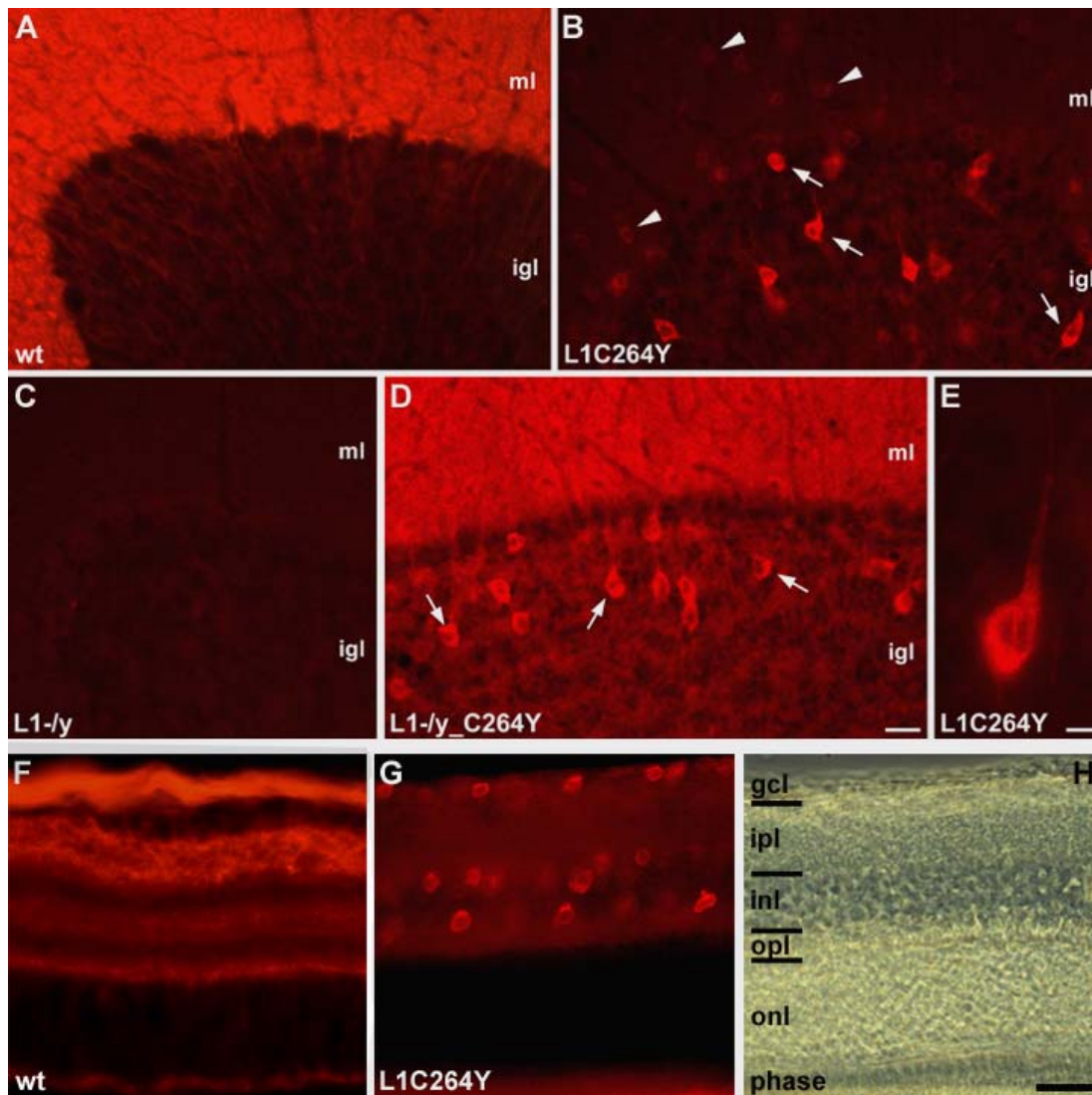


**Figure 18: L1-immunohistochemistry of the cerebellum (A-E) and the retina (F-H) of two-month-old wt, L1C264Y, or L1-/y mice.** Intense and homogenously distributed L1-immunoreactivity is visible in the fiber-rich brain regions of wt mice, such as the molecular layer of the cerebellum (A), and the nerve fiber layer and plexiform layers of the retina (F). Regions rich in cell bodies, such as the internal granular layer of the cerebellum (A) or inner and outer nuclear layers of the retina (F) are only weakly L1-immunoreactive in wt mice. In contrast, L1-positive fibers are absent from the cerebellar cortex (B) or the retina (G) of L1C264Y mice. Instead, intense intracellular labeling of Golgi cells (some labeled with arrows in B; E shows a single Golgi cell) and weaker intracellular labeling of basket and stellate cells (some labeled with arrowheads in B) is visible in the cerebellar cortex of L1C264Y mice. In the retina of these mutants, cell bodies of ganglion, horizontal and amacrine cells (G) are strongly stained by L1 antibodies. In L1+/y\_C264Y mice, both, fiber tracts and nerve cell bodies are labeled by L1 antibodies (D; some immunoreactive Golgi cells are labeled with arrows). Sections from L1-/y mice are L1 immunonegative (C). (H) is the phase contrast photomicrograph of (G). gcl: ganglion cell layer; igl: internal granule layer, inl: inner nuclear layer; ipl: inner plexiform layer; ml: molecular layer; onl: outer nuclear layer; opl: outer plexiform layer; Bar in D (for A-D): 25  $\mu$ m; bar in E: 10  $\mu$ m; bar in F (for F-H): 50  $\mu$ m.

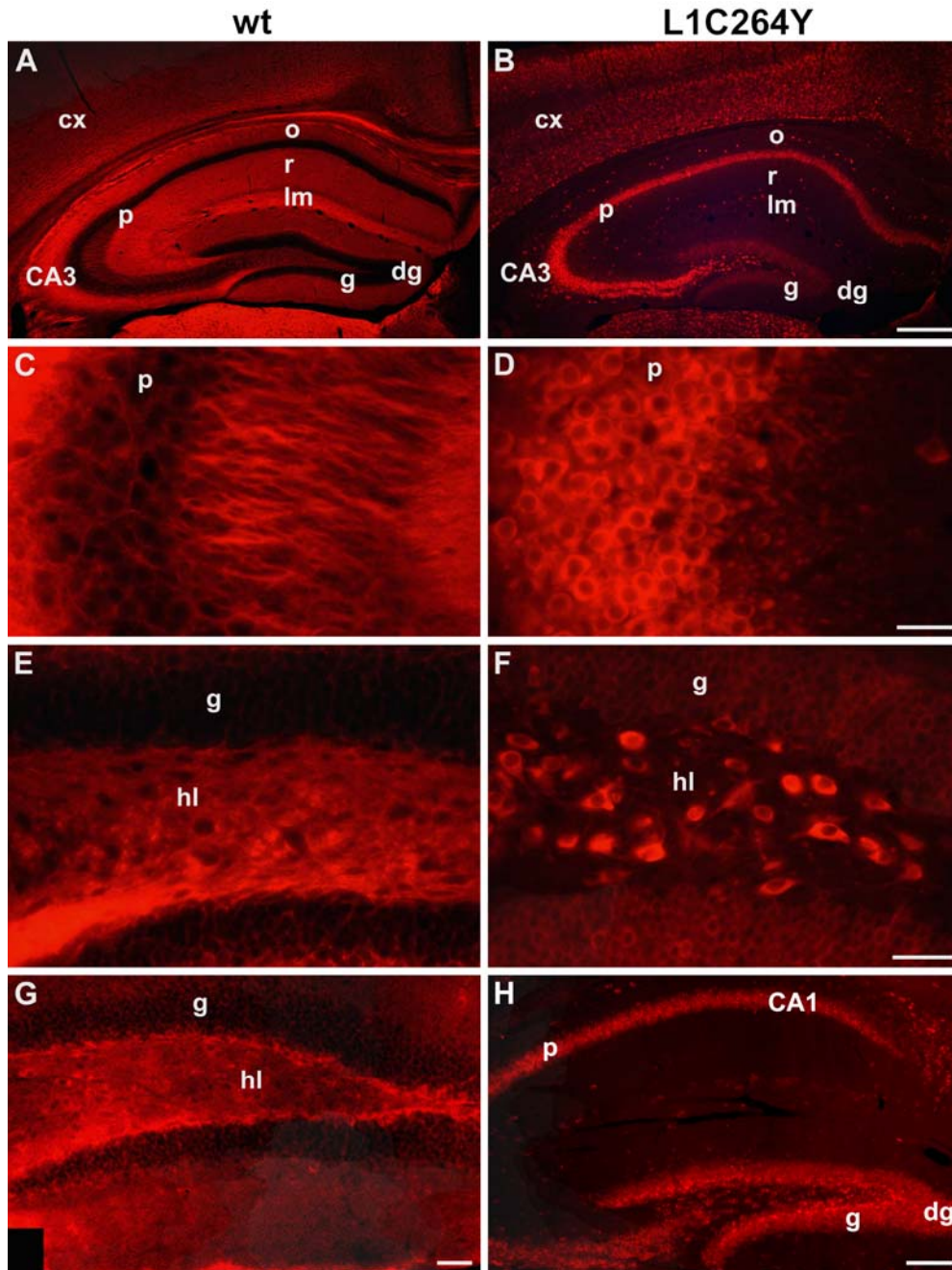


**Figure 19: L1 immunohistochemistry of the hippocampus of two-month- (A-F) and four-week-old (G and H) wt (A, C, E, G) and L1C264Y (B, D, F, H) mice.** In wt mice, L1-immunoreactivity is visible in fiber-rich regions, including the stratum oriens, radiatum, and lacunosum moleculare (A) and the mossy fibers (C and E). In contrast, in L1C264Y mice only cell bodies including pyramidal cells (B and D) and hilar interneurons (F) are intensely labeled. In the two-month-old L1C264Y mice the granule cells are only weakly stained (F), whereas in the four-week-old mice, the granule cells show intense labeling comparable to that of the pyramidal cells (G) with the strongest staining of granule cells in the hilar-near subgranular zone. In four-week-old wt animals, fibers in the subgranular zone are strongly labeled (G), whereas in two-month-old wt mice (E) labeling in this area is reduced. cx: cortex; dg: dentate gyrus; g: granule cell layer; hl: hilus; lm: stratum lacunosum moleculare; ml: molecular layer; o: stratum oriens; p: pyramidal cell layer; r: stratum radiatum. Bar in A (for A and B): 200  $\mu$ m; bar in D (for C and D), F (for E and F), and H (for G and H): 100  $\mu$ m.

within neuronal cell bodies (Fig. 18 D). Sections from L1-*y* mice were L1-immunonegative (Fig. 18 C).

In summary, L1C264Y transgenic mice showed a normal spatio-temporal expression pattern of transgenic L1 in that transgenic L1 was only detectable in cells known to normally express L1 in wt mice, but not in cells known to not express L1 wt mice, such as Purkinje cells in the cerebellum or photoreceptor cells in the retina (Fig. 18 B and G). In addition, expression of L1 in L1C264Y mice was developmentally regulated. For example, in four-week-old L1C264Y mice, granule cells of the dentate gyrus showed a labeling intensity comparable to that of the pyramidal cells of the hippocampus (Fig. 19 H). The most intense labeled granule cells were found in the hilus-near part region. These cells might correspond to young postmitotic cells, since the vast majority of the granule cells are generated postnatally during the first three to four weeks (Bayer, 1980). In contrast, in two-month-old L1C264Y mice, granule cells were only weakly labeled compared to pyramidal cells (Fig. 19 H).

## 2.4 General phenotype of L1C264Y mice

Our combined *in vitro* and *in vivo* data indicate that the pathogenic missense mutation L1C264Y is not expressed at the cell surface. It is thus reasonable to assume that the L1C264Y transgenic mouse might be equivalent to a functional knock-out mutant, and thus might exhibit a phenotype indistinguishable from that of L1-deficient mice. However, it is also possible that an accumulation of mutated L1 protein within the cell or a cell surface localization below detection levels result in a more severe or less severe phenotype, respectively, compared to L1 null mutants. We therefore compared in detail the phenotypes of L1C264Y and L1-*y* mice.

Both, L1-*y* and L1C264Y mice, had a reduced body size compared to their wt littermates, lacrimeous and sunken eyes (Fig. 20), and had difficulties to use their hindlegs when hanging on a grid. These general phenotypes were more striking in young animals until their fourth postnatal week than in older ones. In contrast, L1+*y*\_C264Y mice (males that express both L1C264Y and wild-type L1) showed no general abnormalities and were undistinguishable from wt mice.

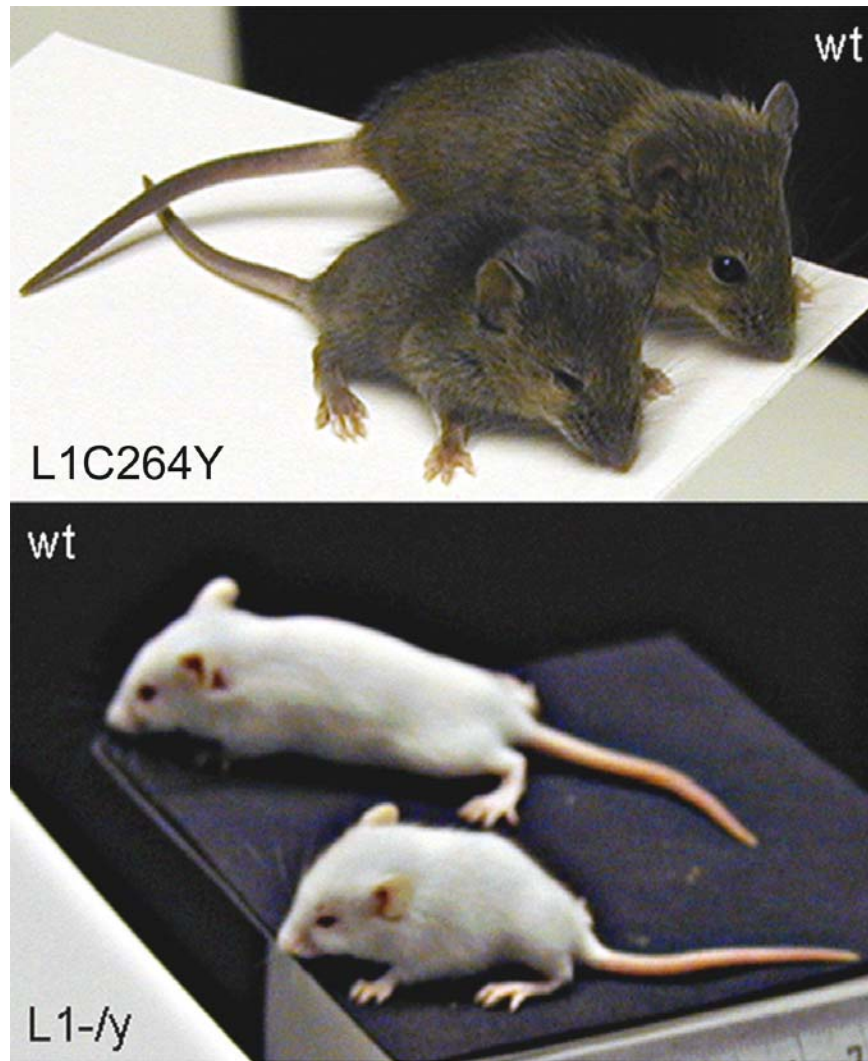


**Figure 20:** Three-week-old L1C264Y transgenic (top) and L1-/y mice (bottom) and their wt litter. Both mutants display a reduced body size and have lacrimous and sunken eyes.

The average body weight of ten-week-old L1-/y ( $25.1 \pm 2.6$  g,  $n = 7$ ) and L1C264Y mice ( $25.5 \pm 1.5$  g,  $n = 7$ ) was reduced when compared to wt ( $29.3 \pm 1.6$  g,  $n = 12$ ) and L1+/y\_L1C264Y littermates ( $28.6 \pm 1.2$  g,  $n = 5$ ; Fig. 21).

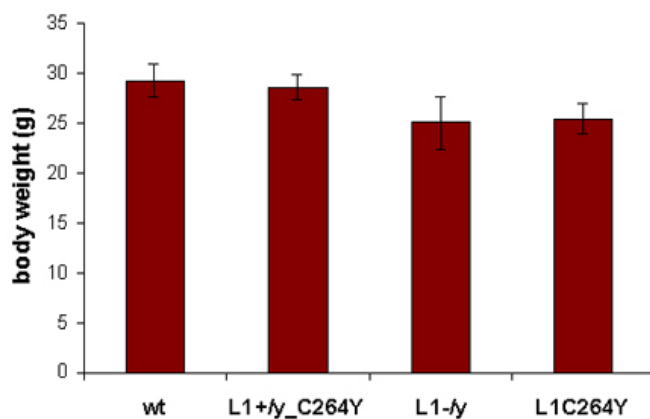


**Figure 21:** Average body weight of ten-week-old wt, L+/y\_L1C264Y, L1-/y, and L1C264Y mice. The body weight of L1-/y and L1C264Y, but not of L1+/y\_L1C264Y mice, is reduced compared to age-matched wt animals. Bars represent the mean values  $\pm$  SD of 5 to 12 animals.

Given an expected ratio of 1:1 between born females and males, the apparent survival rate until weaning was strongly reduced for males (32.7 %; Fig. 22 A) derived from breedings between L1+/-\_C264Y females and wt males. The reduced frequency of male offsprings was due to a decreased survival rate of L1C264Y and L1-/y males compared to wt male littermates. According to Mendelian frequencies, each of the four possible genotypes of males expected to derive from the given crosses should appear with a probability of 25 %. We used the number of wt males (n = 50) to calculate the percentage of males of the different genotypes which reached the age of weaning (Fig. 22 B). According to these calculations, the frequency of L1+/y\_L1C264Y males was only slightly lower (21.2 %, n = 42) than expected (i.e. 25 %), whereas the number of both L1C264Y and L1-/y mutant males was dramatically lower than theoretically expected (L1C264Y: 8.0 %, n = 16; L1-/y: 9.5 %, n = 19).

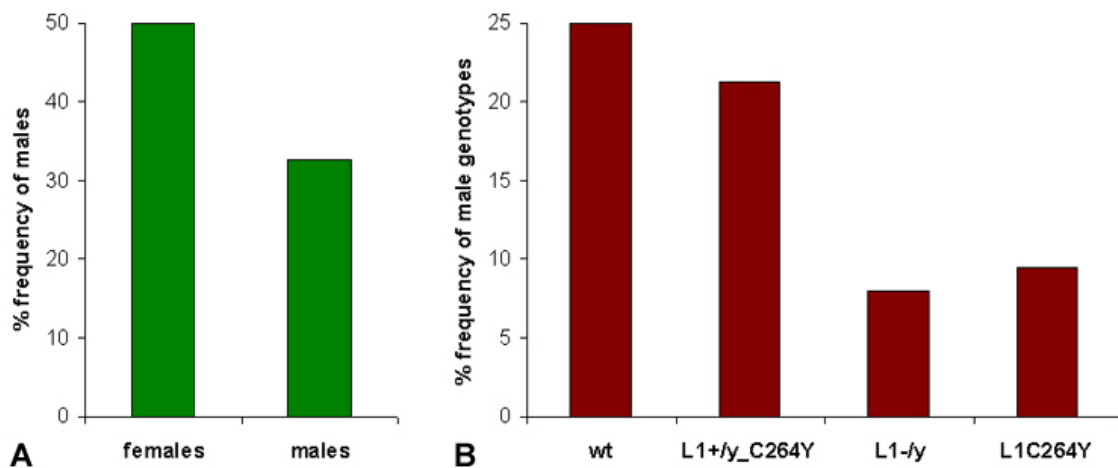


**Figure 22:** The survival rate of males is reduced compared to females (A). L1-/y and L1C264Y males showed a strongly reduced survival rate compared to wt and L1+/y\_C264Y males (B).

## 2.5 L1C264Y and L1-deficient mice display a similar morphological phenotype

Corticospinal axons of L1-deficient mice display pathfinding errors at the pyramidal decussation (Cohen et al., 1998). To evaluate whether similar abnormalities are detectable in L1C264Y mice, the CST of wt, L1-/y, and L1C264Y mice was anterogradely labeled at postnatal day 1-2. The trajectory of the tract at the pyramidal decussation was analyzed 2 days after tracing (Fig. 23).

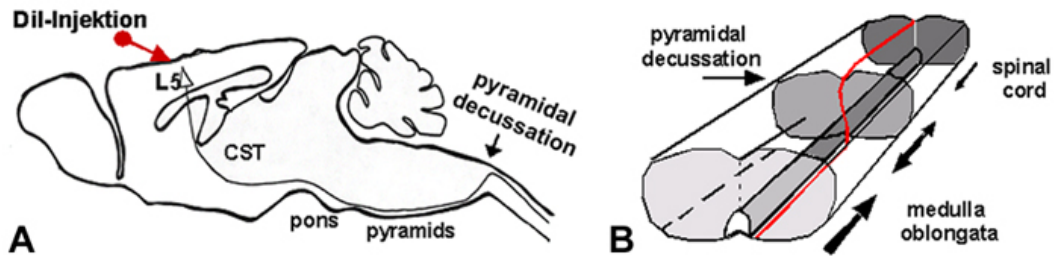


**Figure 23: Tracing and trajectory of the corticospinal tract (CST) from the pyramidal cells in layer 5 (L5) of the cortex through the diencephalon and medulla to the spinal cord (A). At the caudal end of the medulla, the CST turns from ventral to dorsal and crosses the midline to the contralateral side (pyramidal decussation), and enters the dorsal funiculus of the spinal cord (B).**

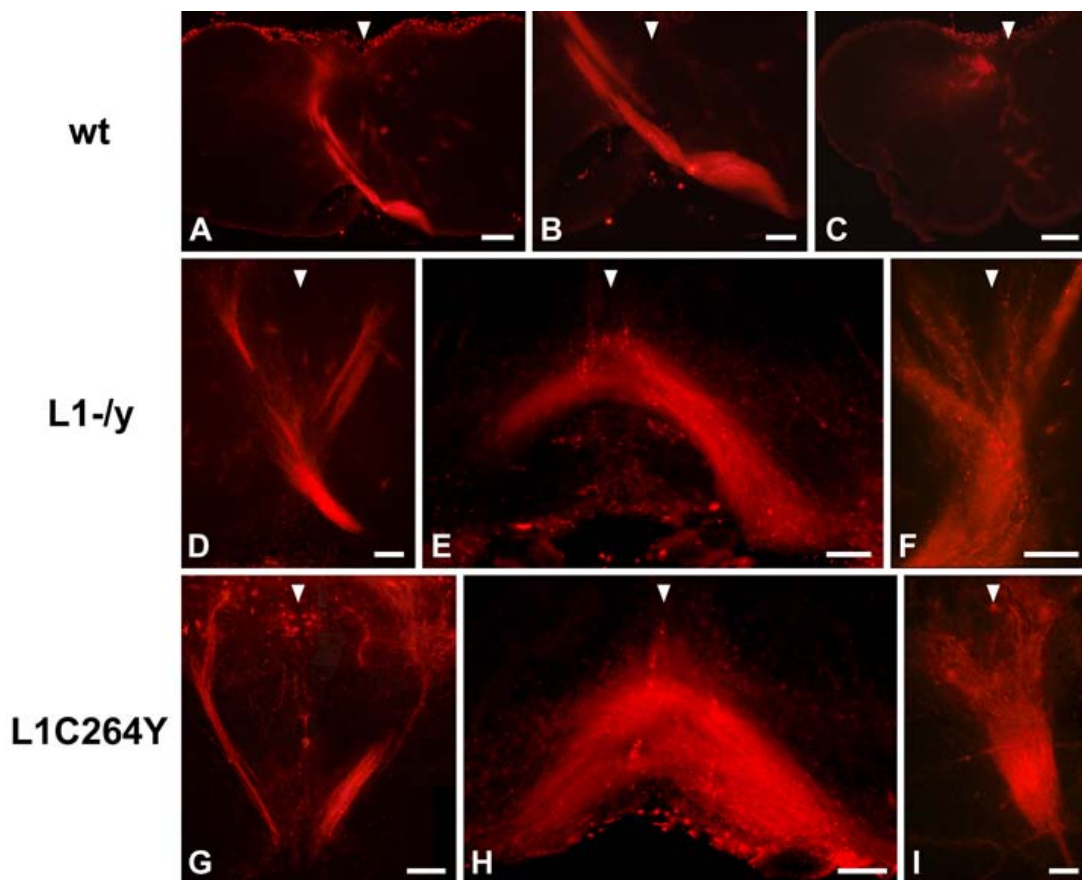


**Figure 24: Anterograde tracing of corticospinal axons in wt (A-C), L1-/y (D-F), and L1C264Y mice (G-I), and analysis of their trajectory at the pyramidal decussation. In wt mice, corticospinal axons cross the midline (indicated by arrowheads in A-I) at the pyramidal decussation (A and B) and extend to the dorsal column, where they enter the dorsal funiculus (C). In L1-/y mice, corticospinal axons display pronounced pathfinding errors at the pyramidal decussation, and either project bilaterally to the dorsal column (D), or cross the midline but stay ventrally instead of projecting dorsally (E). A bilateral projection of corticospinal axons to the dorsal column (G) or a projection to the contralateral pyramid (H) is also detectable in L1C264Y transgenic mice. Both mutants additionally show defasciculation of corticospinal axons (F and I). Bars in A and C: 200  $\mu\text{m}$ ; Bars in B, D-I: 100  $\mu\text{m}$ .**

In wt mice ( $n = 5$ , Fig. 24 A-C), corticospinal axons turned dorsally at the caudal end of the medulla oblongata, crossed the midline (Fig. 24 A and B) and extended into the contralateral dorsal column (Fig. 24 C). In most L1- $/y$  mice ( $n = 4$ , Fig. 24 D-F), in contrast, a significant portion of axons failed to cross the midline but instead projected to the ipsilateral dorsal column (Fig. 24 D). In other L1- $/y$  mice, corticospinal axons stayed ventrally and entered the contralateral pyramid ( $n = 2$ , Fig. 24 E) or stayed ventrally without crossing the midline ( $n = 1$ ). Pathfinding errors of corticospinal axons were also observed at the pyramidal decussation of L1C264Y mice (Fig. 24 G-I). Similar to L1- $/y$  mice, a significant fraction of corticospinal axons projected to the ipsilateral dorsal column ( $n = 3$ , Fig. 24 G), or axons stayed ventrally either without crossing the midline ( $n = 2$ ) or extending to the contralateral pyramid ( $n = 2$ , Fig. 24 H). One L1C264Y mutant displayed no obvious pathfinding errors at the pyramidal decussation. In addition, moderate defasciculation of corticospinal axons was observed in both mutant mouse lines (Fig. 24 F and I).

The size of the CST is significantly reduced in L1-deficient mice (Dahme et al., 1997). Therefore, we determined the area of the CST in ten-week-old wt (Fig. 25 A), L1- $/y$  (Fig. 25 B), L1C264Y (Fig. 24 C), and L1+ $/y$ \_L1C264Y mice at the caudal end of the medulla (Fig. 25 D). The area of the CST of L1- $/y$  mice was significantly

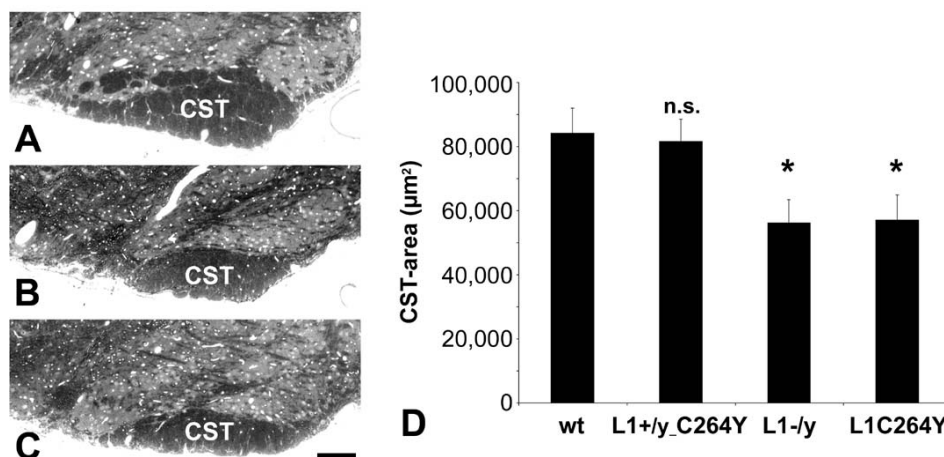


**Figure 25: The size of the CST of L1- $/y$  (B) and L1C264Y mice (C) is significantly reduced compared to wt mice (A).** Quantitative analysis (D) reveals a similar area of the corticospinal tract (CST) in wt ( $n = 7$ ) and L1+ $/y$ \_C264Y ( $n = 3$ ) mice. In contrast, the area of the CST is significantly reduced to a similar extent in L1- $/y$  ( $n = 5$ ) and L1C264Y ( $n = 5$ ) mice. Bars in (D) represent mean values  $\pm$  SD. n.s.: not significantly different from wt;  $\star$ : significantly different from wt ( $p < 0.01$ ; Mann-Whitney-test). CST: corticospinal tract. Bar in A-C: 100 $\mu\text{m}$ .

reduced to 66.8 % ( $56,264 \pm 7179 \mu\text{m}^2$  per tract;  $n = 5$ ) compared to wt mice ( $84,199 \pm 7816 \mu\text{m}^2$  per tract;  $n = 7$ ). The CST of L1C264Y mice was reduced to a similar extent as that of L1-/y mice (67.9 %;  $57,133 \pm 7716 \mu\text{m}^2$  per tract;  $n = 5$ ), while the values for L1+/y\_L1C264 mice ( $96.9 \%$ ;  $81,572 \pm 7043 \mu\text{m}^2$ ,  $n = 3$ ) were not significantly different from that of wt animals.

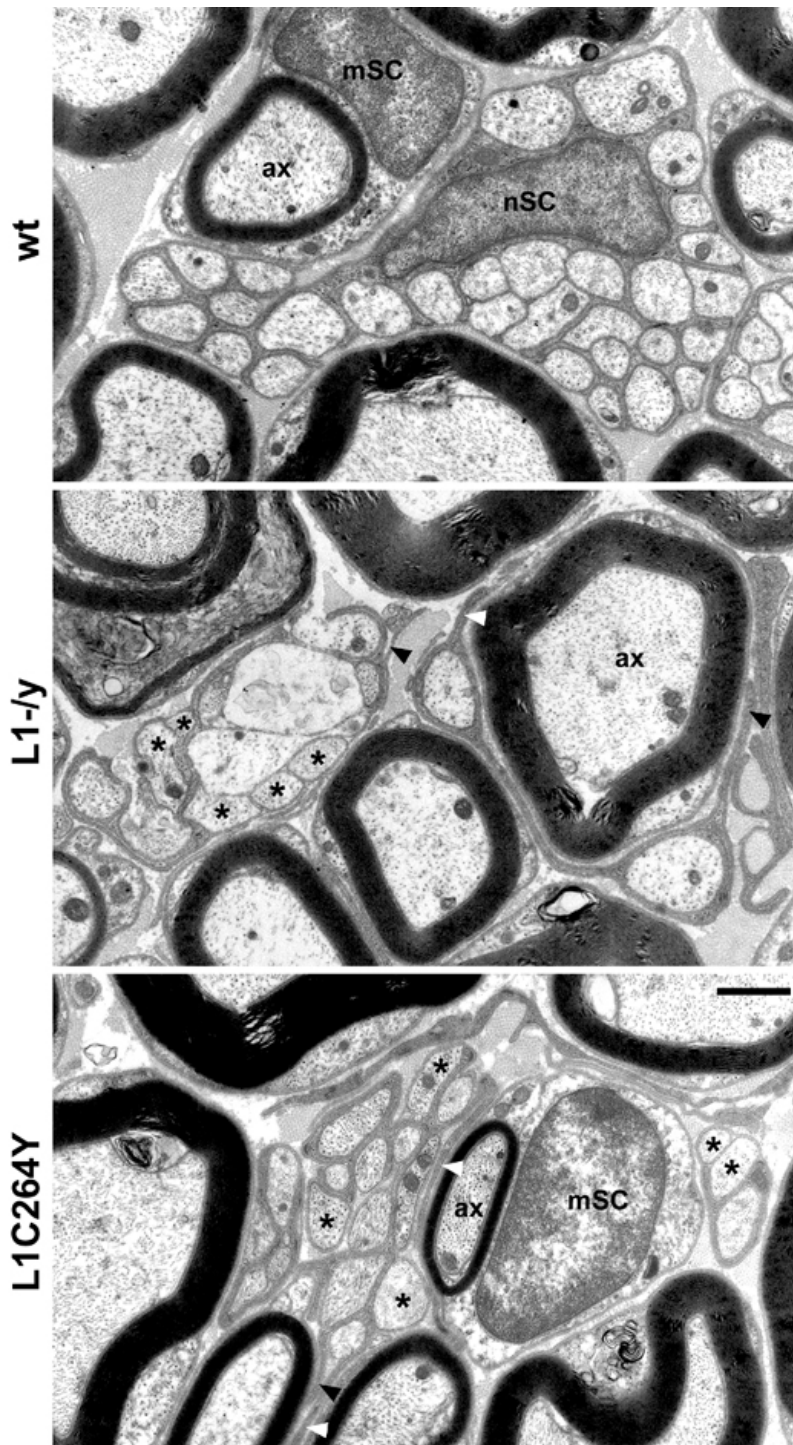


**Figure 26: Ultrastructure of unmyelinated fibers in the sciatic nerve of wt, L1-/y, and L1C264Y mice.** Axons in wt mice are ensheathed and separated from each other by Schwann cell processes. In L1-/y and L1C264Y mice, in contrast, a portion of axons (same labeled with asterisks) is not covered by a Schwann cell process, and numerous nonmyelinating Schwann cells extend processes (labeled with arrowheads) into the endoneurial space. Note the reduced number of axons associated with one nonmyelinating Schwann cell in L1-/y and L1C264Y mice compared to wt animals. ax: myelinated axon; mSC: myelinating Schwann cell; nSC: nonmyelinating Schwann cell. Bar in L1C264Y (for all graphs):  $1\mu\text{m}$ .

Morphological abnormalities of unmyelinated fibers in peripheral nerves of L1-deficient mice include a reduced number of unmyelinated axons per nonmyelinating Schwann cell, Schwann cell processes extending into the endoneurial space, and the presence of incompletely ensheathed unmyelinated axons (Dahme et al., 1997; Haney et al., 1999). To investigate if L1C264Y mice exhibit similar defects, we examined unmyelinated fibers in sciatic nerves of ten- to eleven-week-old wt, L1-*ly*, and L1C264Y mice. In wt animals, nonmyelinating Schwann cell processes ensheathed individual axons whereas in both, L1-*ly* and L1C264Y (Fig. 26; n = 6 for each genotype) mutant mice, a portion of axons were either incompletely or not ensheathed by Schwann cell processes. Instead, these axons were either covered by a basal lamina or were in direct contact with each other (Fig. 26, asterisks).

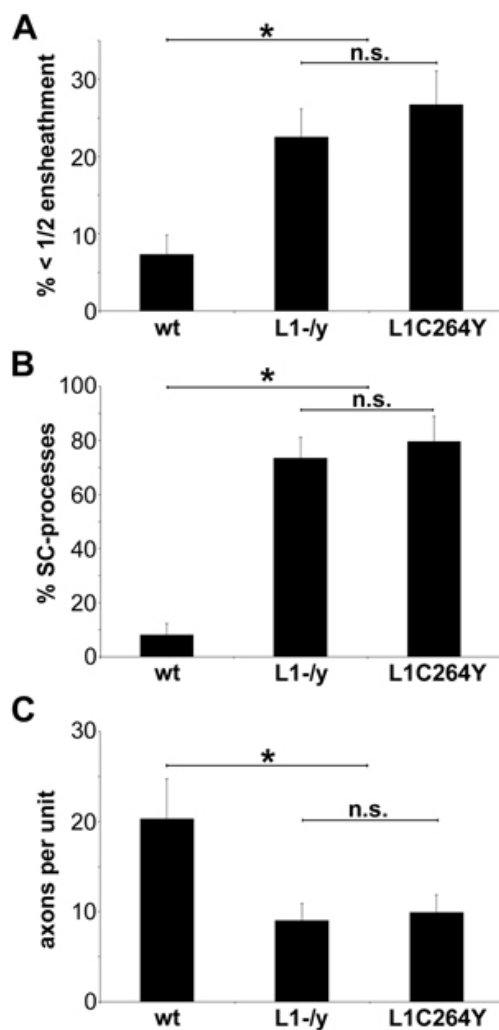


**Figure 27: Quantitative analysis of ultrastructural abnormalities in the sciatic nerve of wt, L1-*ly*, and L1C264Y mice.** The number of incompletely ensheathed axons per nonmyelinating Schwann cell (A), and the number of nonmyelinating Schwann cells extending one or more processes into the endoneurium (B) is significantly increased, and the number of axons associated with a nonmyelinating Schwann cell (C) is significantly decreased in L1-*ly* and L1C264Y mice when compared to wt animals. Note that values for L1-*ly* and L1C264Y mice are not significantly different from each other for all parameters analyzed (A-C). Bars in (A-C) represent mean values  $\pm$  SD from six animals for each genotype. SC-processes: Schwann cell processes; n.s.: not significantly different;  $\star$ : significantly different ( $p < 0.01$ ; Mann-Whitney-test).

The percentage of axons with an incomplete (less than half of the axonal circumference) ensheathment by Schwann cell processes (Fig. 27 A) was significantly increased to a similar extent in L1-*y* ( $22.5 \pm 3.6$  %) and L1C264Y ( $26.7 \pm 4.4$  %) mice, when compared to wt mice ( $7.3 \pm 2.5$  %). Moreover, nonmyelinating Schwann cells of both mutant mouse lines extended additional processes into the endoneurial space (Fig. 26 B and C, arrowheads; Fig. 27 B). In wt mice,  $8.2 \pm 4.2$  % of nonmyelinating Schwann cells extended such additional processes into the endoneurium compared to  $73.4 \pm 7.8$  % and  $79.9 \pm 9.1$  % in L1-*y* and L1C264Y mutants, respectively (Fig. 27 B). Finally, the number of unmyelinated axons associated with one nonmyelinating Schwann cell was significantly and similarly reduced in L1-*y* ( $9.0 \pm 1.9$  axons per unit) and L1C264Y ( $9.9 \pm 2.0$  axons per unit) compared to wt mice ( $20.3 \pm 4.4$  axons per unit; Fig. 27 C).

## IV Discussion

Mutations in all parts of the human L1 gene cause severe neurological diseases, termed L1 spectrum. The disorder is characterized by increased mortality, mental retardation and various malformations of the nervous system (Fransen et al., 1995). Missense mutations in the human L1 gene affecting the extracellular domain often result in a severe phenotype, whereas mutations in the highly conserved cytoplasmic domain generally cause a more moderate clinical picture. In an attempt to understand the reasons for the frequent occurrence of severe missense mutations in the extracellular domain of L1, this study focused on the functional consequences of extracellular and cytoplasmic L1 mutations *in vitro*. To this aim, we used mutated L1 constructs, sL1 or L1 $\Delta$ E2 and L1 $\Delta$ E27, L1ex, L1 $\Delta$ hbs, and L1C264Y, to study their expression in CHO cells. Moreover, a transgenic mouse line was generated expressing the human pathogenic missense mutation C264Y in the extracellular domain. The mutant was used to study the expression of this L1 variant *in vivo* and the consequences of this mutation on the development of the nervous system. The present study demonstrates impaired trafficking of the mutated L1 variants L1 $\Delta$ hbs and L1C264Y to the cell surface *in vitro*. Impaired trafficking of L1C264Y was also observed *in vivo*, resulting in severe morphological deficits of the L1C264Y transgenic mouse that are undistinguishable from the deficits observed in L1-deficient mice.

### 1 The short isoform of L1

Cultures of CHO cells transiently transfected with sL1 showed a reduction of the number of cells with surface L1 immunoreactivity compared to cultures transfected with L1wt. The impaired transport of this L1 variant to the cell surface is due to the lack of exon 2, since cultures transiently or stably transfected with L1 $\Delta$ E2 showed the same reduction in the number of cells with surface L1, whereas the number of L1 $\Delta$ E27-transfected cells with surface L1 was comparable to those transfected with L1wt. However, a reduction of surface sL1 could not be verified by quantification of the amount of cell surface biotinylated L1. A possible explanation

for this observation is that cells with surface expression of sL1 expressed higher amounts of L1 protein than cells expressing L1wt or L1ex.

As exon 2 is not included in L1 expressed by neurons and is located between the signal peptide and the first Ig domain it would be reasonable to assume that the absence of exon 2 alters protein trafficking of L1. This possibility was recently excluded by a study in which cerebellar neurons and chick dorsal root ganglion cells were transfected with L1 lacking exon 2, since no alterations in its distribution on the cell body and along neurites were found in comparison to full-length protein (De Angelis et al., 2001). However, since the amount of surface L1 was not determined in this study, we can not exclude that our observations on sL1-/L1 $\Delta$ E2-transfected CHO cells related to the particular cell type used in our study.

It has also been demonstrated that binding of L1 $\Delta$ E2 to itself or full-length L1 is dramatically or moderately reduced, respectively. In addition heterophilic binding of L1 $\Delta$ E2 to TAX-1 and F3 was impaired (De Angelis et al., 2001). The findings of reduced homophilic binding abilities of L1 $\Delta$ E2 were confirmed and extended by another study showing diminished levels of neurite outgrowth from cerebellar neurons on a L1 $\Delta$ E2 substrate (Jacob et al., 2002). The combined data lead to the suggestion that exon 2 provides a 'spacer', allowing N-terminal residues to interact with the junction between Ig domains 4 and 5 in the proposed horseshoe structure of the first 4 Ig domains (Su et al., 1998; Freigang et al., 2000; De Angelis et al., 2001; Jacob et al., 2002). Therefore the data provides an explanation for certain pathological mutations affecting exon 2 of L1 that cause L1 spectrum (Jouet et al., 1995 b; Finck et al., 2000; De Angelis et al., 2001).

## **2 The L1 mutations L1C264Y and L1 $\Delta$ hbs result in impaired protein trafficking**

When CHO cells were transiently transfected with L1C264Y and L1 $\Delta$ hbs, significantly reduced amounts of protein were found at the cell surface compared to L1wt, sL1, or L1ex. Cell surface levels of L1 $\Delta$ hbs and L1C264Y decreased further with increasing time after transfection. Furthermore, stably transfected CHO cells did not express detectable levels of the L1 $\Delta$ hbs and L1C264Y variants

at their cell surface. However, immunoblot analysis of total cell culture lysates revealed similar amounts of L1 protein for all L1 variants analyzed (i.e. L1wt, sL1, L1 $\Delta$ E2, L1 $\Delta$ E27, L1ex, L1 $\Delta$ hbs, and L1C264Y), demonstrating a similar transfection efficiency for all constructs. While a prominent 220 kD band was observed in L1wt-, sL1-, and L1ex-transfected cells, this band was very weak in short-term and absent in long-term cultures transfected with the L1 $\Delta$ hbs or L1C264Y constructs. Instead, for these two mutations, a 190 kD form of L1 was detected as the prominent L1-immunoreactive band. This 190 kD form was not labeled in cell surface biotinylation experiments, indicative for an intracellular localization of L1 $\Delta$ hbs or L1C264Y. To discuss these and further data about these L1 mutations in more detail, the general mechanisms of how mutated proteins can be retained intracellularly are illustrated in the next chapter.

### 3 Retention of misfolded proteins in the ER

The ER is the subcellular site where glycoproteins such as L1 are synthesized, acquire their proper folding, and become *de novo* N-glycosylated. In addition, the ER contains mechanisms to monitor the fidelity of these early biosynthetic events of the proteins. This has been called 'ER quality control', a mechanism that prevents export of incompletely or improperly folded proteins from the ER to the Golgi apparatus (Hammond and Helenius, 1995; Kopito, 1997). Therefore, cellular systems have evolved sets of ER resident helper proteins termed 'molecular chaperons' which facilitate folding of proteins and counteract misfolding and aggregation during the folding process. Examples for such proteins in the ER are family members of Hsp70 (heat shock protein 70; e.g. BiP (immunoglobulin heavy chain-binding protein); Bukau and Horwich, 1998), Hsp90 (Grp94 (glucose regulated protein); Bose et al., 1999), and lectin (carbohydrate-binding proteins) chaperones (calnexin, calreticulin) (Beissinger and Buchner, 1998). For example, calnexin (CNX), a membrane-associated lectin, is involved in the processing of N-linked glycoproteins and is part of the ER quality control, by which misfolded proteins may be retained in the ER (Parodi, 2000 a, b).

Biosynthesis of all N-linked oligosaccharides starts in the rough ER with cotranslational transfer of a dolichol-*P-P*-linked precursor oligosaccharide

(Glc<sub>3</sub>Man<sub>9</sub>GlcNAc<sub>2</sub>) to Asn residues in nascent polypeptide chains (Fig. 30; step 1). From the triglycosylated core glycan three glucose and one mannose residues are cleaved off by three different enzymes (glucosyltransferase I and II,  $\alpha$ -mannosidase; Fig. 30; step 2 and 3). During this process of glycan trimming, glycoproteins get also folded, assisted by chaperones and mediated by isomerases. Correctly folded proteins are then able to exit from the ER to the Golgi network for further processing of the glycans. The ER resident enzyme glucosyltransferase is able to add one glucose residue to the Man<sub>7-9</sub> oligosaccharide which is linked to unfolded or misfolded, thus not correctly folded glycoproteins (Fig. 30; step 3a). This enzyme is therefore a sensor for the folding state of glycoproteins. Subsequently, CNX selectively binds monoglucosylated glycans and prevents folding of the adjacent amino acid segments. The removal of the terminal glucose by glucosyltransferase II releases the ligand from CNX. If protein folding is still incomplete, a next cycle of CNX binding is initiated to drive the folding process towards completion. Thus, CNX prevents premature folding and aggregation of newly made proteins, therefore allowing a functional interaction

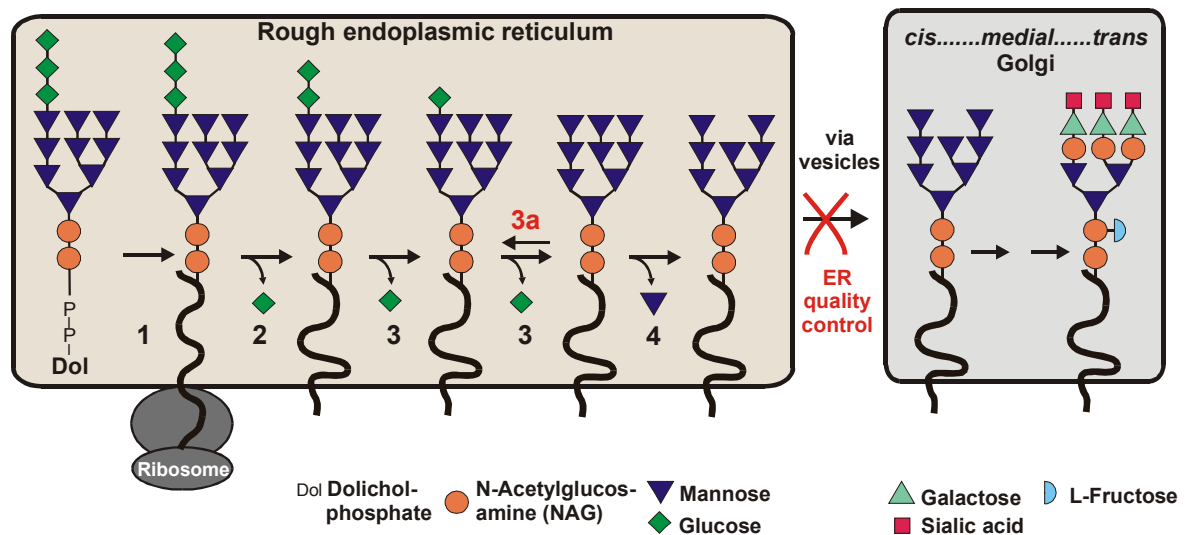


**Figure 28: Addition and initial processing of N-linked oligosaccharides in the rough ER of vertebrate cells and decision of further transport to the Golgi network by the ER quality control.** The Glc<sub>3</sub>Man<sub>9</sub>GlcNAc<sub>2</sub> precursor is transferred from the dolichol carrier to a susceptible Asn residue on a nascent protein as soon as the asparagine crosses to the luminal side of the ER (step 1). In three separate reactions, one glucose residue (step 2), then two glucose residues (step 3), and finally one mannose residue (step 4) are removed. Re-addition of one glucose residue (step 3a) is part of the ER quality control process. Following these reactions, the newly made protein is transported in a vesicle to the Golgi network for further processing of the glycans resulting in more complex oligosaccharide structures.

between the glycoproteins and classical ER chaperones (e.g. Bip) and other folding assistant proteins. At the same time CNX retains unfolded or misfolded glycoproteins within the ER (Ou et al., 1993; Sousa et al., 1992; Chen et al., 1995; for reviews see: Trombetta and Helenius, 1998; Chevet et al, 1999; Parodi, 2000 a, b). In addition to CNX, other chaperones are involved in the retention of misfolded proteins, such as BiP (Bonnerot et al., 1994) and GRP94 (Melnick et al, 1992).

Cells respond to accumulation of unfolded proteins in the rough ER, e.g. by elevating the transcription of sets of target genes or by slowing general translation. This reaction to ER stress is known as the 'unfolded protein response' (UPR). As sensors for misfolded proteins, several transmembrane kinases are suggested (e.g.: PERK /PEK (Silverman and Williams, 1999; Shi et al., 1998); Ire1p and Ern1p (Shamu and Walter, 1996; Shamu, 1998; Tirasophon et al, 1998; Okamara et al., 2000)), which communicate the ER stress to the cytosol. Signal transduction mechanisms finally induce the transcription of genes with an UPR promoter element, found for diverse genes, including chaperones and components of the quality control but also elements of the apoptotic machinery. Therefore, the UPR might function to increase the probability of correct folding as well as the ability to retain and degrade misfolded proteins or to induce cell death after long-term stress. These tasks are important for the cell, since a failure of correct folding of proteins not only disturbs the ER function but also exposes the cell to the potential toxic effect of unfolded proteins. (for review: Patil and Walter, 2001; Chevet et al., 1999; Imaizumi et al., 2001).

#### **4 L1 $\Delta$ hbs and L1C264Y are retained in the ER**

The occurrence of L1 $\Delta$ hbs and L1C264Y protein with a reduced molecular weight of 190 kD suggested differences in the glycosylation state when compared to L1wt. Indeed, L1 $\Delta$ hbs and L1C264Y protein was sensitive to endo H digestion, an enzyme which cleaves N-glycans with terminal mannose residues. Since such glycans are characteristic for glycoproteins within the ER and early Golgi compartments, and since the ER is the 'checkpoint' for further transport to the Golgi network, whereas the glycans of glycoproteins are rapidly further modified in

the Golgi network, it is evident that L1 $\Delta$ hbs and L1C264Y are retained within the ER most likely because of a misfolding of the mutated proteins. Such a misfolding is conceivable in the case of L1C264Y due to the fact that the substituted cysteine residue is essential for the formation of a disulfide bridge in the third Ig-like domain of L1. The amino acid Arg at position 184 which is affected by the 14 amino acid deletion of L1 $\Delta$ hbs is suggested to be a key residue, affecting the structure of the corresponding Ig domain in L1 (Bateman et al., 1996). Therefore, it is likely that the proposed structural changes might lead to ER retention. Two pathogenic missense mutations of the Arg-184 residues, R184Q and R184W, cause indeed severe phenotypes in humans (Jouet et al., 1994; Fransen et al., 1996).

An intracellularly located 190 kD protein in addition to a full length cell surface expressed 200 kD protein form was also found in lysates of cells transfected with L1wt, sL1 or L1ex. This finding was also observed in other studies (e.g. Moulding et al., 2000) and might be related to artificial effects of the cell culture system. The above-mentioned expression of high levels of highly glycosylated L1 (putatively 21 N-glycosylation sites) might overstrain the postranslational processing machinery of the ER. Therefore, part of the L1 protein is not yet surface-expressed rather than permanently retained in the ER. Similarly, in CHO cells transfected with N-CAM (containing 6 N-glycosylation sites), also significant amounts of the N-CAM protein was endo H-sensitive. In comparison to L1-transfected CHO cells, the amount of endo H-sensitive N-CAM protein in relation to the cell surface expressed protein was lower (Markus Delling, ZMNH, personal communication). In addition, mice which overexpress L1 in neurons (transgenic expression of L1 under the control of the Thy-1 promoter; about 200-300 % of L1 levels found in wt mice) a significant amount of L1 is present as an endo H-sensitive 190 kD protein (Meike Zerwas, ZMNH, personal communication).

## **5 Studies on L1 extracellular missense mutations**

The extracellular pathogenic L1 missense mutations R184Q and D598N have recently been studied *in vitro* and reported to be expressed at only very low levels at the cell surface and to be incompletely processed for up to 24 hours after infection (Moulding et al., 2000). In addition, variable degrees of reduced cell

surface expression have recently been demonstrated for a variety of extracellular missense mutations, including R184Q and C264Y, whereas the D598N mutation was shown to be expressed at the cell surface (De Angelis et al., 2002). Low levels of cell surface expression of mutated L1 proteins detected in these studies are in line with our observation of weak cell surface expression of L1 $\Delta$ hbs and L1C264Y in short-term, transient transfection experiments. However, this weak cell surface expression disappeared after prolonged culture periods. We suggest that the early cell surface expression of L1 $\Delta$ hbs and L1C264Y is the result of an ineffective retention of misfolded proteins within the ER at initial stages of expression, rather than a targeting of the 190 kD form of L1 to the cell surface (as supposed by Moulding et al., 2000). Indeed, biotinylation experiments with live cells revealed labeling of the 220 kD form of L1 and its proteolytic cleavage fragments, but not of the 190 kD form. An initially ineffective ER retention of misfolded protein might be likely for cell culture systems in which high levels of protein are expressed from the introduced DNA (driven by a constitutive CMV promoter). Since accumulation of misfolded proteins triggers an UPR in the ER which subsequently initiates increased expression of chaperones and components of the ER quality control, ER retention of misfolded proteins might become more effective after prolonged time periods in culture.

The recently published report of apparent cell surface expression of the missense mutation R184Q in HEK 293 cells (Needham et al., 2001) is probably explained by the use of paraformaldehyde-fixed cells for immunocytochemical analysis, given that such a treatment permeabilizes cells and thus results in labeling of intracellularly located L1 protein (Moulding et al., 2000; the present study). Indeed, in a previous study five missense mutations, including R184Q and C264Y, were proposed to be cell surface expressed based on immunocytochemistry of paraformaldehyde-fixed cells (De Angelis et al., 1999). Amendatory, these L1 mutations were later demonstrated to be intracellularly located (De Angelis et al., 2001).

The combined *in vitro* observations of the present and previous studies (De Angelis et al., 2002) demonstrate that mutations in the extracellular domain of L1 interfere with the targeting of the protein to the cell surface, suggesting that many mutations in the extracellular domain of L1 might correspond to loss of function mutations.

## 6 Mutations of the intracellular domain

In contrast to mutations in the extracellular domain, L1ex, which lacks most of the intracellular domain of L1, is expressed at similarly high levels at the cell surface as L1wt. Strong cell surface expression has also been reported for the intracellularly located pathogenic mutation S1194L (Moulding et al., 2000). Based on these findings, we hypothesize that the intracellular domain of L1 is unlikely to be important for correct folding of the protein, i.e. it is not subject of the quality control within the ER. However, pathogenic mutations in the intracellular domain might affect one or more functions of this domain, e.g. interactions with the skeleton or signal transduction cascades. For example, the two missense mutations (S1224L (the contribution of this Ser residue to ankyrin was previously unknown), and Y1229H) which alter amino acids within or nascent to the ankyrin binding motif (Fig. 4) were shown to reduce the ability of L1 to recruit ankyrin to the plasma membrane; the mutation S1224L was additionally shown to enhance clatherin-dependent endocytosis (Needham et al., 2001).

## 7 The L1C264Y-transgenic mouse

To evaluate whether an intracellular retention of L1C264Y indeed causes loss of L1 function and therefore lead to the severe clinical picture of patients carrying this mutation (Jouet et al., 1993), we generated a transgenic mouse line expressing L1C264Y under regulatory elements of the L1 gene (Kallunki et al., 1998). The transgenic animals were crossed into a L1-deficient background (Dahme et al., 1997; Rolf et al., 2001) to study expression of the transgene and its effects on the development of the nervous system. The spatial and temporal expression of L1C264Y was comparable to L1 expression in wt mice. However, we found an exclusive expression of a 190 kD form of L1 which lacks Golgi-type sugar processing by immunoblot analysis, and an intracellular localization of the L1 protein by immunohistochemistry, in line with our observations *in vitro*. Thus, L1C264Y transgenic mice are likely to represent functional null mutants. Analysis of transgenic mice and L1-deficient animals indeed revealed similar phenotypes of both mutant mouse lines. Both, L1C264Y transgenic and L1-deficient animals

were smaller in size, exhibited increased mortality, displayed hypoplasia of the CST and pathfinding errors of corticospinal axons at the pyramidal decussation, and showed impaired interactions between nonmyelinating Schwann cells and axons in peripheral nerves (Dahme et al., 1997; Cohen et al., 1998; Haney et al., 1999).

## **8 The fate of intracellularly retained misfolded protein**

The similar pathology of L1C264Y transgenic and L1-deficient mice allows speculations about the fate of intracellularly located L1 mutant protein. For a detailed discussion a general overview of the molecular consequences of mutations is given. Missense mutations and short deletions and insertions can be divided into two groups with respect to their molecular consequences at the protein level: 1) mutations affecting functional sites, which are characterized by the presence of normal amounts of protein at the correct place, but impaired functional activity (Fig. 29-1), and 2) mutations that decrease or abolish the level of mutant protein at their designated cellular location (Fig. 29-2A/B; Bross et al., 1999). Frequent causes for the second group of mutations are disturbances of the folding process of proteins. Diseases which are linked to these molecular mechanisms are termed conformational or protein folding diseases (Thomas et al., 1995; Beissinger and Buchner, 1998), and two subgroups are distinguishable.

In the first subgroup aberrant folded proteins form insoluble aggregates and thus can not be translocated into transport vesicles or into the cytosol for degradation (Fig. 29-2A; see below; Pfeffer and Rothman, 1987). Ongoing accumulation of undegraded, misfolded proteins in the ER, triggers the UPR and is likely to clog the secretory pathway and to become toxic to the cells (Kaufman, 1999; Klausner and Sita, 1990; Stevens and Argon, 1999). For example, in special forms of  $\alpha$ 1-antitrypsin deficiency (about 10-15 % of all  $\alpha$ 1-antitrypsin deficiency causing mutations), missense mutations in the gene encoding  $\alpha$ 1-antitrypsin lead to the formation of crystalline-like aggregates that are not exported from the ER. As a result, the secretion of other proteins is also impaired, ultimately leading to cell death (Carlson et al., 1989; Lomas et al., 1992; Lomas, 1996). Therefore, patients with such mutations develop liver diseases in addition to emphysema, the

general syndrome of  $\alpha$ 1-antitrypsin deficiency (Perlmutter, 1998; Wu et al., 1994). Similarly, cell toxic effects have been found for mutated and misfolded PLP (proteolipid protein; Jung et al., 1996). Mutations in the PLP gene result in severe dysmyelination of the CNS of *jimpy* mice or cause Pelizaeus-Merzbacher disease in humans, largely due to the death of oligodendrocytes (Knapp et al., 1986; Vermeesch et al., 1990; Gencic and Hudson, 1990). With regard to the occurrence of cell death or impaired maturation of other proteins in the ER as a consequence of aggregated misfolded protein, it is evident that the underlying mutations act in a "dominant-negative" fashion or exhibit a combination of loss- and gain-of-function effects. Indeed, the phenotype of the natural occurring *jimpy* mouse could not be completely rescued by the introduction of a wild-type PLP transgene (Nadon et al., 1994; Schneider et al., 1995). In contrast, dysmyelination was reduced to moderate levels when the expression of the mutated allele was down-regulated (Boison and Stoffel, 1994; Boison et al., 1995).

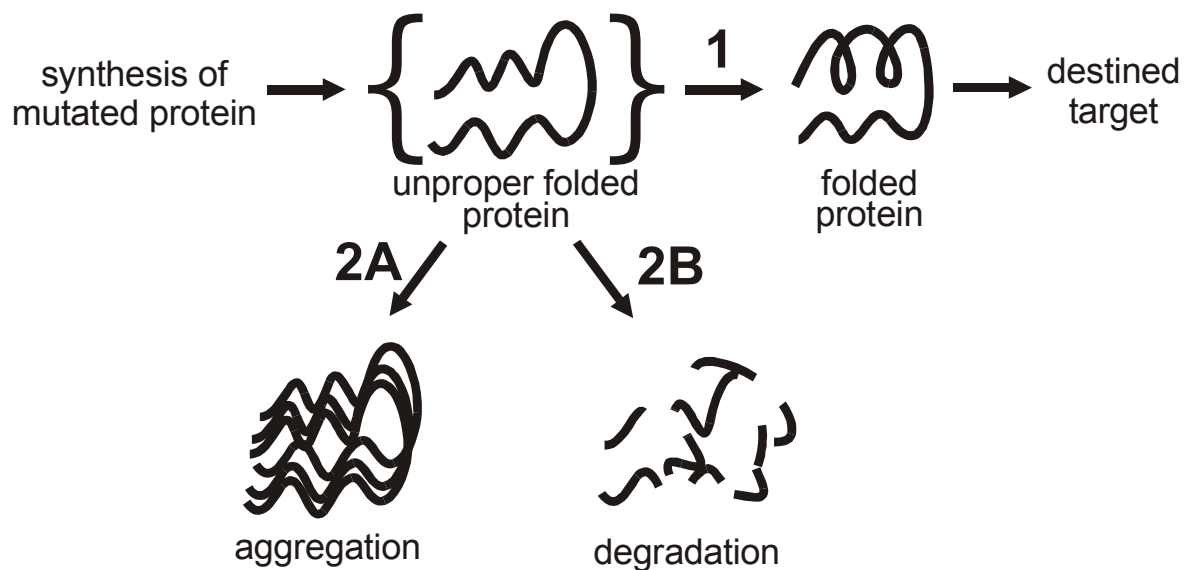


**Figure 29: Possible fate of mutated proteins.** Mutated proteins that are correctly folded are further transported to their destined targets (1). Misfolded proteins with folding mutations can either form insoluble aggregates (2A) or become degraded (2B).

The second group of conformational diseases is characterized by a rapid degradation of misfolded proteins (Fig. 29-2B), the so-called ER-associated degradation (ERAD; McCracken and Brodsky, 1996). The development of a system that is not only able to recognize irreversibly misfolded proteins, but to

target them for degradation, is an essential function for cell survival. The major mechanism of ERAD is the dislocation of misfolded proteins from the ER, presumably via reverse translocation through the ER translocon (Wiertz et al., 1996; Plemper and Wolf, 1999) to the cytosol for selective protein degradation by the ubiquitin-proteasome pathway (Ciechanover, 1994; Goldberg, 1995; Jentsch, 1995; Hiller et al., 1996). The steps involved in this process include partial proteolysis of the misfolded protein within the ER, ubiquitination, extraction from the ER, and the removal of all previously attached N-linked carbohydrates before complete proteasomal digestion (Kopito, 1997; Coux et al., 1996). The core complex of proteasomes is composed of four stacked seven-membered rings of subunits, which build a cylindrical structure and contain the proteolytic enzymes and two apertures, one at each side of the cylinder, which allow access to the cavity only for unfolded proteins (Groll et al., 1997). A prominent example for such a mechanism is cystic fibrosis, in which the most common CFTR (cystic fibrosis transmembrane conductance regulator) mutation ( $\Delta F508$ ) is retained in the ER for longer times than the wild-type form, followed by ubiquitination and retrograde transport to the cytosol where it is degraded by the proteasome (Jensen et al., 1995; Ward et al., 1995). Further examples are most forms of  $\alpha 1$ -antitrypsin deficiency (gene:  $\alpha 1$ -antitrypsin; Mahadeva et al., 1998), Tay-Sachs disease (gene:  $\beta$ -hexosaminidase; Lau and Neufeld, 1989), Charcot-Marie-Tooth (gene: connexin 32; Deschenes et al., 1997; Bone et al., 1997), familial hypercholesterolemia (gene: LDL receptor; Hobbs et al., 1990), and retinitis pigmentosa (gene: rhodopsin; Olsson et al., 1992). In general, rapid ERAD of the mutated and misfolded protein leads to loss of function of the affected protein.

The L1C264Y transgenic mouse line expresses about 30 % of the amount of L1 protein found in wt mice. This is the highest amount found in five founder lines. It is likely that this reduced amount of L1 might be due to a decreased half-life of the mutated L1 protein as a result of rapid degradation, which is typical for diseases leading to ERAD of proteins with folding mutations (Bross et al., 1999). For example the  $\Delta F508$  variant that causes cystic fibrosis is degraded almost to completion (Ward and Kopito, 1994). Therefore, the apparent amount of L1 protein in L1C264Y transgenic, compared to that in wt mice, allows no direct statement on the amount of *de novo* synthesized L1C264Y versus L1 wt protein. More

information about the expression levels of L1 in L1C264Y versus wt mice might be obtained from quantification of mRNA levels.

The phenotype of L1C264Y transgenic mice is similar to that of L1-deficient mice. Therefore, we do not assume negative effects of intracellularly retained L1C264Y on cell viability or function, as seen in other diseases characterized by an aggregation of proteins within cells. Indeed, we have not observed any obvious decrease in the number of cells that normally express L1 at the cell surface in the L1C264Y mutant in comparison to the L1-deficient mouse. Furthermore, the area of the CST was not further reduced in L1C264Y in comparison to L1-*y* mice. The cortical pyramidal neurons are likely to be affected in case of decreased cell viability as a result of intracellular accumulation of mutated protein, since these cells normally express high levels of L1 protein. In addition, we did not observe any abnormalities in L1+/*y*\_C264Y mice (which express L1C264Y in addition to the endogenous wild-type L1) in comparison to wt mice in terms of body weight, survival, or size of the CST, arguing against the possibility of dominant-negative effects of the L1C264Y protein. We thus hypothesize that mutated L1 variants that are retained within the ER become degraded by proteasomes after release to the cytosol without exerting negative effects on cell survival or function.

## 9 Concluding remarks and outlook

In summary, we have confirmed and extended observations that demonstrate a reduction or lack of cell surface expression of mutated L1 variants *in vitro* (Moulding et al., 2000; De Angelis et al., 2002). More importantly, we have demonstrated for the first time that a pathogenic missense mutation of L1 results in lack of cell surface expression *in vivo*, causing a phenotype indistinguishable from that of the L1-deficient mouse. Other extracellular missense mutations of L1 have been shown to be transported to the cell surface (De Angelis et al., 2001) affecting homophilic and/or heterophilic binding, e.g. to axonin-1/TAG-1/TAX-1 or contactin /F11/F3. Thus, impaired trafficking of L1 to the cell surface, in addition to abnormal heterophilic and homophilic interactions of mutated L1 proteins that reach the cell surface (De Angelis et al., 1999 and 2002), potentially explains the

high phenotypic variability caused by L1 mutations, particularly within the extracellular domain of the protein.

Whether our results of impaired cell surface expression of the L1C264Y mutation and the proposed underlying mechanisms (see below) can be extrapolated to other L1 mutations that are not expressed at the cell surface remains to be investigated. Results of the present study have important implications for the design of such investigations in cell culture systems. A complete retention of mutated L1 and exclusive expression of the 190 kD protein in L1 $\Delta$ hbs- and L1C264Y-transfected cells was found only after prolonged culture times and thus closely resembles the *in vivo* findings, namely the exclusive occurrence of an intracellularly located 190 kD protein in L1C264Y transgenic mice. Therefore, prolonged times in culture might be important to make reliable predictions on whether a pathological missense mutation is expressed *in vivo* on the cell surface or not. Moreover, our findings suggest that the occurrence of a 190 kD form of mutated L1 which lacks Golgi-type sugar processing is sufficient to predict an intracellular retention of mutated L1 variants.

We suggest ER retention followed by ERAD as the most likely underlying molecular pathomechanism of the L1C264Y mutated protein, which ultimately results in the complete loss of L1 function. This assumption has to be verified in further experiments *in vitro*, for example by inhibition of the proteasome degradation pathway (e.g. with lactacystin, Novoradovskaya et al., 1998), estimation of degradation rates (e.g. by pulse-chase experiments), or direct verification or inhibition of protein binding to chaperones involved in ER retention (e.g. to CNX; e.g. by co-immunoprecipitation). Similar investigations, particularly the binding/colocalization to chaperones or inhibition of supposed interactions and pathways can be performed *in vivo* using the L1C264Y transgenic mouse as a model system or by using primary neurons isolated from L1C264Y transgenic mice. Analysis of mice carrying two L1C264Y transgenic alleles in a L1-deficient background, and thus presumably expressing higher levels of mutated L1 protein, might give further insights into the fate of intracellularly located, mutated L1.

Some of these experiments may also provide important insights into possible therapeutical approaches. First attempts to develop such approaches are based on the regulation of ER retention and degradation systems by compounds that

target some of its members, with the final aim to restore the transport of the protein to the cell surface. In several studies, rescue of the ER-sequestered mutant proteins was achieved using either chemical (Sato et al., 1996; Tamarappoo and Verkman, 1998) or specific pharmacological (Morello et al., 2000) chaperones, or inhibitors of the degradation pathway, for example lactacystin, which can result in accumulation of the protein but in some cases also in a partial restoration of protein transport to the cell surface (Novoradovskaya et al., 1998). If such approaches are applicable for distinct L1 mutations depends, among other factors, on whether a particular mutation interferes with the normal function of the L1 protein. Investigations using purified mutated L1-Fc fragments have indeed demonstrated that many of the pathogenic L1 mutations that are now known not to reach the cell surface impair homophilic and/or heterophilic binding to TAX-1, among them R184Q and C264Y (De Angelis et al., 1999 and 2002).

## V References

- Angst BD, Marcozzi C, Magee AI (2001) The cadherin superfamily: diversity in form and function. *J Cell Sci* 114: 629-641.
- Aplin AE, Howe A, Alahari SK, Juliano RL (1998) Signal transduction and signal modulation by cell adhesion receptors: the role of integrins, cadherins, immunoglobulin-cell adhesion molecules, and selectins. *Pharmacol Rev* 50: 197-263.
- Appel F, Holm J, Conscience JF, Schachner M (1993) Several extracellular domains of the neural cell adhesion molecule L1 are involved in neurite outgrowth and cell body adhesion. *J Neurosci* 13: 4764-4775.
- Appel F, Holm J, Conscience JF, von Bohlen und Halbach F, Faissner A, James P, Schachner M. (1995) Identification of the border between fibronectin type III homologous repeats 2 and 3 of the neural cell adhesion molecule L1 as a neurite outgrowth promoting and signal transducing domain. *J Neurobiol* 28: 297-312.
- Archer FR, Doherty P, Collins D, Bolsover SR (1999) CAMs and FGF cause a local submembrane calcium signal promoting axon outgrowth without a rise in bulk calcium concentration. *Eur J Neurosci* 11: 3565-3573.
- Asou H, Miura M, Kobayashi M, Uyemura K (1992) The cell adhesion molecule L1 has a specific role in neural cell migration. *Neuroreport* 3: 481-484.
- Ausrubel, FM (1996). *Current Protocols in Molecular Biology*. (Brooklyn, New York: Greene Publishing Associates, Inc.).
- Bartsch U, Kirchhoff F, Schachner M (1989) Immunohistological localization of the adhesion molecules L1, N-CAM, and MAG in the developing and adult optic nerve of mice. *J Comp Neurol* 284: 451-462.
- Bateman A, Jouet M, MacFarlane J, Du JS, Kenwrick S, Chothia C (1996) Outline structure of the human L1 cell adhesion molecule and the sites where mutations cause neurological disorders. *EMBO J* 15: 6050-6059.

- Bayer SA (1980) Development of the hippocampal region in the rat. I. Neurogenesis examined with 3H-thymidine autoradiography. *J Comp Neurol* 190: 87-114.
- Beer S, Oleszewski M, Gutwein P, Geiger C, Altevogt P (1999) Metalloproteinase-mediated release of the ectodomain of L1 adhesion molecule. *J Cell Sci* 112 (Pt 16): 2667-2675.
- Beissinger M, Buchner (1998) How chaperones fold proteins. *Biol Chem* 379: 245-259.
- Bennett V, Chen L (2001) Ankyrins and cellular targeting of diverse membrane proteins to physiological sites. *Curr Opin Cell Biol* 13: 61-67.
- Bianchine JW, Lewis RC, Jr. (1974) The MASA syndrome: a new heritable mental retardation syndrome. *Clin Genet* 5: 298-306.
- Bickers D, Adams R (1949) Hereditary stenosis of the aqueduct of Sylvius as a cause of congenital hydrocephalus. *Brain* 72: 246-262.
- Boison D, Bussow H, D'Urso D, Muller HW, Stoffel W (1995) Adhesive properties of proteolipid protein are responsible for the compaction of CNS myelin sheaths. *J Neurosci* 15:5502-5513.
- Boison D, Stoffel W (1994) Disruption of the compacted myelin sheath of axons of the central nervous system in proteolipid protein-deficient mice. *Proc Natl Acad Sci U S A* 91: 11709-11713.
- Bone LJ, Deschenes SM, Balice-Gordon RJ, Fischbeck KH, Scherer SS (1997) Connexin32 and X-linked Charcot-Marie-Tooth disease. *Neurobiol Dis* 4: 221-230.
- Bonnerot C, Marks MS, Cosson P, Robertson EJ, Bikoff EK, Germain RN, Bonifacio JS (1994) Association with BiP and aggregation of class II MHC molecules synthesized in the absence of invariant chain. *EMBO J* 13: 934-944.
- Bose S, Weikl T, Gugl H, Buchner J (1999) Chaperone function of Hsp90-associated proteins. *Science* 274: 1715-1717.

- Brackenbury R, Thiery JP, Rutishauser U, Edelman GM (1977) Adhesion among neural cells of the chick embryo. I. An immunological assay for molecules involved in cell-cell binding. *J Biol Chem* 252: 6835-6840.
- Brittis PA, Silver J, Walsh FS, Doherty P (1996) Fibroblast Growth Factor Receptor Function Is Required for the Orderly Projection of Ganglion Cell Axons in the Developing Mammalian Retina. *Mol Cell Neurosci* 8: 120-128.
- Bross P, Corydon TJ, Andresen BS, Jorgensen MM, Bolund L, Gregersen N (1999) Protein misfolding and degradation in genetic diseases. *Hum Mutat* 14: 186-198.
- Brummendorf T, Hubert M, Treubert U, Leuschner R, Tarnok A, Rathjen FG (1993) The axonal recognition molecule F11 is a multifunctional protein: specific domains mediate interactions with Ng-CAM and restrictin. *Neuron* 10: 711-727.
- Brummendorf T, Rathjen FG (1995) Cell adhesion molecules 1: immunoglobulin superfamily. *Protein Profile* 2: 963-1108.
- Brummendorf T, Kenwrick S, Rathjen FG (1998) Neural cell recognition molecule L1: from cell biology to human hereditary brain malformations. *Curr Opin Neurobiol* 8: 87-97.
- Buchstaller A, Kunz S, Berger P, Kunz B, Ziegler U, Rader C, Sonderegger P (1996) Cell adhesion molecules NgCAM and axonin-1 form heterodimers in the neuronal membrane and cooperate in neurite outgrowth promotion. *J Cell Biol* 135: 1593-1607.
- Bukau B, Horwich AL (1998) The Hsp70 and Hsp60 chaperone machines. *Cell* 92: 351-366.
- Burden-Gulley SM, Payne HR, Lemmon V (1995) Growth cones are actively influenced by substrate-bound adhesion molecules. *J Neurosci* 15: 4370-4381.
- Burgoon MP, Grumet M, Mauro V, Edelman GM, Cunningham BA (1991) Structure of the chicken neuron-glia cell adhesion molecule, Ng-CAM: origin of the polypeptides and relation to the Ig superfamily. *J Cell Biol* 112: 1017-1029.

- Burgoon MP, Hazan RB, Phillips GR, Crossin KL, Edelman GM, Cunningham BA (1995) Functional analysis of posttranslational cleavage products of the neuron-glia cell adhesion molecule, Ng-CAM. *J Cell Biol* 130: 733-744.
- Carlson JA, Rogers BB, Sifers RN, Finegold MJ, Clift SM, DeMayo FJ, Bullock DW, Woo SL (1989) Accumulation of PiZ alpha 1-antitrypsin causes liver damage in transgenic mice. *J Clin Invest* 83: 1183-1190.
- Castellani V, Chedotal A, Schachner M, Faivre-Sarrailh C, Rougon G (2000) Analysis of the L1-deficient mouse phenotype reveals cross-talk between Sema3A and L1 signaling pathways in axonal guidance. *Neuron* 27: 237-249.
- Chang S, Rathjen FG, Raper JA (1987) Extension of neurites on axons is impaired by antibodies against specific neural cell surface glycoproteins. *J Cell Biol* 104: 355-362.
- Chapman VM, Keitz BT, Stephenson DA, Mullins LJ, Moos M, Schachner M (1990) Linkage of a gene for neural cell adhesion molecule, L1 (CamL1) to the Rsvp region of the mouse X chromosome. *Genomics* 8: 113-118.
- Chen W, Helenius J, Braakman I, Helenius A (1995) Cotranslational folding and calnexin binding during glycoprotein synthesis. *Proc Natl Acad Sci U S A* 92: 6229-6233.
- Chevet E, Jacob CA, Thomas DY, Bereron JJ (1999) Calnexin family members as modulators of genetic diseases. *Semin Cell Dev Biol* 10: 473-480.
- Ciechanover A (1994) The ubiquitin-proteasome proteolytic pathway. *Cell* 79: 13-21.
- Clark EA, Brugge JS (1995) Integrins and signal transduction pathways: the road taken. *Science* 268: 233-239.
- Cohen NR, Taylor JS, Scott LB, Guillery RW, Soriano P, Furley AJ (1998) Errors in corticospinal axon guidance in mice lacking the neural cell adhesion molecule L1. *Curr Biol* 8: 26-33.
- Coutelle O, Nyakatura G, Taudien S, Elgar G, Brenner S, Platzer M, Drescher B, Jouet M, Kenwrick S, Rosenthal A (1998) The neural cell adhesion molecule L1:

- genomic organisation and differential splicing is conserved between man and the pufferfish *Fugu*. *Gene* 208: 7-15.
- Coux O, Tanaka K, Goldberg AL (1996) Structure and functions of the 20S and 26S proteasomes. *Annu Rev Biochem* 65: 801-847.
- Cunningham BA (1995) Cell adhesion molecules as morphoregulators. *Curr Opin Cell Biol* 7: 628-633.
- Dahlin-Huppe K, Berglund EO, Ranscht B, Stallcup WB (1997) Mutational analysis of the L1 neuronal cell adhesion molecule identifies membrane-proximal amino acids of the cytoplasmic domain that are required for cytoskeletal anchorage. *Mol Cell Neurosci* 9: 144-156.
- Dahme M, Bartsch U, Martini R, Anliker B, Schachner M, Mantei N (1997) Disruption of the mouse L1 gene leads to malformations of the nervous system. *Nat Genet* 17: 346-349.
- Davis JQ, Bennett V (1993) Ankyrin-binding activity of nervous system cell adhesion molecules expressed in adult brain. *J Cell Sci Suppl* 17: 109-117.
- Davis JQ, Bennett V (1994) Ankyrin binding activity shared by the neurofascin/L1/NrCAM family of nervous system cell adhesion molecules. *J Biol Chem* 269: 27163-27166.
- Dayhoff MO, Barker WC, Hunt LT (1983) Establishing homologies in protein sequences. *Methods Enzymol* 91: 524-545.
- De Angelis E, MacFarlane J, Du JS, Yeo G, Hicks R, Rathjen FG, Kenwrick S, Brummendorf T (1999) Pathological missense mutations of neural cell adhesion molecule L1 affect homophilic and heterophilic binding activities. *EMBO J* 18: 4744-4753.
- De Angelis E, Brummendorf T, Cheng L, Lemmon V, Kenwrick S (2001) Alternative use of a mini exon of the L1 gene affects L1 binding to neural ligands. *J Biol Chem* 276: 32738-32742.

- De Angelis E, Watkins A, Schafer M, Brummendorf T, Kenwrick S (2002) Disease-associated mutations in L1 CAM interfere with ligand interactions and cell-surface expression. *Hum Mol Genet* 11: 1-12.
- DeBernardo AP, Chang S (1996) Heterophilic interactions of DM-GRASP: GRASP-NgCAM interactions involved in neurite extension. *J Cell Biol* 133: 657-666.
- Debiec H, Christensen EI, Ronco PM (1998) The cell adhesion molecule L1 is developmentally regulated in the renal epithelium and is involved in kidney branching morphogenesis. *J Cell Biol* 143: 2067-2079.
- Demyanenko GP, Tsai AY, Maness PF (1999) Abnormalities in neuronal process extension, hippocampal development, and the ventricular system of L1 knockout mice. *J Neurosci* 19: 4907-4920.
- Deschenes SM, Walcott JL, Wexler TL, Scherer SS, Fischbeck KH (1997) Altered trafficking of mutant connexin32. *J Neurosci*. 1997 Dec 1;17(23):9077-84.
- Djabali M, Mattei MG, Nguyen C, Roux D, Demengeot J, Denizot F, Moos M, Schachner M, Goridis C, Jordan BR (1990) The gene encoding L1, a neural adhesion molecule of the immunoglobulin family, is located on the X chromosome in mouse and man. *Genomics* 7: 587-593.
- Doherty P, Williams E, Walsh FS (1995) A soluble chimeric form of the L1 glycoprotein stimulates neurite outgrowth. *Neuron* 14: 57-66.
- Doherty P, Walsh FS (1996) CAM-FGF receptor interactions: a model for axonal growth. *Mol Cell Neurosci* 8: 99-111.
- Doherty P, Smith P, Walsh FS (1996) Shared cell adhesion molecule (CAM) homology domains point to CAMs signalling via FGF receptors. *Perspect Dev Neurobiol* 4: 157-168.
- Ebeling O, Duczmal A, Aigner S, Geiger C, Schollhammer S, Kemshead JT, Moller P, Schwartz-Albiez R, Altevogt P (1996) L1 adhesion molecule on human lymphocytes and monocytes: expression and involvement in binding to alpha v beta 3 integrin. *Eur J Immunol* 26: 2508-2516.

- Edelman GM, Cunningham BA, Gall WE, Gottlieb PD, Rutishauser U, Waxdal MJ (1969) The covalent structure of an entire gammaG immunoglobulin molecule. *Proc Natl Acad Sci U S A* 63: 78-85.
- Edelman G, (1986) Cell adhesion and the molecular processes of morphogenesis. *Annu Rev Biochem* 54: 135-169.
- Engel J (1991) Common structural motifs in proteins of the extracellular matrix. *Curr Opin Cell Biol* 3: 779-785.
- Faissner A, Kruse J, Nieke J, Schachner M (1984) Expression of neural cell adhesion molecule L1 during development, in neurological mutants and in the peripheral nervous system. *Brain Res* 317: 69-82.
- Faissner A, Teplow DB, Kubler D, Keilhauer G, Kinzel V, Schachner M (1985) Biosynthesis and membrane topography of the neural cell adhesion molecule L1. *EMBO J* 4: 3105-3113.
- Felding-Habermann B, Silletti S, Mei F, Siu CH, Yip PM, Brooks PC, Cheresh DA, O'Toole TE, Ginsberg MH, Montgomery AM (1997) A single immunoglobulin-like domain of the human neural cell adhesion molecule L1 supports adhesion by multiple vascular and platelet integrins. *J Cell Biol* 139: 1567-1581.
- Finckh U, Schroder J, Ressler B, Veske A, Gal A (2000) Spectrum and detection rate of L1CAM mutations in isolated and familial cases with clinically suspected L1-disease. *Am J Med Genet* 92: 40-46.
- Fischer G, Kunemund V, Schachner M (1986) Neurite outgrowth patterns in cerebellar microexplant cultures are affected by antibodies to the cell surface glycoprotein L1. *J Neurosci* 6: 605-612.
- Fransen E, Schrandt-Stumpel C, Vits L, Coucke P, van Camp G, Willems PJ (1994) X-linked hydrocephalus and MASA syndrome present in one family are due to a single missense mutation in exon 28 of the L1CAM gene. *Hum Mol Genet* 3: 2255-2256.
- Fransen E, Lemmon V, van Camp G, Vits L, Coucke P, Willems PJ (1995) CRASH syndrome: clinical spectrum of corpus callosum hypoplasia, retardation,

adducted thumbs, spastic paraparesis and hydrocephalus due to mutations in one single gene, L1. *Eur J Hum Genet* 3: 273-284.

Fransen E, Vits L, van Camp G, Willems PJ (1996) The clinical spectrum of mutations in L1, a neuronal cell adhesion molecule. *Am J Med Genet* 64: 73-77.

Fransen E, van Camp G, Vits L, Willems PJ (1997) L1-associated diseases: clinical geneticists divide, molecular geneticists unite. *Hum Mol Genet* 6: 1625-1632.

Fransen E, D'Hooge R, van Camp G, Verhoye M, Sijbers J, Reyniers E, Soriano P, Kamiguchi H, Willemsen R, Koekkoek SK, De Zeeuw CI, De Deyn PP, Van der LA, Lemmon V, Kooy RF, Willems PJ (1998a) L1 knockout mice show dilated ventricles, vermis hypoplasia and impaired exploration patterns. *Hum Mol Genet* 7: 999-1009.

Fransen E, van Camp G, D'Hooge R, Vits L, Willems PJ (1998b) Genotype-phenotype correlation in L1 associated diseases. *J Med Genet* 35: 399-404.

Freigang J, Proba K, Leder L, Diederichs K, Sonderegger P, Welte W (2000) The crystal structure of the ligand binding module of axonin-1/TAG-1 suggests a zipper mechanism for neural cell adhesion. *Cell* 101:425-33.

Garver TD, Ren Q, Tuvia S, Bennett V (1997) Tyrosine phosphorylation at a site highly conserved in the L1 family of cell adhesion molecules abolishes ankyrin binding and increases lateral mobility of neurofascin. *J Cell Biol* 137: 703-714.

Gencic S, Hudson LD (1990) Conservative amino acid substitution in the myelin proteolipid protein of jimpymsd mice. *J Neurosci* 10: 117-124

Goldberg AL (1995) Functions of the proteasome: the lysis at the end of the tunnel. *Science* 268:522-523.

Goodman CS, Shatz CJ (1993) Developmental mechanisms that generate precise patterns of neuronal connectivity. *Cell* 72 Suppl: 77-98.

Gordon-Weeks PR, Fischer I (2000) MAP1B expression and microtubule stability in growing and regenerating axons. *Microsc Res Tech* 48: 63-74.

- Groll M, Ditzel L, Lowe J, Stock D, Bochtler M, Bartunik HD, Huber R (1997) Structure of 20S proteasome from yeast at 2.4 Å resolution. *Nature* 386: 463-471.
- Grumet M, Friedlander DR, Edelman GM (1993) Evidence for the binding of Ng-CAM to laminin. *Cell Adhes Commun* 1: 177-190.
- Gumbiner BM (1993) Proteins associated with the cytoplasmic surface of adhesion molecules. *Neuron* 11: 551-564.
- Gutwein P, Oleszewski M, Mechtersheimer S, Agmon-Levin N, Krauss K, Altevogt P (2000) Role of src kinases in the ADAM-mediated release of L1 adhesion molecule from human tumor cells. *J Biol Chem* 275: 15490-15497.
- Halliday J, Chow CW, Wallace D, Danks DM (1986) X linked hydrocephalus: a survey of a 20 year period in Victoria, Australia. *J Med Genet* 23: 23-31.
- Hammond C, Helenius A (1995) Quality control in the secretory pathway. *Curr Opin Cell Biol* 7: 523-529.
- Haney CA, Sahenk Z, Li C, Lemmon VP, Roder J, Trapp BD (1999) Heterophilic binding of L1 on unmyelinated sensory axons mediates Schwann cell adhesion and is required for axonal survival. *J Cell Biol* 146: 1173-1184.
- Hankin MH, Lagenaur CF (1994) Cell adhesion molecules in the early developing mouse retina: retinal neurons show preferential outgrowth in vitro on L1 but not N-CAM. *J Neurobiol* 25: 472-487.
- Helenius A, Aebi M (2001) Intracellular functions of N-linked glycans. *Science* 291: 2364-2369.
- Hiller MM, Finger A, Schweiger M, Wolf DH (1996) ER degradation of a misfolded luminal protein by the cytosolic ubiquitin-proteasome pathway. *Science* 273: 1725-1728.
- Hobbs HH, Russell DW, Brown MS, Goldstein JL (1990) The LDL receptor locus in familial hypercholesterolemia: mutational analysis of a membrane protein. *Annu Rev Genet* 24:133-170.

- Hogan BLM, Beddington R, Constantini F, Lacy E (1994) *Manipulating the Mouse Embryo: A Laboratory Manual*. Cold Spring, New York: Cold Spring Harbor Publications.
- Holm J, Appel F, Schachner M (1995) Several extracellular domains of the neural cell adhesion molecule L1 are involved in homophilic interactions. *J Neurosci Res* 42: 9-20.
- Horstkorte R, Schachner M, Magyar JP, Vorherr T, Schmitz B (1993) The fourth immunoglobulin-like domain of NCAM contains a carbohydrate recognition domain for oligomannosidic glycans implicated in association with L1 and neurite outgrowth. *J Cell Biol* 121: 1409-1421.
- Hortsch M, Wang YM, Marikar Y, Bieber AJ (1995) The cytoplasmic domain of the *Drosophila* cell adhesion molecule neuroglian is not essential for its homophilic adhesive properties in S2 cells. *J Biol Chem* 270: 18809-18817.
- Hortsch M (1996) The L1 family of neural cell adhesion molecules: old proteins performing new tricks. *Neuron* 17: 587-593.
- Hortsch M, O'Shea KS, Zhao G, Kim F, Vallejo Y, Dubreuil RR (1998) A conserved role for L1 as a transmembrane link between neuronal adhesion and membrane cytoskeleton assembly. *Cell Adhes Commun* 5: 61-73.
- Hortsch M (2000) Structural and functional evolution of the L1 family: are four adhesion molecules better than one? *Mol Cell Neurosci* 15: 1-10.
- Ignelzi MA, Jr., Miller DR, Soriano P, Maness PF (1994) Impaired neurite outgrowth of src-minus cerebellar neurons on the cell adhesion molecule L1. *Neuron* 12: 873-884.
- Imaizumi K, Miyoshi K, Katayama T, Yoneda T, Taniguchi M, Kudo T, Tohyama M (2001) The unfolded protein response and Alzheimer's disease. *Biochim Biophys Acta* 1536: 85-96.
- Inoue H, Nojima H, Okayama H (1990) High efficiency transformation of *Escherichia coli* with plasmids. *Gene* 96: 23-28.

- Itoh K, Sakurai Y, Asou H, Umeda M. (2000) Differential expression of alternatively spliced neural cell adhesion molecule L1 isoforms during oligodendrocyte maturation. *J Neurosci Res* 60: 579-586.
- Jacob J, Haspel J, Kane-Goldsmith N, Grumet M (2002) L1 mediated homophilic binding and neurite outgrowth are modulated by alternative splicing of exon 2. *J Neurobiol* 51 :177-89.
- Jensen TJ, Loo MA, Pind S, Williams DB, Goldberg AL, Riordan JR (1995) Multiple proteolytic systems, including the proteasome, contribute to CFTR processing. *Cell* 83: 129-135.
- Jentsch S, Schlenker S (1995) Selective protein degradation: a journey's end within the proteasome. *Cell* 82: 881-884.
- Jouet M, Rosenthal A, MacFarlane J, Kenwrick S, Donnai D (1993) A missense mutation confirms the L1 defect in X-linked hydrocephalus (HSAS). *Nat Genet* 4: 331.
- Jouet M, Rosenthal A, Armstrong G, MacFarlane J, Stevenson R, Paterson J, Metzenberg A, Ionasescu V, Temple K, Kenwrick S (1994) X-linked spastic paraplegia (SPG1), MASA syndrome and X-linked hydrocephalus result from mutations in the L1 gene. *Nat Genet* 7: 402-407.
- Jouet M, Rosenthal A, Kenwrick S (1995a) Exon 2 of the gene for neural cell adhesion molecule L1 is alternatively spliced in B cells. *Brain Res Mol Brain Res* 30: 378-380.
- Jouet M, Kenwrick S (1995) Gene analysis of L1 neural cell adhesion molecule in prenatal diagnosis of hydrocephalus. *Lancet* 345: 161-162.
- Jouet M, Moncla A, Paterson J, McKeown C, Fryer A, Carpenter N, Holmberg E, Wadelius C, Kenwrick S (1995b) New domains of neural cell-adhesion molecule L1 implicated in X-linked hydrocephalus and MASA syndrome. *Am J Hum Genet* 56: 1304-1314.

- Juliano RL (2002) Signal transduction by cell adhesion receptors and the cytoskeleton: functions of integrins, cadherins, selectins, and immunoglobulin-superfamily members. *Annu Rev Pharmacol Toxicol* 42: 283-323.
- Jung M, Sommer I, Schachner M, Nave KA (1996) Monoclonal antibody O10 defines a conformationally sensitive cell-surface epitope of proteolipid protein (PLP): evidence that PLP misfolding underlies dysmyelination in mutant mice. *J Neurosci* 16: 7920-7929.
- Kadmon G, Kowitz A, Altevogt P, Schachner M (1990) The neural cell adhesion molecule N-CAM enhances L1-dependent cell-cell interactions. *J Cell Biol* 110: 193-208.
- Kadmon G, Bohlen und HF, Horstkorte R, Eckert M, Altevogt P, Schachner M (1995) Evidence for cis interaction and cooperative signalling by the heat-stable antigen nectadrin (murine CD24) and the cell adhesion molecule L1 in neurons. *Eur J Neurosci* 7: 993-1004.
- Kallunki P, Edelman GM, Jones FS (1997) Tissue-specific expression of the L1 cell adhesion molecule is modulated by the neural restrictive silencer element. *J Cell Biol* 138: 1343-1354.
- Kallunki P, Edelman GM, Jones FS (1998) The neural restrictive silencer element can act as both a repressor and enhancer of L1 cell adhesion molecule gene expression during postnatal development. *Proc Natl Acad Sci U S A* 95: 3233-3238.
- Kamiguchi H, Lemmon V (1998) A neuronal form of the cell adhesion molecule L1 contains a tyrosine- based signal required for sorting to the axonal growth cone. *J Neurosci* 18: 3749-3756.
- Kamiguchi H, Long KE, Pendergast M, Schaefer AW, Rapoport I, Kirchhausen T, Lemmon V (1998) The neural cell adhesion molecule L1 interacts with the AP-2 adaptor and is endocytosed via the clathrin-mediated pathway. *J Neurosci* 18: 5311-5321.
- Kamiguchi H, Lemmon V (2000) Recycling of the cell adhesion molecule L1 in axonal growth cones. *J Neurosci* 20: 3676-3686.

- Kamiguchi H, Yoshihara F (2001) The role of endocytic L1 trafficking in polarized adhesion and migration of nerve growth cones. *J Neurosci* 21: 9194-9203.
- Kaplan P (1983) X linked recessive inheritance of agenesis of the corpus callosum 5. *J Med Genet* 20: 122-124.
- Kater SB, Rehder V (1995) The sensory-motor role of growth cone filopodia. *Curr Opin Neurobiol* 5: 68-74.
- Kaufman RJ (1999) Stress signaling from the lumen of the endoplasmic reticulum: coordination of gene transcriptional and translational controls. *Genes Dev* 13:1211-1233.
- Kayyem JF, Roman JM, de la Rosa EJ, Schwarz U, Dreyer WJ (1992) Bravo/Nr-CAM is closely related to the cell adhesion molecules L1 and Ng-CAM and has a similar heterodimer structure. *J Cell Biol* 118: 1259-1270.
- Kenwrick S, Ionasescu V, Ionasescu G, Searby C, King A, Dubowitz M, Davies KE (1986) Linkage studies of X-linked recessive spastic paraplegia using DNA probes. *Hum Genet* 73: 264-266.
- Kenwrick S, Watkins A, Angelis ED (2000) Neural cell recognition molecule L1: relating biological complexity to human disease mutations. *Hum Mol Genet* 9: 879-886.
- Klausner RD, Sitia R (1990) Protein degradation in the endoplasmic reticulum. *Cell* 62: 611-614.
- Knapp PE, Skoff RP, Redstone DW (1989) Oligodendroglial cell death in jimpy mice: an explanation for the myelin deficit. *J Neurosci* 6:2813-2822.
- Kohl A, Giese KP, Mohajeri MH, Montag D, Moos M, Schachner M (1992) Analysis of promoter activity and 5' genomic structure of the neural cell adhesion molecule L1. *J Neurosci Res* 32: 167-177.
- Kopito RR (1997) ER quality control: the cytoplasmic connection. *Cell* 88 :427-430.

- Kornblihtt AR, Umezawa K, Vibe-Pedersen K, Baralle FE (1985) Primary structure of human fibronectin: differential splicing may generate at least 10 polypeptides from a single gene. *EMBO J* 4: 1755-1759.
- Kowitz A, Kadmon G, Eckert M, Schirmmacher V, Schachner M, Altevogt P (1992) Expression and function of the neural cell adhesion molecule L1 in mouse leukocytes. *Eur J Immunol* 22: 1199-1205.
- Kuhn TB, Stoeckli ET, Condrau MA, Rathjen FG, Sonderegger P (1991) Neurite outgrowth on immobilized axonin-1 is mediated by a heterophilic interaction with L1(G4). *J Cell Biol* 115: 1113-1126.
- Kujat R, Miragall F, Krause D, Dermietzel R, Wrobel KH (1995) Immunolocalization of the neural cell adhesion molecule L1 in non-proliferating epithelial cells of the male urogenital tract. *Histochem Cell Biol* 103: 311-321.
- Kunz S, Ziegler U, Kunz B, Sonderegger P (1996) Intracellular signaling is changed after clustering of the neural cell adhesion molecules axonin-1 and NgCAM during neurite fasciculation. *J Cell Biol* 135: 253-267.
- Laemmli, UK (1970). Cleavage of structural proteins during the assembly of the head of bacteriophage T4. *Nature* 227, 680-685.
- Lagenaur C, Lemmon V (1987) An L1-like molecule, the 8D9 antigen, is a potent substrate for neurite extension. *Proc Natl Acad Sci U S A* 84: 7753-7757.
- Lau MM, Neufeld EF (1989) A frameshift mutation in a patient with Tay-Sachs disease causes premature termination and defective intracellular transport of the alpha-subunit of beta-hexosaminidase. *J Biol Chem* 264: 21376-2180.
- Lemmon V, Farr KL, Lagenaur C (1989) L1-mediated axon outgrowth occurs via a homophilic binding mechanism. *Neuron* 2: 1597-1603.
- Letourneau PC, Shattuck TA (1989) Distribution and possible interactions of actin-associated proteins and cell adhesion molecules of nerve growth cones. *Development* 105: 505-519.
- Lindner J, Rathjen FG, Schachner M (1983) L1 mono- and polyclonal antibodies modify cell migration in early postnatal mouse cerebellum. *Nature* 305: 427-430.

- Lom B, Hopker V, McFarlane S, Bixby JL, Holt CE (1998) Fibroblast growth factor receptor signaling in *Xenopus* retinal axon extension. *J Neurobiol* 37: 633-641.
- Lomas DA, Evans DL, Finch JT, Carrell RW (1992) The mechanism of Z alpha 1-antitrypsin accumulation in the liver. *Nature* 357:605-607.
- Lomas DA (1996) New insights into the structural basis of alpha 1-antitrypsin deficiency. *QJM* 89:807-812.
- Luthi A, Mohajeri H, Schachner M, Laurent JP (1996) Reduction of hippocampal long-term potentiation in transgenic mice ectopically expressing the neural cell adhesion molecule L1 in astrocytes. *J Neurosci Res* 46: 1-6.
- Luthi A, Laurent JP, Figurov A, Muller D, Schachner M (1994) Hippocampal long-term potentiation and neural cell adhesion molecules L1 and NCAM. *Nature* 372: 777-779.
- Mahadeva R, Stewart S, Bilton D, Lomas DA (1998) Alpha-1 antitrypsin deficiency alleles and severe cystic fibrosis lung disease. *Thorax* 53:1022-1024.
- Martini R, Schachner M (1986) Immunoelectron microscopic localization of neural cell adhesion molecules (L1, N-CAM, and MAG) and their shared carbohydrate epitope and myelin basic protein in developing sciatic nerve. *J Cell Biol* 103: 2439-2448.
- Martini R, Schachner M (1988) Immunoelectron microscopic localization of neural cell adhesion molecules (L1, N-CAM, and myelin-associated glycoprotein) in regenerating adult mouse sciatic nerve. *J Cell Biol* 106: 1735-1746.
- McCracken AA, Brodsky JL (1996) Assembly of ER-associated protein degradation in vitro: dependence on cytosol, calnexin, and ATP. *J Cell Biol* 132: 291-298.
- Mechtersheimer S, Gutwein P, Agmon-Levin N, Stoeck A, Oleszewski M, Riedle S, Fogel M, Lemmon V, Altevogt P (2001) Ectodomain shedding of L1 adhesion molecule promotes cell migration by autocrine binding to integrins. *J Cell Biol* 155: 661-674.

- Meech R, Kallunki P, Edelman GM, Jones FS (1999) A binding site for homeodomain and Pax proteins is necessary for L1 cell adhesion molecule gene expression by Pax-6 and bone morphogenetic proteins. *Proc Natl Acad Sci U S A* 96: 2420-2425.
- Meiri KF, Saffell JL, Walsh FS, Doherty P (1998) Neurite outgrowth stimulated by neural cell adhesion molecules requires growth-associated protein-43 (GAP-43) function and is associated with GAP-43 phosphorylation in growth cones. *J Neurosci* 18: 10429-10437.
- Melnick J, Aviel S, Argon Y (1992) The endoplasmic reticulum stress protein GRP94, in addition to BiP, associates with unassembled immunoglobulin chains. *J Biol Chem* 267: 21303-21306.
- Michaelis RC, Du YZ, Schwartz CE (1998) The site of a missense mutation in the extracellular Ig or FN domains of L1CAM influences infant mortality and the severity of X linked hydrocephalus. *J Med Genet* 35: 901-904.
- Milev P, Friedlander DR, Sakurai T, Karthikeyan L, Flad M, Margolis RK, Grumet M, Margolis RU (1994) Interactions of the chondroitin sulfate proteoglycan phosphacan, the extracellular domain of a receptor-type protein tyrosine phosphatase, with neurons, glia, and neural cell adhesion molecules. *J Cell Biol* 127: 1703-1715.
- Milev P, Meyer-Puttlitz B, Margolis RK, Margolis RU (1995) Complex-type asparagine-linked oligosaccharides on phosphacan and protein-tyrosine phosphatase-zeta/beta mediate their binding to neural cell adhesion molecules and tenascin. *J Biol Chem* 270: 24650-24653.
- Miura M, Kobayashi M, Asou H, Uyemura K (1991) Molecular cloning of cDNA encoding the rat neural cell adhesion molecule L1. Two L1 isoforms in the cytoplasmic region are produced by differential splicing. *FEBS Lett* 289: 91-95.
- Miura M, Asou H, Kobayashi M, Uyemura K (1992) Functional expression of a full-length cDNA coding for rat neural cell adhesion molecule L1 mediates homophilic intercellular adhesion and migration of cerebellar neurons. *J Biol Chem* 267: 10752-10758.

- Montgomery AM, Becker JC, Siu CH, Lemmon VP, Cheresch DA, Pancook JD, Zhao X, Reisfeld RA (1996) Human neural cell adhesion molecule L1 and rat homologue NILE are ligands for integrin alpha v beta 3. *J Cell Biol* 132: 475-485.
- Moos M, Tacke R, Scherer H, Teplow D, Fruh K, Schachner M (1988) Neural adhesion molecule L1 as a member of the immunoglobulin superfamily with binding domains similar to fibronectin. *Nature* 334: 701-703.
- Morello JP, Petaja-Repo UE, Bichet DG, Bouvier M (2000) Pharmacological chaperones: a new twist on receptor folding. *Trends Pharmacol Sci* 2000 21: 466-469.
- Moulding HD, Martuza RL, Rabkin SD (2000) Clinical mutations in the L1 neural cell adhesion molecule affect cell- surface expression. *J Neurosci* 20: 5696-5702.
- Moya GE, Michaelis RC, Holloway LW, Sanchez JM (2002) Prenatal Diagnosis of L1 Cell Adhesion Molecule Mutations. capabilities and limitations. *Fetal Diagn Ther* 17: 115-119.
- Nadon NL, Arnheiter H, Hudson LD (1994) A combination of PLP and DM20 transgenes promotes partial myelination in the jimpy mouse. *J Neurochem* 63: 822-833.
- Nayeem N, Silletti S, Yang X, Lemmon VP, Reisfeld RA, Stallcup WB, Montgomery AM (1999) A potential role for the plasmin(ogen) system in the posttranslational cleavage of the neural cell adhesion molecule L1. *J Cell Sci* 112 (Pt 24): 4739-4749.
- Needham LK, Thelen K, Maness PF (2001) Cytoplasmic Domain Mutations of the L1 Cell Adhesion Molecule Reduce L1- Ankyrin Interactions. *J Neurosci* 21: 1490-1500.
- Nolte C, Moos M, Schachner M (1999) Immunolocalization of the neural cell adhesion molecule L1 in epithelia of rodents. *Cell Tissue Res* 298: 261-273.

- Novoradovskaya N, Lee J, Yu ZX, Ferrans VJ, Brantly M (1998) Inhibition of intracellular degradation increases secretion of a mutant form of alpha1-antitrypsin associated with profound deficiency. *J Clin Invest* 101: 2693-26701.
- Nybroe O, Dalseg AM, Bock E (1990) A developmental study of soluble L1. *Int J Dev Neurosci* 8: 273-281.
- Okamura K, Kimata Y, Higashio H, Tsuru A, Kohno K (2000) Dissociation of Kar2p/BiP from an ER sensory molecule, Ire1p, triggers the unfolded protein response in yeast. *Biochem Biophys Res Commun* 279: 445-450.
- Oleszewski M, Gutwein P, von Der LW, Rauch U, Altevogt P (2000) Characterization of the L1-neurocan binding site. Implications for L1- L1 homophilic binding. *J Biol Chem.* 275: 34478-85.
- Olsson JE, Gordon JW, Pawlyk BS, Roof D, Hayes A, Molday RS, Mukai S, Cowley GS, Berson EL, Dryja TP (1992) Transgenic mice with a rhodopsin mutation (Pro23His): a mouse model of autosomal dominant retinitis pigmentosa. *Neuron* 9: 815-830.
- Orr HT, Lancet D, Robb RJ, Lopez de Castro JA, Strominger JL (1979) The heavy chain of human histocompatibility antigen HLA-B7 contains an immunoglobulin-like region. *Nature* 282: 266-270.
- Ou WJ, Cameron PH, Thomas DY, Bergeron JJ (1993) Association of folding intermediates of glycoproteins with calnexin during protein maturation. *Nature* 364: 771-776.
- Parodi AJ (2000a) Protein glucosylation and its role in protein folding. *Annu Rev Biochem* 69: 69-93.
- Parodi AJ (2000a) Role of N-oligosaccharide endoplasmic reticulum processing reactions in glycoprotein folding and degradation. *Biochem J* 348 Pt 1: 1-13.
- Patil C, Walter P (2001) Intracellular signaling from the endoplasmic reticulum to the nucleus: the unfolded protein response in yeast and mammals. *Curr Opin Cell Biol* 13: 349-355.

- Payne HR, Burden SM, Lemmon V (1992) Modulation of growth cone morphology by substrate-bound adhesion molecules. *Cell Motil Cytoskeleton* 21: 65-73.
- Perlmutter DH (1998) Alpha-1-antitrypsin deficiency. *Semin Liver Dis* 18: 217-225.
- Persohn E, Schachner M (1987) Immunoelectron microscopic localization of the neural cell adhesion molecules L1 and N-CAM during postnatal development of the mouse cerebellum. *J Cell Biol* 105: 569-576.
- Pfeffer SR, Rothman JE (1987) Biosynthetic protein transport and sorting by the endoplasmic reticulum and Golgi. *Annu Rev Biochem* 56: 829-852.
- Plempner RK, Wolf DH (1999) Retrograde protein translocation: ERADication of secretory proteins in health and disease. *Trends Biochem Sci* 24: 266-270.
- Pridmore RD (1987) New and versatile cloning vectors with kanamycin-resistance marker. *Gene* 56: 309-312.
- Purves D, Lichtman JW (1983) Specific connections between nerve cells. *Annu Rev Physiol* 45: 553-565.
- Rader C, Kunz B, Lierheimer R, Giger RJ, Berger P, Tittmann P, Gross H, Sonderegger P (1996) Implications for the domain arrangement of axonin-1 derived from the mapping of its NgCAM binding site. *EMBO J* 15: 2056-2068.
- Rathjen FG, Schachner M (1984) Immunocytological and biochemical characterization of a new neuronal cell surface component (L1 antigen) which is involved in cell adhesion. *EMBO J* 3: 1-10.
- Rauch U, Gao P, Janetzko A, Flaccus A, Hilgenberg L, Tekotte H, Margolis RK, Margolis RU (1991) Isolation and characterization of developmentally regulated chondroitin sulfate and chondroitin/keratan sulfate proteoglycans of brain identified with monoclonal antibodies. *J Biol Chem* 266: 14785-14801.
- Rauch U, Feng K, Zhou XH (2001) Neurocan: a brain chondroitin sulfate proteoglycan. *Cell Mol Life Sci* 58: 1842-1856.
- Rolf B, Kutsche M, Bartsch U (2001) Severe hydrocephalus in L1-deficient mice. *Brain Res* 891: 247-252.

- Ronn LC, Doherty P, Holm A, Berezin V, Bock E (2000) Neurite outgrowth induced by a synthetic peptide ligand of neural cell adhesion molecule requires fibroblast growth factor receptor activation. *J Neurochem* 75: 665-671.
- Rose SP (1995) Glycoproteins and memory formation. *Behav Brain Res* 66: 73-78.
- Rosenthal A, Jouet M, Kenwrick S (1992) Aberrant splicing of neural cell adhesion molecule L1 mRNA in a family with X-linked hydrocephalus [published erratum appears in *Nat Genet* 1993 Mar;3(3):273]. *Nat Genet* 2: 107-112.
- Ruiz JC, Cuppens H, Legius E, Fryns JP, Glover T, Marynen P, Cassiman JJ (1995) Mutations in L1-CAM in two families with X linked complicated spastic paraplegia, MASA syndrome, and HSAS. *J Med Genet* 32: 549-552.
- Ruoslahti E, Pierschbacher MD (1987) New perspectives in cell adhesion: RGD and integrins. *Science* 238: 491-497.
- Ruppert M, Aigner S, Hubbe M, Yagita H, Altevogt P (1995) The L1 adhesion molecule is a cellular ligand for VLA-5. *J Cell Biol* 131: 1881-1891.
- Sadoul K, Sadoul R, Faissner A, Schachner M (1988) Biochemical characterization of different molecular forms of the neural cell adhesion molecule L1. *J Neurochem* 50: 510-521.
- Sadoul R, Kirchhoff F, Schachner M (1989) A protein kinase activity is associated with and specifically phosphorylates the neural cell adhesion molecule L1. *J Neurochem* 53: 1471-1478.
- Saffell JL, Williams EJ, Mason IJ, Walsh FS, Doherty P (1997) Expression of a dominant negative FGF receptor inhibits axonal growth and FGF receptor phosphorylation stimulated by CAMs. *Neuron* 18: 231-242.
- Salton SR, Shelanski ML, Greene LA (1983) Biochemical properties of the nerve growth factor-inducible large external (NILE) glycoprotein. *J Neurosci* 3: 2420-2430.
- Sambrook J, Fritsch EF, Maniatis T (1989) *Molecular cloning: A Laboratory Manual*, 2<sup>nd</sup> edition (Cold Spring Harbor, NY: Cold Spring Harbor Laboratory).

- Sammar M, Gulbins E, Hilbert K, Lang F, Altevogt P (1997) Mouse CD24 as a signaling molecule for integrin-mediated cell binding: functional and physical association with src-kinases. *Biochem Biophys Res Commun* 234: 330-334.
- Sato S, Ward CL, Krouse ME, Wine JJ, Kopito RR (1996) Glycerol reverses the misfolding phenotype of the most common cystic fibrosis mutation. *J Biol Chem* 1996 271: 635-638.
- Schmid RS, Graff RD, Schaller MD, Chen S, Schachner M, Hemperly JJ, Maness PF (1999) NCAM stimulates the Ras-MAPK pathway and CREB phosphorylation in neuronal cells. *J Neurobiol* 38: 542-558.
- Schmid RS, Pruitt WM, Maness PF (2000) A MAP kinase-signaling pathway mediates neurite outgrowth on L1 and requires src-dependent endocytosis. *J Neurosci* 20: 4177-4188.
- Schmidt A, Hannah MJ, Huttner WB (1997) Synaptic-like microvesicles of neuroendocrine cells originate from a novel compartment that is continuous with the plasma membrane and devoid of transferrin receptor. *J Cell Biol* 137: 445-458.
- Schneider AM, Griffiths IR, Readhead C, Nave KA (1995) Dominant-negative action of the jimpy mutation in mice complemented with an autosomal transgene for myelin proteolipid protein. *Proc Natl Acad Sci U S A* 92: 4447-4451.
- Schrander-Stumpel C, Fryns JP (1998) Congenital hydrocephalus: nosology and guidelines for clinical approach and genetic counselling. *Eur J Pediatr* 157: 355-362.
- Scotland P, Zhou D, Benveniste H, Bennett V (1998) Nervous system defects of AnkyrinB (-/-) mice suggest functional overlap between the cell adhesion molecule L1 and 440-kD AnkyrinB in premyelinated axons. *J Cell Biol* 143: 1305-1315.
- Seilheimer B, Persohn E, Schachner M. (1989) Antibodies to the L1 adhesion molecule inhibit Schwann cell ensheathment of neurons in vitro. *J Cell Biol* 1989 109: 3095-3103.

- Serville F, Lyonnet S, Pelet A, Reynaud M, Louail C, Munnich A, Le Merrer M (1992) X-linked hydrocephalus: clinical heterogeneity at a single gene locus. *Eur J Pediatr* 151: 515-518.
- Shamu CE, Walter P (1996) Oligomerization and phosphorylation of the Ire1p kinase during intracellular signaling from the endoplasmic reticulum to the nucleus. *EMBO J* 15: 3028-3039.
- Shamu CE (1998) Splicing: HACKing into the unfolded-protein response. *Curr Biol* 8: R121-123.
- Shi Y, Vattem KM, Sood R, An J, Liang J, Stramm L, Wek RC (1998) Identification and characterization of pancreatic eukaryotic initiation factor 2 alpha-subunit kinase, PEK, involved in translational control. *Mol Cell Biol* 18: 7499-7509.
- Silverman RH, Williams BR (1999) Translational control perks up. *Nature* 397: 208-211.
- Simon H, Klinz T, Fahrig T, Schachner M (1991) Molecular association of the neural adhesion molecules L1 and N-CAM in the surface membrane of neuroblastoma cells is shown by chemical cross-linking. *Eur Neurosci* 3:634-640.
- Sousa MC, Ferrero-Garcia MA, Parodi AJ (1992) Recognition of the oligosaccharide and protein moieties of glycoproteins by the UDP-Glc:glycoprotein glucosyltransferase. *Biochemistry* 31: 97-105.
- Stevens FJ, Argon Y (1999) Protein folding in the ER. *Semin Cell Dev Biol* 10: 443-454.
- Su XD, Gastinel LN, Vaughn DE, Faye I, Poon P, Bjorkman PJ (1998) Crystal structure of hemolin: a horseshoe shape with implications for homophilic adhesion. *Science* 281: 991-995.
- Takeda Y, Asou H, Murakami Y, Miura M, Kobayashi M, Uyemura K (1996) A nonneuronal isoform of cell adhesion molecule L1: tissue-specific expression and functional analysis. *J Neurochem* 66: 2338-2349.

- Takei K, Chan TA, Wang FS, Deng H, Rutishauser U, Jay DG (1999) The neural cell adhesion molecules L1 and NCAM-180 act in different steps of neurite outgrowth. *J Neurosci* 19: 9469-9479.
- Tamarappoo BK, Verkman AS (1998) Defective aquaporin-2 trafficking in nephrogenic diabetes insipidus and correction by chemical chaperones. *J Clin Invest* 101: 2257-2267.
- Tepass U, Truong K, Godt D, Ikura M, Peifer M (2000) Cadherins in embryonic and neural morphogenesis. *Nat Rev Mol Cell Biol* 1: 91-100.
- Thiery JP, Brackenbury R, Rutishauser U, Edelman GM (1977) Adhesion among neural cells of the chick embryo. II. Purification and characterization of a cell adhesion molecule from neural retina. *J Biol Chem* 252: 6841-6845.
- Thomas GR, Forbes JR, Roberts EA, Walshe JM, Cox DW (1995) The Wilson disease gene: spectrum of mutations and their consequences. *Nat Genet* 9: 210-217.
- Thor G, Probstmeier R, Schachner M (1987) Characterization of the cell adhesion molecules L1, N-CAM and J1 in the mouse intestine. *EMBO J* 6: 2581-2586.
- Tirasophon W, Welihinda AA, Kaufman RJ (1998) A stress response pathway from the endoplasmic reticulum to the nucleus requires a novel bifunctional protein kinase/endoribonuclease (Ire1p) in mammalian cells. *Genes Dev* 12: 1812-1824.
- Towbin H, Staehelin T, Gordon J (1979) Electrophoretic transfer of proteins from polyacrylamide gels to nitrocellulose sheets: procedure and some applications. *Proc Natl Acad Sci U S A* 76: 4350-4354.
- Trombetta ES, Helenius A (1998) Lectins as chaperones in glycoprotein folding. *Curr Opin Struct Biol* 8: 587-592.
- van Camp G, Fransen E, Vits L, Raes G, Willems PJ (1996) A locus-specific mutation database for the neural cell adhesion molecule L1CAM (Xq28). *Hum Mutat* 8: 391.

- Vermeesch MK, Knapp PE, Skoff RP, Studzinski DM, Benjamins JA (1990) Death of individual oligodendrocytes in jimpy brain precedes expression of proteolipid protein. *Dev Neurosci* 12: 303-315.
- Vits L, van Camp G, Coucke P, Fransen E, De Boulle K, Reyniers E, Korn B, Poustka A, Wilson G, Schrandt-Stumpel C (1994) MASA syndrome is due to mutations in the neural cell adhesion gene L1CAM. *Nat Genet* 7: 408-413.
- Walsh FS, Doherty P (1997) Neural cell adhesion molecules of the immunoglobulin superfamily: role in axon growth and guidance. *Annu Rev Cell Dev Biol* 13: 425-456.
- Ward CL, Kopito RR (1994) Intracellular turnover of cystic fibrosis transmembrane conductance regulator. Inefficient processing and rapid degradation of wild-type and mutant proteins. *J Biol Chem* 269: 25710-25718.
- Ward CL, Omura S, Kopito RR (1995) Degradation of CFTR by the ubiquitin-proteasome pathway. *Cell* 83: 121-127.
- Wiertz EJ, Tortorella D, Bogoy M, Yu J, Mothes W, Jones TR, Rapoport TA, Ploegh HL (1996) Sec61-mediated transfer of a membrane protein from the endoplasmic reticulum to the proteasome for destruction. *Nature* 384: 432-438.
- Williams AF, Barclay AN (1988) The immunoglobulin superfamily--domains for cell surface recognition. *Annu Rev Immunol* 6: 381-405.
- Williams EJ, Doherty P, Turner G, Reid RA, Hemperly JJ, Walsh FS (1992) Calcium influx into neurons can solely account for cell contact-dependent neurite outgrowth stimulated by transfected L1. *J Cell Biol* 119: 883-892.
- Williams EJ, Walsh FS, Doherty P (1994a) Tyrosine kinase inhibitors can differentially inhibit integrin-dependent and CAM-stimulated neurite outgrowth. *J Cell Biol* 124: 1029-1037.
- Williams EJ, Furness J, Walsh FS, Doherty P (1994b) Activation of the FGF receptor underlies neurite outgrowth stimulated by L1, N-CAM, and N-cadherin. *Neuron* 13: 583-594.

- Wong EV, Cheng G, Payne HR, Lemmon V (1995a) The cytoplasmic domain of the cell adhesion molecule L1 is not required for homophilic adhesion. *Neurosci Lett* 200: 155-158.
- Wong EV, Kenwrick S, Willems P, Lemmon V (1995b) Mutations in the cell adhesion molecule L1 cause mental retardation. *Trends Neurosci* 18: 168-172.
- Wong EV, Schaefer AW, Landreth G, Lemmon V (1996a) Involvement of p90rsk in neurite outgrowth mediated by the cell adhesion molecule L1. *J Biol Chem* 271: 18217-18223.
- Wong EV, Schaefer AW, Landreth G, Lemmon V (1996b) Casein kinase II phosphorylates the neural cell adhesion molecule L1. *J Neurochem* 66: 779-786.
- Wood P, Moya F, Eldridge C, Owens G, Ranscht B, Schachner M, Bunge M, Bunge R (1990a) Studies of the initiation of myelination by Schwann cells. *Ann N Y Acad Sci* 605: 1-14.
- Wood PM, Schachner M, Bunge RP (1990b) Inhibition of Schwann cell myelination in vitro by antibody to the L1 adhesion molecule. *J Neurosci* 10: 3635-3645.
- Wu Y, Whitman I, Molmenti E, Moore K, Hippenmeyer P, Perlmutter DH (1994) A lag in intracellular degradation of mutant alpha 1-antitrypsin correlates with the liver disease phenotype in homozygous PiZZ alpha 1-antitrypsin deficiency. *Proc Natl Acad Sci U S A* 91: 9014-90188.
- Yamasaki M, Arita N, Hiraga S, Izumoto S, Morimoto K, Nakatani S, Fujitani K, Sato N, Hayakawa T (1995) A clinical and neuroradiological study of X-linked hydrocephalus in Japan. *J Neurosurg* 83: 50-55.
- Yamasaki M, Thompson P, Lemmon V (1997) CRASH syndrome: mutations in L1CAM correlate with severity of the disease. *Neuropediatrics* 28: 175-178.
- Zhang X, Davis JQ, Carpenter S, Bennett V (1998) Structural requirements for association of neurofascin with ankyrin. *J Biol Chem* 273: 30785-30794.

- Zhao X, Siu CH (1995) Colocalization of the homophilic binding site and the neuritogenic activity of the cell adhesion molecule L1 to its second Ig-like domain. *J Biol Chem* 270: 29413-29421.
- Zhao X, Yip PM, Siu CH (1998) Identification of a homophilic binding site in immunoglobulin-like domain 2 of the cell adhesion molecule L1. *J Neurochem* 71: 960-971.
- Zisch AH, Stallcup WB, Chong LD, Dahlin-Huppe K, Voshol J, Schachner M, Pasquale EB (1997a) Tyrosine phosphorylation of L1 family adhesion molecules: implication of the Eph kinase Cck5. *J Neurosci Res* 47: 655-665.
- Zisch AH, Pasquale EB (1997b) The Eph family: a multitude of receptors that mediate cell recognition signals. *Cell Tissue Res* 290: 217-226.

## VI Appendix

### 1 Abbreviations

μ	micro (10 <sup>-6</sup> )	LB	Luria Bertani
xg	g-force	m	milli (10 <sup>-3</sup> )
°C	grad celsius	MEM	minimal essential medium
aa	amino acid	min	minute
A	adenine	MOPS	(4-(N-morpholino)-propan)-sulfonic acid
Amp	ampicillin	mRNA	messenger ribonucleic acid
APS	ammoniumperoxidisulfate	n	nano (10 <sup>-9</sup> )
bp	base pairs	OD	optic density
BSA	bovine serum albumine	p	pico (10 <sup>-12</sup> )
C	cytosine	PAGE	polyacrylamide gel electrophoresis
cDNA	complementary deoxyribonucleic acid	PBS	phosphat buffer
CHO	Chinese Hamster Ovarian	PCR	polymerase chain reaction
Cm	chloramphenicol	rpm	rounds per minute
CMV	cytomegalie virus	RNA	ribonucleic acid
CST	corticospinal tract	RT	room temperature
dNTP	2'-desoxyribonucleotide-5'-triphosphate	SDS	sodium dodecyl sulfate
ECM	extracellular matrix	T	thymin
EDTA	ethylendiamintetraacetic acid	TEMED	N,N,N',N'-tetraethylenamine
FCS	fetal calf serum	Tm	melting temperature
g	gram	Tris	tris(-hydroxymethyl)-aminomethane
G	guanosine	U	unit (enzymaticP
h	hour(s)	V	volt
IPTG	isopropyl-β-D-thiogalactoside	vol	volume
Kan	kanamycin	v/v	volume per volume
kb	kilo base pairs	w/v	veight per volume
l	liter		

Amino acids were abbreviated using the one letter code

## 2 Oligonucleotides

### 2.1 Primer for sequencing of mouse L1 cDNA

Start and end bp indicate the position of the primers on the EcoRI-fragment with L1cDNA of the pGEM2-L1 plasmid.

name	start bp	end bp	sequence
<b>Forward primer</b>			
L1X1	44	64	5'-TGA TGC TGC GGT ACG TGT GGC-3'
DEIa1	444	463	5'-GTG GCC GAA GGA GAC TGT AA-3'
DEIa2	484	503	5'-GGA GAA TCA GTA GTT CTG CC-3'
L1B1	501	528	5'-GCC TTG CAA CCC TCC ACC CAG TGC AGC C-3'
DEIIa	933	952	5'-CAA TGT GGG CGA AGA GGA CG-3'
L1B2	976	1000	5'-GAG AAC TCG CTG GGC AGT GCC CGG C-3'
DEIIIa	1407	1427	5'-CCA GTG GCT GGA TGA AGA AGG-3'
L1B3	1494	1515	5'-CCA GGC CAA TGA CAC TGG ACG C-3'
DEIVa	1945	1965	5'-GCT GAA GAC CAC AAC TCT CCC-3'
L15'.2	2253	2285	5'-GAT GGA TTG GAA TGC CCC CCA GAT TCA GTA CCG-3'
Apa 1	2355	2381	5'-GGT GTC TAA CAC TTC CAC ATT TGT GCC-3'
Seq 1	2485	2505	5'-CTT GAA GAC ATC ACA ATC TTC-3'
Apa 2	2835	2863	5'-GCT ACT GCA CTG GCA GCC ACC ACT CAG CC-3'
Apa 3.2	3336	3365	5'-CCA TCT GGA TGT GAA GAC TAA TGG-3'
L13'dn	3781	3811	5'-GCT ACC TCT CCT ATC AAT CCT GCA GTA GCC C-3'
<b>Reward primer</b>			
L1 5'up	112	80	5'-ATT CGT CTG GAA TCT GTA TGA GCA GGC AGG GGC-3'
L1X4	291	268	5'-CAC TAC ACC CAA TTC TTC CTT GGG-3'
DEIVb	2488	2469	5'-CAA GTT CAG GGC TCA CCT GG-3'
Seq 2	2892	2872	5'-GAG CAG GTA GCC AGT GAG CAC-3'
DEIIb	3055	3036	5'-CTG GCT TGC CAA ACA GGG CC-3'
DEIb2	3482	3501	5'-TGA GTA TTT GCC ACC CTT GC-3'
DEIb1	3498	3517	5'-CCT CCT TGT CCT TCA CTG AG-3'

## 2.2 Primer for sequencing of transgenic construct

After cloning the transgenic construct, the borders between L1 promoter, mL1cDNA, and NRSE sequence were controlled by sequencing.

PL1.1	5'-gtg gcc acc acc aaa atc aag c-3'
PL1.2	5'-cag gag ggt agt gga atc tgg c-3'
Amp-down	5'-atg ttg aat act cat act ctt-3'
PL1-up	5'-tat cca ctc cct tca tac tct-3'
gal-up	5'-aag atc gca ctc cag cca gct-3'
NRSE1	5'-agt gct ctt cag tta ctc ac-3'

## 2.3 Primer for genotyping

L1-A'	5'-tgg gaa gac aat agc agg cat-3'
L1-C	5'-ggg agg cag gag ata agg tca-3'
L1-D	5'-cag tca ttg atc ctg gag tgc-3'
L1-ki	5'-tcg cga tga ctt agt aaa gca cat-3'
L1-5'up2	5'-aga ggc cac acg tac cgc agc atc-3'
tTa-up3	5'-tac atg cca ata caa tgt agg ctg c-3'
L1arm	5'-att gtt gat gct gca gat gca gct g-3'
L1-292	5'-gca ccc tat tct ggc tcc tt-3'
L1-709	5'-atg ctg ttg gtg ggc ttg ac-3'

## 2.4 Primer for PCR mutagenesis

DE2-A	5'-catg <b>ctcttc</b> attgctagagccacctgtcatcac-3'
DE2-B	5'-acgt <b>ctcttc</b> acaattcgtctggaatctgtatgagc-3'
DE27-A	5'-catg <b>ctcttc</b> cacagtgacaatgaagagaaggcctt-3'
DE27-B	5'-acgt <b>ctcttc</b> actgtactcgccgaagggtctctct-3'
Dhbs-A	5'-catg <b>ctcttc</b> aggacctatattttgccaatgtgc-3'
Dhbs-B	5'-acgt <b>ctcttc</b> atccaaaatcttgctgttcatccag-3'
SCY-A	5'-catg <b>ctcttc</b> atacattgctgagggattcccta-3'
SCY-B	5'-acgt <b>ctcttc</b> agtactccaggatcaatgactggc-3'

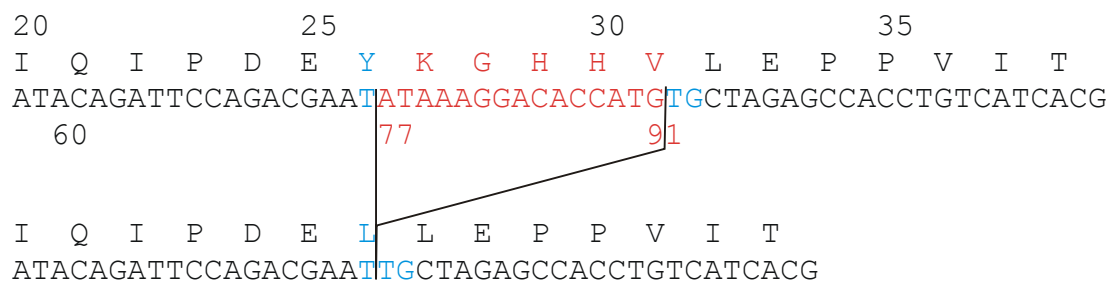
Bold letters indicate the Eam1104I-restriction site.

### 3 Mutations in the of L1cDNA

For cell culture investigations and generation of a transgenic mouse line different mutated L1cDNAs were created by PCR mutagenesis. The indicated nucleotide and amino acid (aa) position are in relation to the mouse L1cDNA beginning with ATG as nucleotide position1.

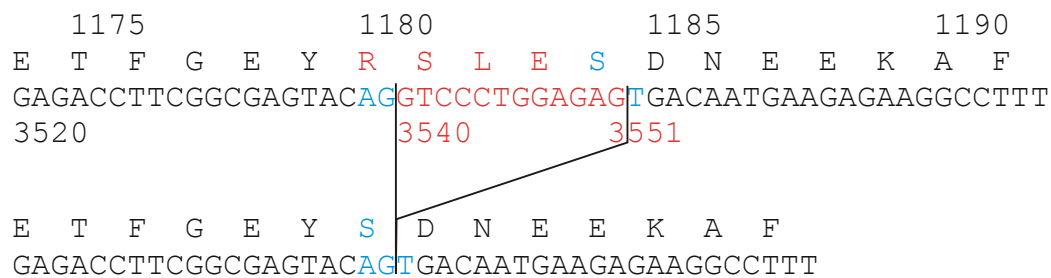
#### L1 $\Delta$ E2 – deletion of exon 2

In L1 $\Delta$ E2 the nucleotides 77 – 91 were deleted (red) encoding aa 26 – 31 which comprises exon 2 leading to a single leucine blue residue in place of six amino acids, using the primers DE2-A and -B. Above the original, below the mutated DNA and aa sequences are shown.



#### L1 $\Delta$ E27 – deletion of exon 27

In L1 $\Delta$ E27 the nucleotides 3540 – 3551 were deleted (red) encoding aa 1180 – 1183 which comprises exon 27 by usage of primers DE27-A and -B. Above the original, below the mutated DNA and aa sequences are shown.



### L1ex – the extracellular domain of L1

L1ex comprise the whole extracellular (blue) and transmembrane part (orange), and the first nine amino acids of the intracellular domain (green; remains aa 1 – 1152 of L1cDNA) in fusion with a HA-tag (violet; cloned by P. Kallunki).

```

3398 catctggatg tgaagactaa tggaactggc cctgtgogag tttctactac
1100 H L D V K T N G T G P V R V S T T
3348 agggagcttt gcctccgagg gctggttcat cgcctttgtc agcgctatca
1117 A S E G W F I A F V S A I I L L L
3398 ttctcttgct cctcatcctg ctcatcctct gttcatcaa acgcagcaag
1134 L I G S F L L I L C F I K R S K
3448 ggcgcccta tgatcccata cgatgttcca gattacgcct ag
1151 G G P M I P Y D V P D Y A -

```

### L1Δhbs – deletion of the putative homophilic binding site

In L1Δhbs the nucleotides 529–570 were deleted encoding for the putative homophilic binding site of L1 (Zhao et al., 1998) using primers Dhbs-A and -B. Above the original, below the mutated DNA and aa sequences are shown.

```

174      177      190
K I F H I K Q D E R V S M G Q N G D L Y
AAGATTTTG CACATCAAACAAGATGAGCGGGTGTCCATGGGCCAGAATGGA GACCTATAT
520      529      570

K I F D L Y
AAGATTTTG GACCTATAT

```

### L1C264Y – missense mutation

In L1C264Y a guanine at nucleotide position 788 (red) was replaced by an adenine leading to an exchange of Cys to Tyr at aa 263 (corresponding to nucleotide 264 in human L1). The primers SCY-A and -B were used. Above the original, below the mutated DNA and aa sequences are shown.

```

          263
S L I L G C I A G G F
TCATTGATCCTGGAGTGCATTGCTGAGGGATTC

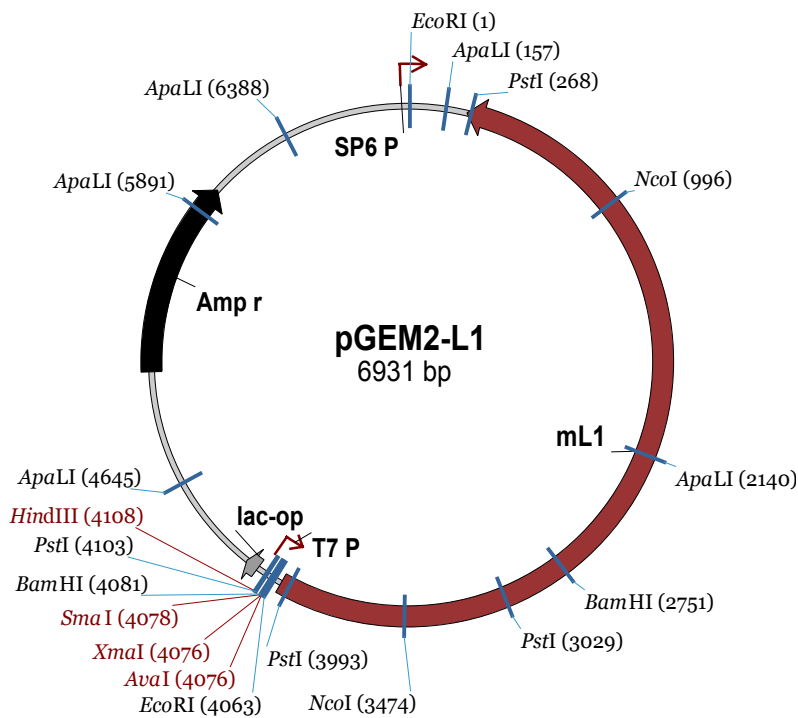
          788
S L I L G Y I A G G F
TCATTGATCCTGGAGTACATTGCTGAGGGATTC

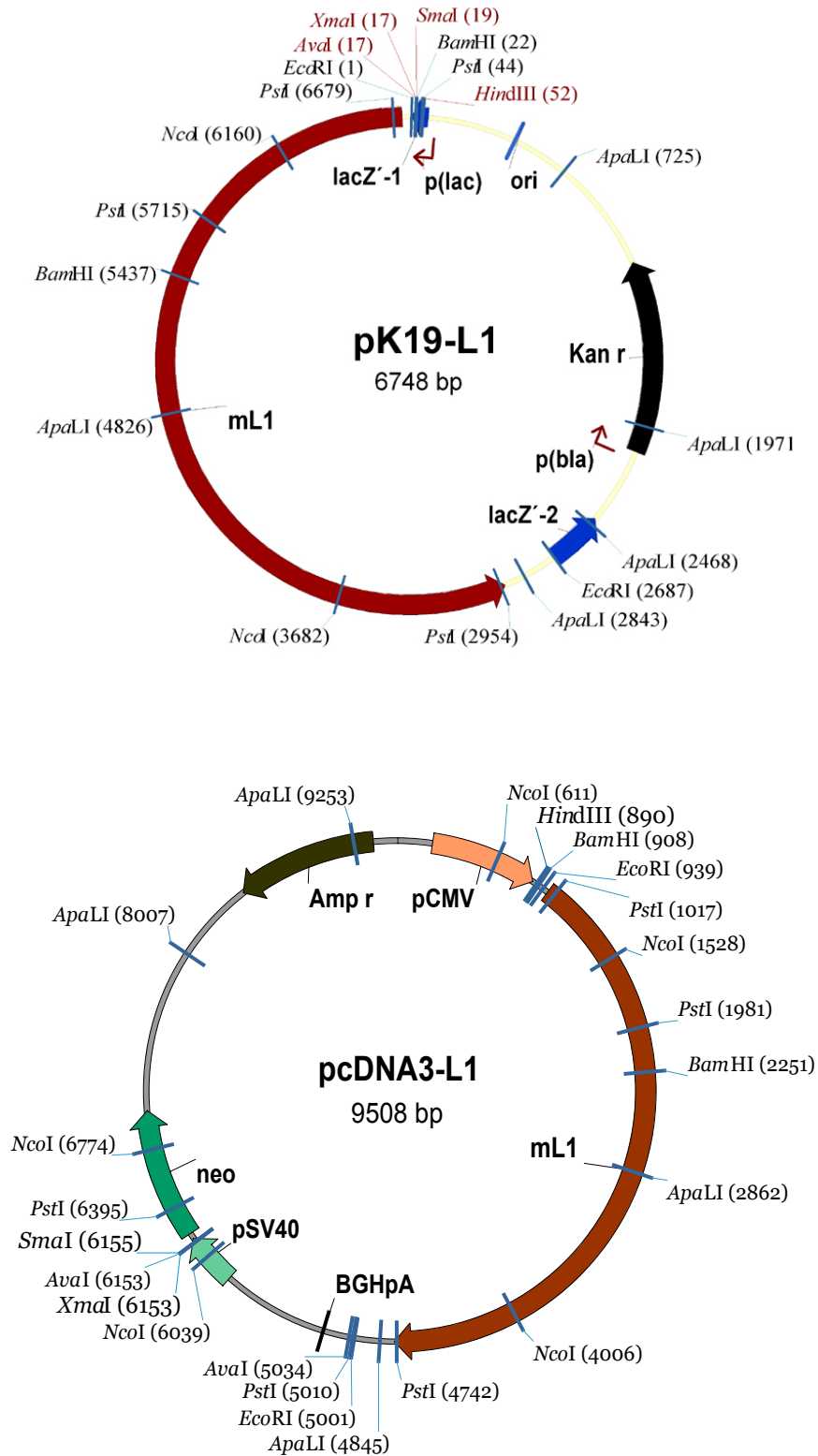
```

## 4 L1 plasmids

### 4.1 Cloning of mutated L1cDNAs into a mammalian expression vector

Different mutated L1cDNAs were created by PCR mutagenesis using the vector pGEM2-L1wt was differently mutated via PCR. Subsequently, the mutated L1cDNAs were cloned into the cloning vector pK19 (derived from the pUC19 vector by replacing the Amp<sup>r</sup> with an Kan<sup>r</sup>-resistance gene) and further cloned into the pcDNA3 expression vector, each time using the EcoRI restriction sites. mL1 indicates all mutated L1 constructs (L1 $\Delta$ E2, L1 $\Delta$ E27, sL1, L1 $\Delta$ hbs, L1C264Y, L1wt).

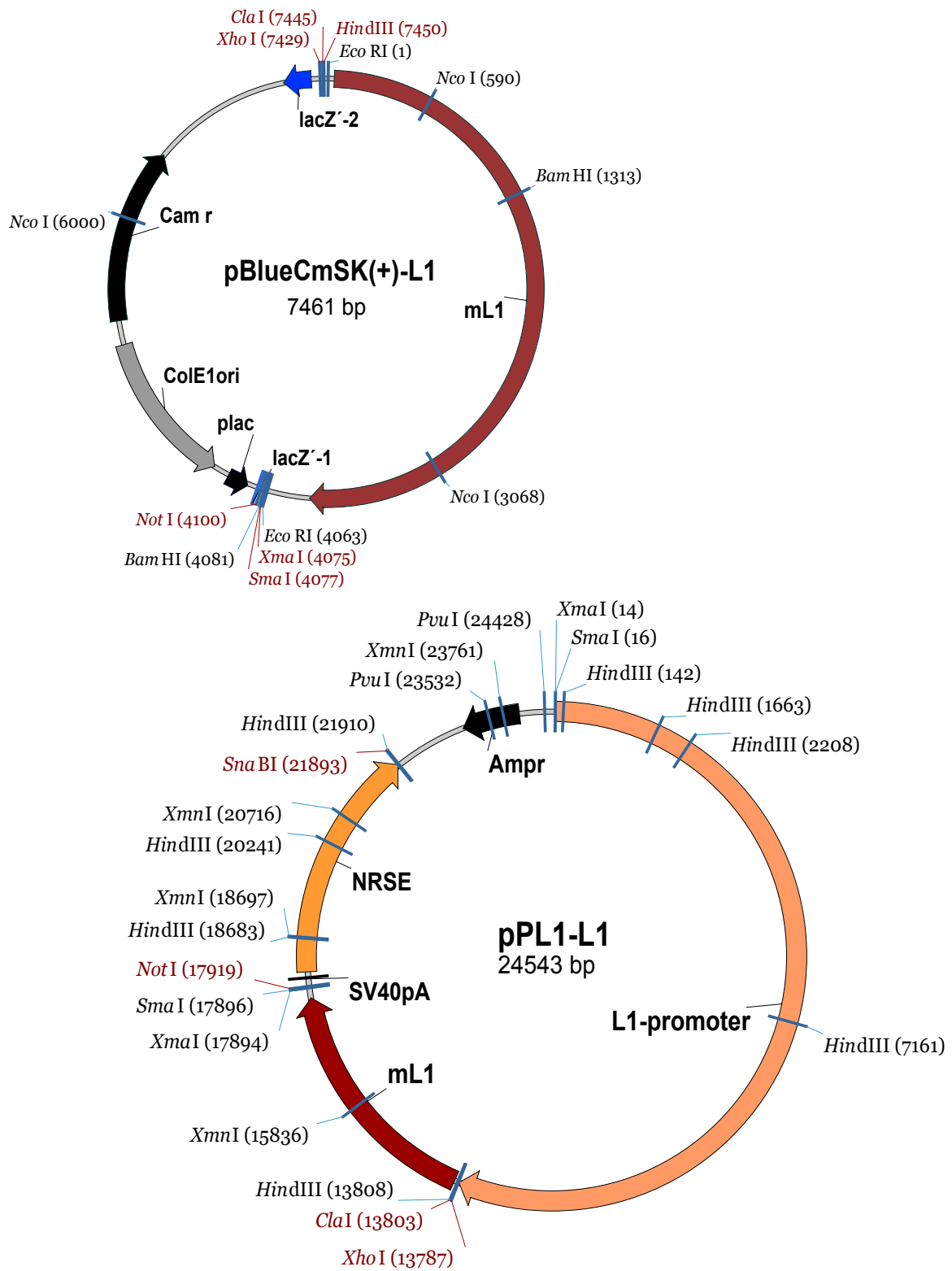




#### 4.2 Cloning of the L1C264Y transgenic construct

An *Eco*RI-PvuI-fragment of pcDNA3-L1C264Y was initially cloned into the *Eco*RI-opened vector pBlueCAM-SK(+). The *lacZ* gene was removed from vector L1lacZ (kind gift of P. Kallunki; Kallunki et al., 1997 and 1998; Meech et al., 1997) by

digestion with *NotI* and *XhoI* and replaced with L1C264Y. The 22 kb-transgenic construct was excised from the plasmid by digestion with *PvuI* and *SnaBI*



## Publications

Rünker AE, Hildebrandt K, Teuchert-Noodt G (1998) Postnatal synaptogenesis in the dentate gyrus of the altricial gerbil (*Meriones unguiculatus*) and the precocial spiny mouse (*Acomys cahirinus*). In: Elsner N., Schnitzler H.-U. (eds.): Göttingen Neurobiology Report 1998: 289. Thieme, Stuttgart.

Rünker AE, Schachner M (2001) A pathological L1 missense mutation leads to a lack of cell surface expression *in vitro* and *in vivo*. In: Elsner N., Schnitzler H.-U. (eds.): Göttingen Neurobiology Report 2001: 40. Thieme, Stuttgart.

Rünker AE, Bartsch U, Nave KA, Schachner M (2002) Mutations in the extracellular domain of L1 impair protein trafficking *in vitro* and *in vivo*. J. Neurosci, submitted.

Rünker AE, Fink T, Blazyca H, Loers G, Feltri L, Martini R, Schachner M. Pathology of a mouse mutation in the Schwann cell-related recognition molecule P0 resembles that of a human Charcot-Marie-Tooth type 1B phenotype. In preparation.

## Danksagung

Im Rahmen dieser Dissertationsschrift möchte ich all denen danken, die mich in den letzten vier Jahren sowohl beruflich als auch privat begleitet haben.

Ich danke Professor Dr. Melitta Schachner für die Überlassung des Themas und die Möglichkeit dieses unter den hervorragenden Bedingungen am Institut für Biosynthese Neuraler Strukturen (ZMNH) durchführen zu können, sowie für ihre stets hilfsbereiten und informativen Beiträge.

Herrn Dr. Jörg Bartsch gilt mein besonderer Dank für die Bereitschaft, diese Arbeit als externe Promotion zu betreuen.

Dr. Udo Bartsch danke ich für seine zahllosen fachkundigen Ratschläge und besonders für seine diskussionsfreudige Begleitung dieser Arbeit.

Bei Dr. Michael Kutsche bedanke ich mich für seine vielen Tricks, die mir auf dem, mir vormals wenig vertrauten, Terrain der Molekularbiologie eine große Hilfe waren.

Ich danke Dr. Marius Ader für seine vielfache Unterstützung bis hin zu Korrekturen des Skripts.

Ein herzlicher Dank geht an mein Labor, Bettina Rolf, Sandra Schmidt und Meike Zerwas, und an die restlichen 'Morphos' nebenan für die gute Atmosphäre und die Unterstützung im Laboralltag. Weiterer Dank gilt vielen Kolleginnen und Kollegen, die mir durch fachliche Gespräche und ihre Hilfsbereitschaft die Durchführung dieser Arbeit erleichtert haben.